Development of a Fatigue Analysis Tool to Predict Cable Flex Life

Chris McCorquodale

40073739

A thesis submitted in partial fulfilment of the requirements of Edinburgh Napier University, for the award of Master of Research

June 2014

Statement of Authenticity: I certify that the work presented in this thesis is of my own creation, and that any work adopted from other sources is duly cited and referenced as such.

Abstract

Fatigue failure by flexing is a common failure mode for cables in a high flex environment. As a result, the specialist cable supplier, Axon' Cable LTD found a need for a flex life analysis tool to aid the design process of their products.

The purpose of this project was to develop a fatigue analysis tool to predict cable flex life and this report looks at the steps taken to do so.

This was achieved by a calculation based model which considers material properties to generate flex life curves. The calculation model for metals was based on the Method of Universal Curves and for polymers based on an empirical fatigue method. Material properties, which were characterised by tensile and fatigue testing, unique to each individual material were incorporated in to these models to differentiate between material flex life performance.

The flex life curves were then validated by a flex life test programme carried out on two custom designed cable flex life test rigs which were developed using 3D CAD software.

Once validated at room temperature, flex life models and test procedures were expanded to incorporate temperature as a factor.

With the final development of a user interface to control the inputs and flex life models, the project concluded with Axon' Cable having a functioning design tool now used in the engineering department.

Acknowledgements

I would first like to thank Professor John Sharp of Edinburgh Napier University for his continued support and supervision throughout the course of the project. I would also like to thank the company, Axon' Cable LTD, for offering me the opportunity to take on such a challenge that has provided highs and lows throughout. My gratitude also goes out to Dr Neil Shearer for being a secondary supervisor to the project and to Technicians at the University for the role they played in the fabrication of test rigs and use of test equipment.

Nomenclature

β = Strand/ element lay angle

Δ (or d) = Change in

ε = Strain

ε_f (or D) = Ductility

ϕ = Position angle

σ = Stress

a = Crack length

A = Area

b = Elastic fatigue exponent

c = Plastic fatigue exponent

C = Paris' constant

d (or y) = Distance to central axis

D = Ductility or diameter

E = Young's Modulus

F = Force

I = Moment of inertia

L = Length

m = Fatigue exponent

M = Bending moment

n = Number of cycles undergone

N (or N_f) = Number of cycles to failure

R = Radius or R-value

List of Subscripts

1 = Primary or 1

2 = Secondary or 2

3 = Relating to twisted bundle or 3

4 = Relating to element in bundle or 4

a = Amplitude

ar = Reversed bending amplitude

bend = Relating to bend

e = Elastic

f = Failure, fracture or

final = Final state

i = State i

initial = Initial state

inner = Inner

insulation = Relating to insulation

max = Maximum

min = Minimum

outer = Outer

p = Plastic

SC = Relating to screen

strand = Relating to strand

y = Yield

List of Abbreviations

CAD = Computer aided design

CuBe = Beryllium copper

DCR = Direct current resistance

ESC = Environmental stress cracking

ETFE = Ethylene tetrafluoroethylene

FEA = Finite element analysis

FEP = Fluorinated ethylene propylene

GUI = Graphical user interface

KTP = Knowledge transfer partnership

PTFE = Polytetrafluoroethylene

RA = Reduction in area

SCA = Silver plated copper alloy

SCF = Strain concentration factor

UTS = Ultimate tensile strength

UV = Ultraviolet

Contents

1.0 Introduction

This report is based on the work undertaken as part of a Knowledge Transfer Partnership (KTP) between Axon’ Cable LTD and Edinburgh Napier University.

Axon' Cable LTD is a UK based subsidiary of a French cable company. The company is based in Rosyth, Fife and specialises in the design and manufacture of wires, cables and harnesses for advanced technologies, offering complete interconnect solutions to a wide range of applications:

- General industry
- Consumer
- Automotive
- Aeronautics
- Space
- Military
- Telecommunications
- Medical
- Research centres
- Oil industry

Due to the nature of Axon' customers, their products are often placed in demanding conditions, thus exposing them to unexpected failure. Repeated flexing is commonplace for cables and with the increasing demand on reliability and performance, it was considered necessary to invest in the development of a fatigue analysis tool to predict cable flex life.

1.1 Project Objectives

The main objectives of the project are as follows:

1. To increase company knowledge and awareness of fatigue and cable flex life.
2. To have a cable flex life analysis method within the company.
3. The ‘tool’ should have the ability to model different flex conditions, materials and cable constructions subject to different environmental temperatures.
4. There is to be an easy to use user interface to do simulations, allowing engineers to quickly and easily conduct a cable flex life analysis.

Successfully delivered, the project will provide the company with a competitive edge by demonstrating an understanding of a complex subject affecting their products. This in conjunction with flex life predictions will offer customers 'peace of mind' that the cable supplied is suitable. In addition, more efficient design reviews can take place, leading to an improved product. This is because the tool can be used to identify weak areas of a cable to reinforce or identify areas where a low grade, cheaper material could be used in order to reduce the cost of the cable without compromising cable integrity.

These factors all contribute to aid sales, help to win contracts and ultimately move a step ahead of competitors, both financially and technically.

1.2 Project Plan

The tool is to be calculation based. All calculations are to refer back to a base stress, strain and fatigue methodology and this was to be validated by experimental data. A validation approach was decided for two reasons:

- Time frame of project is relatively short (30 months).
- Calculation based allows for the development of a universal model that could be adapted to tailor for different cable designs.

The project is to be progressive in style, i.e. starting off with a simple case and gradually introducing complexities with time.

The project had several key stages and sub-stages which are summarised below.

1. Research
    a. Subject area
    b. Test methods
    c. Materials and characterisation
2. Design of flex test equipment
    a. Review of cable flex test equipment
    b. Design and build
3. Single strand conductor
    a. Gauge initial understanding of fatigue and determine material impact on flex life
    b. Material characterisation for 4+ conductor materials
    c. Validation on flex test equipment
    d. Validation at temperature

4. Multi-strand conductor
    a. Determine construction impact on flex life
    b. Validation on flex test equipment
5. Insulations
    a. Material characterisation for 4+ insulation materials
    b. Validation on flex test equipment
    c. Validation at temperature
6. Screens
    a. Determine weave impact on flex life
    b. Materials used similar to conductor materials
    c. Validation on flex test equipment
7. Implementation
    a. Development of user interface for tool

These were assigned times to completion and a Gantt chart was created to try and ensure the project stayed on track with targets being assigned target dates.

2.0 Stress/ Strain Analysis

Before a fatigue prediction can be made, an initial stress or strain analysis needs to be carried out. This determines the state to which the component is repeatedly subject to. This chapter introduces some basic methods used to analyse and correlate stress and strain.

The strain induced in a component is a function of how much it has been deformed. This can be represented by the following relation:

$$\varepsilon = \frac{\Delta L}{L} \tag{1}$$

Not all calculations will be as simple as equation 1, above, but in most cases it should be possible to refer back to it. Once the strain state is determined, the stress can then be analysed. Typically, for linear elastic materials such as metals below yield:

$$\sigma = E\varepsilon \tag{2}$$

For non-linear materials, a more complex calculation is used to determine stress from strain. The approach is similar, where a modulus is used and multiplied by the strain. However the modulus is a function as opposed to a number. This is discussed in more detail in chapter 11.1, polymer material models.

2.1 Types of Stress

There are different types of stress that can occur in a component. Depending on the material, different types of stress can induce different stress-strain behaviour. The main types of stress are listed with a brief description below.

- Tensile stress – occurs when a pull is applied and the component is under tension.
- Compressive stress – occurs when the component is pushed in on itself and compressed.
- Shear stress – occurs when the stress on a component acts in opposite directions at the same time.
- Torsion stress – occurs when a twist is applied to the component.
- Bending stress – occurs when a bend is applied to the component. A tensile stress is apparent on the outside of the bend and a compressive stress is apparent on the inside of the bend.

In this project, bending is the main motion of interest. Elastic bending theory is a common method used to calculate the tensile stress induced by a bend. Equation 3 below summarises this theory [RoyMech].

$$\frac{M}{I} = \frac{E}{R} = \frac{\sigma}{y} \tag{3}$$

2.2 Mean Stress Effects

A lot of fatigue models are based on either stress amplitude or maximum stress induced. These models generally have different R values (R = $\sigma_{max}/\sigma_{min}$) and are good for modelling specific applications, however, for a more flexible model that can cover a wide range of flex conditions it may be necessary to consider the potential effects of mean stress.

Mean stress describes how the effective induced stress or strain is dependent on the following parameters:

- Stress/ strain range
- Amplitude stress/ strain
- Maximum stress/ strain
- Minimum stress/ strain

In a sine wave loading case, the maximum and minimum stresses are shown in figure 1, below.

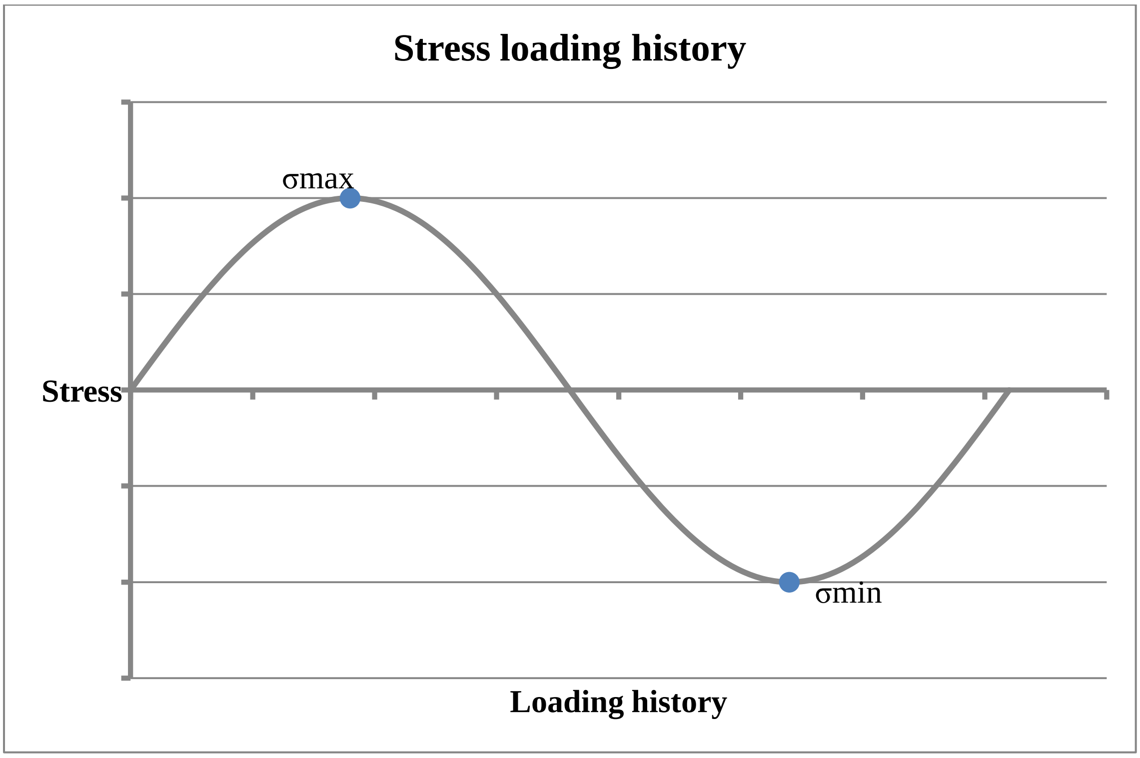

Figure 1; Loading history of component

The stress range is given by:

$$\Delta\sigma = \sigma_{\max} - \sigma_{\min} \tag{4}$$

The stress amplitude is given by:

$$\sigma_a = \frac{\sigma_{\max} - \sigma_{\min}}{2} \tag{5}$$

And the mean stress is given by:

$$\sigma_m = \frac{\sigma_{\max} + \sigma_{\min}}{2} \tag{6}$$

[Dowling, 2004]

The plot in figure 2 illustrates how a shift in mean stress (and different R values), can result in a significantly different loading history with the same stress range and amplitude.

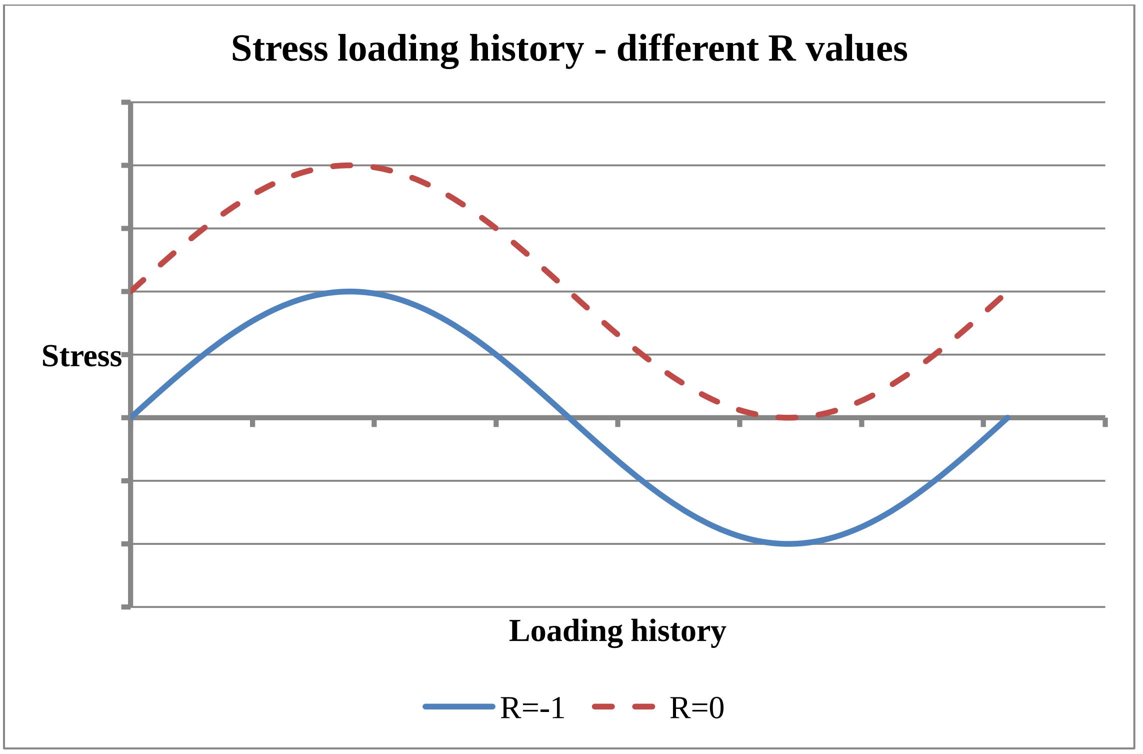

Figure 2; Same wave shape with different mean stresses

The shape of the wave is the same, however for the R=-1 case the load is both compressive and tensile. In the R=0 case, the load is tension only.

2.3 Smith Watson Topper Mean Stress Approach

One of the more common methods is known as the Smith Watson Topper (SWT) method. This method considers the above factors, and offers an 'effective stress amplitude' which should be used (assumes an R value of -1). The following three SWT equations all equate to the same thing:

$$\sigma_{ar} = \sqrt{\sigma_{\max}\sigma_a} \tag{7}$$

$$\sigma_{ar} = \sigma_{\max}\sqrt{\frac{1-R}{2}} \tag{8}$$

$$\sigma_{ar} = \sigma_a\sqrt{\frac{2}{1-R}} \tag{9}$$

[Dowling, 2004]

Figure 3 illustrates the result of using the SWT equations to determine the effective stress amplitude (for R=-1) of a loading pattern with an R value of 0.

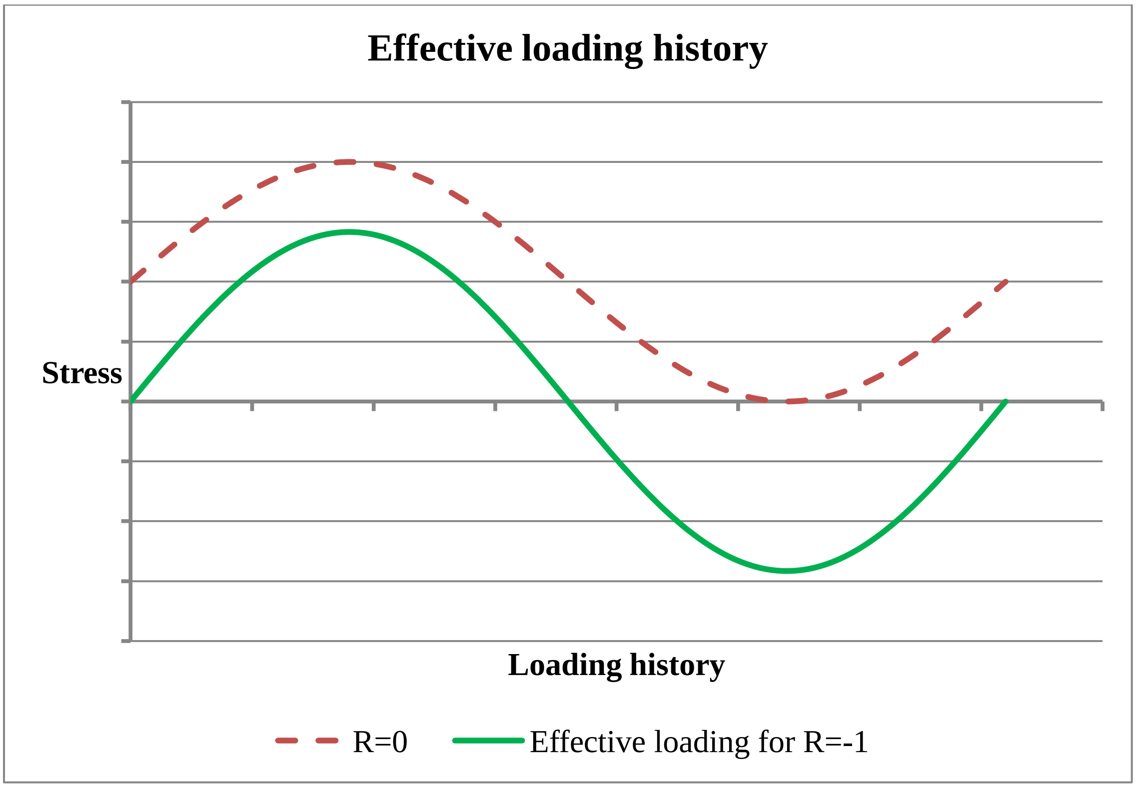

Figure 3; Effective loading cycle compared with actual

As can be seen, from the effective loading line compared to the R=0 line, the maximum stress is effectively reduced, but the amplitude stress is increased.

3.0 Material Characterisation

In order to differentiate between materials, each material needs to be characterised to quantify its stress-strain behaviour by producing a unique set of material properties for it. This chapter looks at some of the method used to do this.

3.1 Tensile Testing

Tensile testing is used to obtain key material properties for various materials. Once a specimen is loaded in to the tensile machine, one end of the specimen remains fixed and the other end is pulled, putting the specimen under tension. A load cell determines the equivalent load for the amount of displacement the specimen has undergone and the specimen is tensioned at a constant rate until it has broken. Figure 4, is a picture of an Instron mini 44, which is a universal test machine and can be programmed to perform numerous tests with different fixtures. The picture is annotated to illustrate the key parts of it.

Figure 4; Tensile testing machine

The highlighted aspects of the machine are summarised below.

A. Area where specimen would be loaded.
B. Load cell.
C. Clamps.
D. Emergency stop button.

Software that is connected to the tensile machine takes the data fed back from the machine and uses it to plot a graph of load against displacement which can then be processed to stress and strain. This is illustrated in figure 5, which illustrates a typical stress strain curve for a linear elastic material such as a metal.

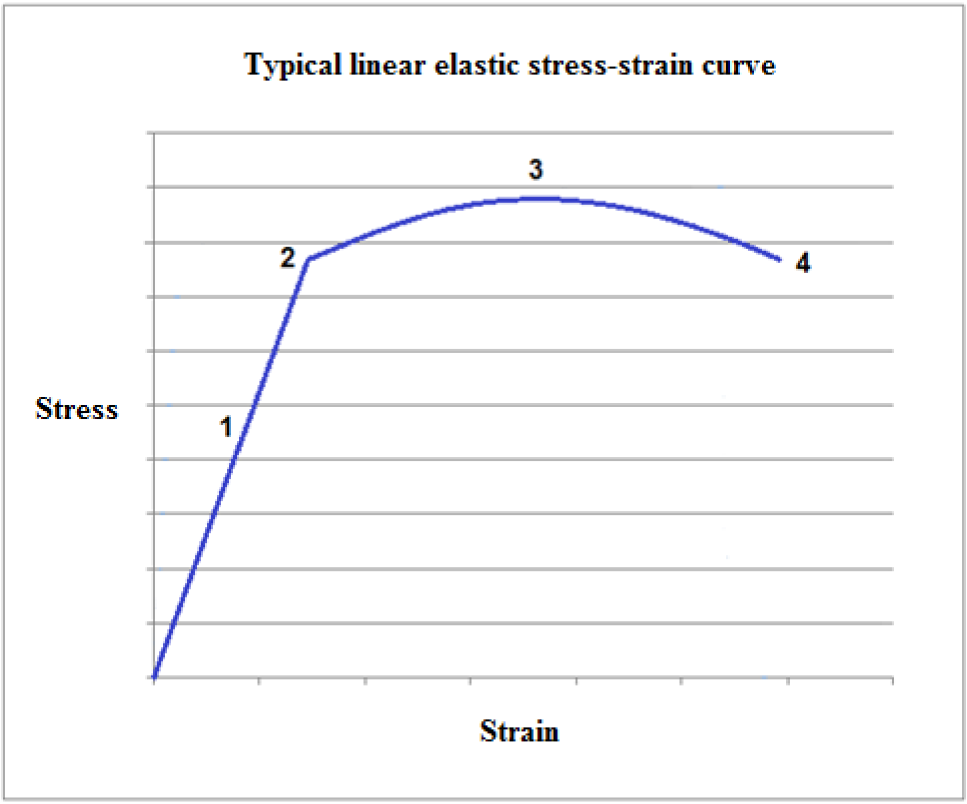

Figure 5; Typical graph from tensile test for metals

From this graph, some key material properties can be determined:

1. The gradient of the initial straight part is the Young's modulus (E) – this is the ratio of stress to strain for the material.

$$E = \frac{\sigma}{\varepsilon} \tag{10}$$

2. Yield strength (σ_y) – this is the stress at which plastic deformation occurs.

$$\sigma_y = \frac{F_y}{A_{initial}} \tag{11}$$

3. Ultimate tensile strength (UTS) – this is the maximum engineering stress the material can withstand.

$$UTS = \frac{F_{\max}}{A_{initial}} \tag{12}$$

4. Total elongation – the total strain of the material at rupture.

$$Elongation = \frac{\Delta L(total)}{L} \tag{13}$$

3.2 Compressive testing

Compressive testing is another form of testing a material to destruction. The concept is the same as that for tensile testing except the specimen is compressed instead of pulled. A similar graph is produced where the compressive Young's modulus, Ultimate and compressive yield strengths can be determined.

3.3 Optical Measuring

Once a specimen has failed in a tensile test, sometimes it is desirable to know the reduction in area at the failure point. It is an alternative indication of ductility to total elongation. This is done using optical measuring microscope which is a high quality microscope connected to a digital screen with measuring capabilities. Figure 6 is a picture of the image that can be viewed and measured on screen, from the equipment. It is a picture of a wire sample that has necked and broken in a tensile test.

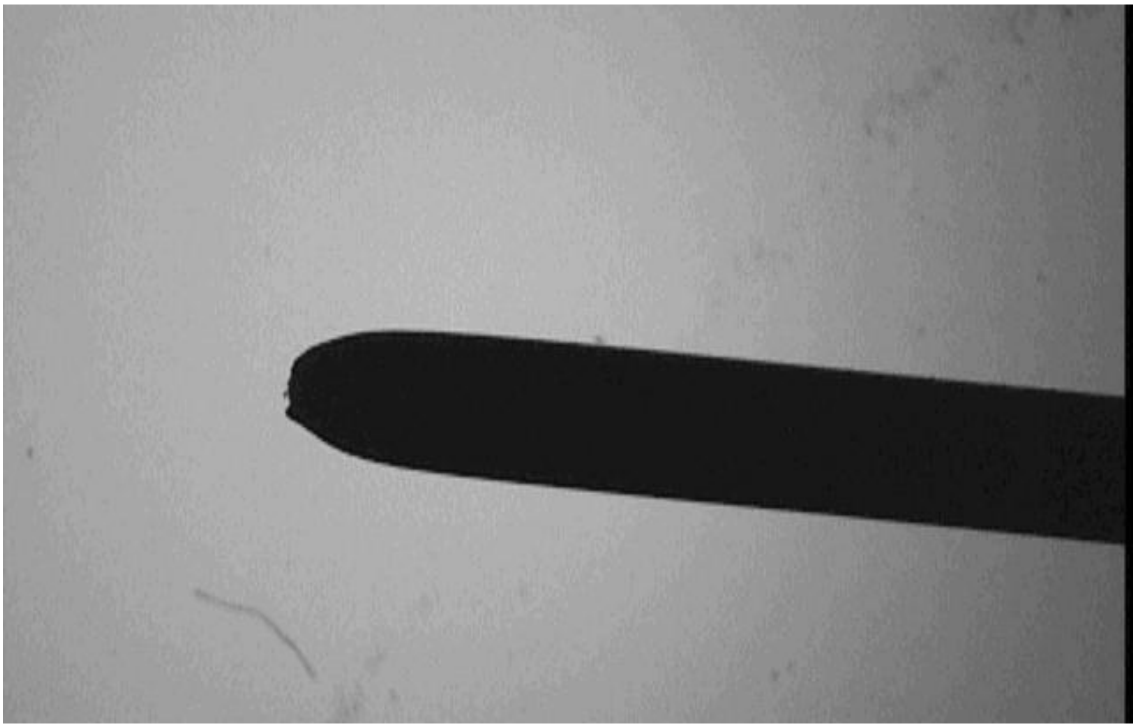

Figure 6; Wire sample necked and failed in a tensile test

With a wire sample of cross sectional area, the initial wire diameter should be known, and the final wire diameter is measured at the point of necking. The area of can be simply calculated from:

$$A = \frac{\pi D^2}{4} \tag{14}$$

The reduction in area is then calculated by:

$$RA = \frac{A_{initial} - A_{final}}{A_{initial}} \tag{15}$$

This can be represented as either a fraction or a percentage.

4.0 Fatigue Prediction Methods

Fatigue describes the accumulative damage process that occurs in a component when it is subject to repeated stress or strain. Failure as a result of this is known as fatigue failure and forms the basis of this project.

In order to estimate how many cycles a component can withstand, a stress or strain analysis needs to be conducted first. This determines the state that the component is repeatedly subject to. The flow chart in figure 7 summarised this process.

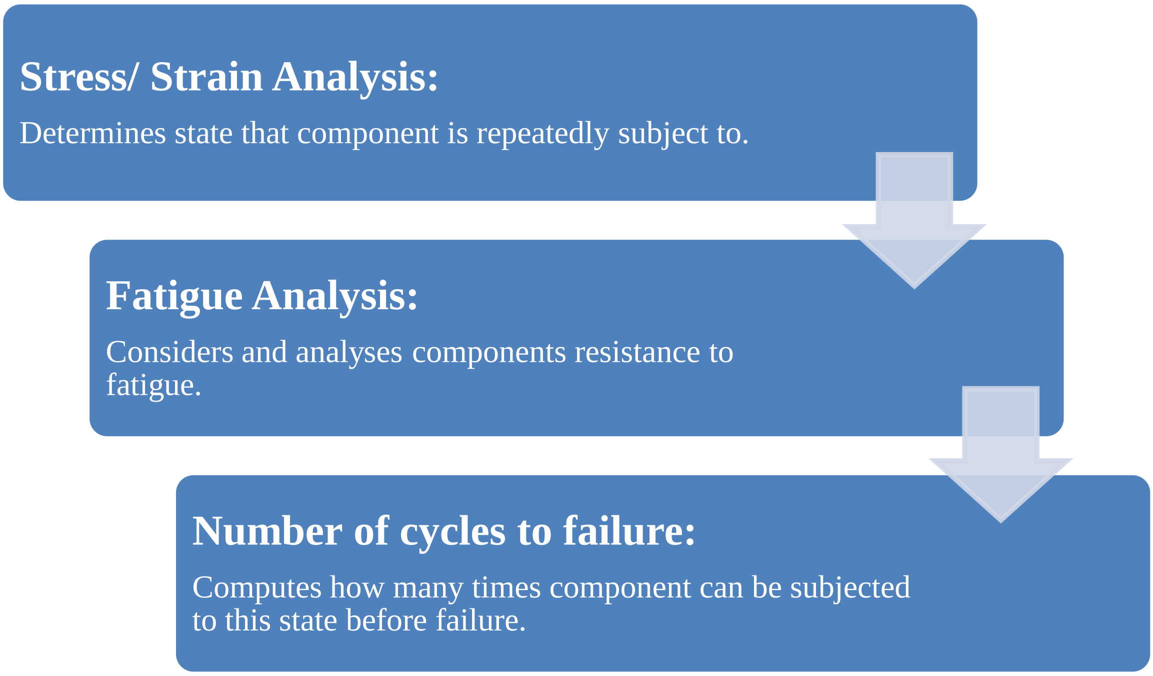

Figure 7; Fatigue prediction flowchart

Stress/strain analysis is generally done by means of calculation or FEA. This chapter looks at fatigue analysis methods, the step after the initial stress or strain analysis and how this leads to an estimation of number of cycles to failure.

4.1 High Cycle Fatigue

When a component is deformed, it can be subject to two types of deformation, elastic deformation and plastic deformation.

A high cycle fatigue method is used when the component is deformed elastically. Elastic deformation occurs when the strain is small and therefore the stress is low. When this stress is removed, the component returns to its original state. The high cycle method considers the materials elastic properties to carry out a fatigue analysis.

$$\frac{\Delta\varepsilon_e}{2} = \frac{\sigma_f'}{E}(2N_f)^b \tag{16}$$

[ASM vol. 19, 1996, P234]

4.2 Low Cycle Fatigue

A low cycle (or strain-life) fatigue method is used when plastic deformation occurs. Plastic deformation happens when the strain induces a stress which exceeds the yield strength of the material. Post yield, if the stress is then removed, the component is permanently deformed but not necessarily broken. The low cycle method considers the materials post yield behaviour in order to carry out a fatigue analysis.

$$\frac{\Delta\varepsilon_p}{2} = \varepsilon_f'(2N_f)^c \tag{17}$$

[ASM vol. 19, 1996, P233]

4.3 Coffin-Manson Method

Despite there being two different methods for fatigue prediction of elastic deformation and plastic deformation, it is believed that the total strain on a component is the sum of the plastic strain and elastic strain. The Coffin-Manson method considers both the elastic and plastic material behaviour to give a more complete equation that considers both the elastic and plastic strain in the fatigue prediction:

$$\frac{\Delta\varepsilon}{2} = \varepsilon_f'(2N_f)^c + \frac{\sigma_f'}{E}(2N_f)^b \tag{18}$$

[ASM vol. 19, 1996, P963]

Knowing the material parameters, N_f can be found iteratively. The fatigue strength exponent (or elastic fatigue exponent), b, is believed to vary between about -0.05 and -0.12. The fatigue ductility exponent (or plastic fatigue exponent), c, is believed to vary between -0.5 and -0.7.

4.4 Method of Universal Curves

The method of universal curves is similar in structure to the Coffin-Manson relation above, but it is more generalised to cover a wider range of metals. The relation is as follows:

$$\Delta\varepsilon = 3.5\frac{UTS}{E}N_f^{-0.12} + \varepsilon_f^{0.6}N_f^{-0.6} \tag{19}$$

[ASM vol. 19, 1996, P963]

This method makes the assumption that all metals possess the same fatigue exponents (-0.12 and -0.6). However, this is not necessarily the case so this method could be made more accurate by curve fitting to data to obtain more accurate fatigue exponents for a material. The other properties in this relation (E, UTS, ε_f) can all be obtained from a tensile test.

4.5 Four Point Method

The four point method attempts to characterise the two parts of the metal fatigue curve (elastic line and plastic line) individually, by relating fatigue to the metal's tensile properties. The total fatigue curve is the sum of the two lines characterised. The following points are the procedures to follow to create the curve.

Points to create elastic line:

1. At N_f=0.25, $\Delta\varepsilon_e$=2.5(σ_f/E)
2. At N_f=10^5, $\Delta\varepsilon_e$=0.9(UTS/E)

These points relate to the elastic tensile properties of the metal. Point 1 is plotted at $\Delta\varepsilon_e$=2.5(σ_f/E), when N=0.25 (1/4 of a loading cycle). σ_f is the fracture stress of the material. Point 2 indicates that when stressed at 90% of its ultimate tensile stress, N = 100,000 cycles.

Points to create plastic line:

3. At N_f=10, $\Delta\varepsilon_p$=0.25$D^{3/4}$
4. At N_f=10^4, $\Delta\varepsilon_p$=(0.0132 - $\Delta\varepsilon_e$)/1.91

These points relate to the plastic tensile properties of the material. Point 3 is plotted at ε_p=0.25$D^{3/4}$, when N=10. D (or ε_f) is the ductility of the material. Point 4 denotes where the plastic and elastic lines intersect; at approximately 10,000 cycles, when $\Delta\varepsilon_p$=(0.0132 - $\Delta\varepsilon_e$)/1.91.

[ASM vol. 19, 1996, P963]

Summing the two lines generates a curve as figure 8 shows:

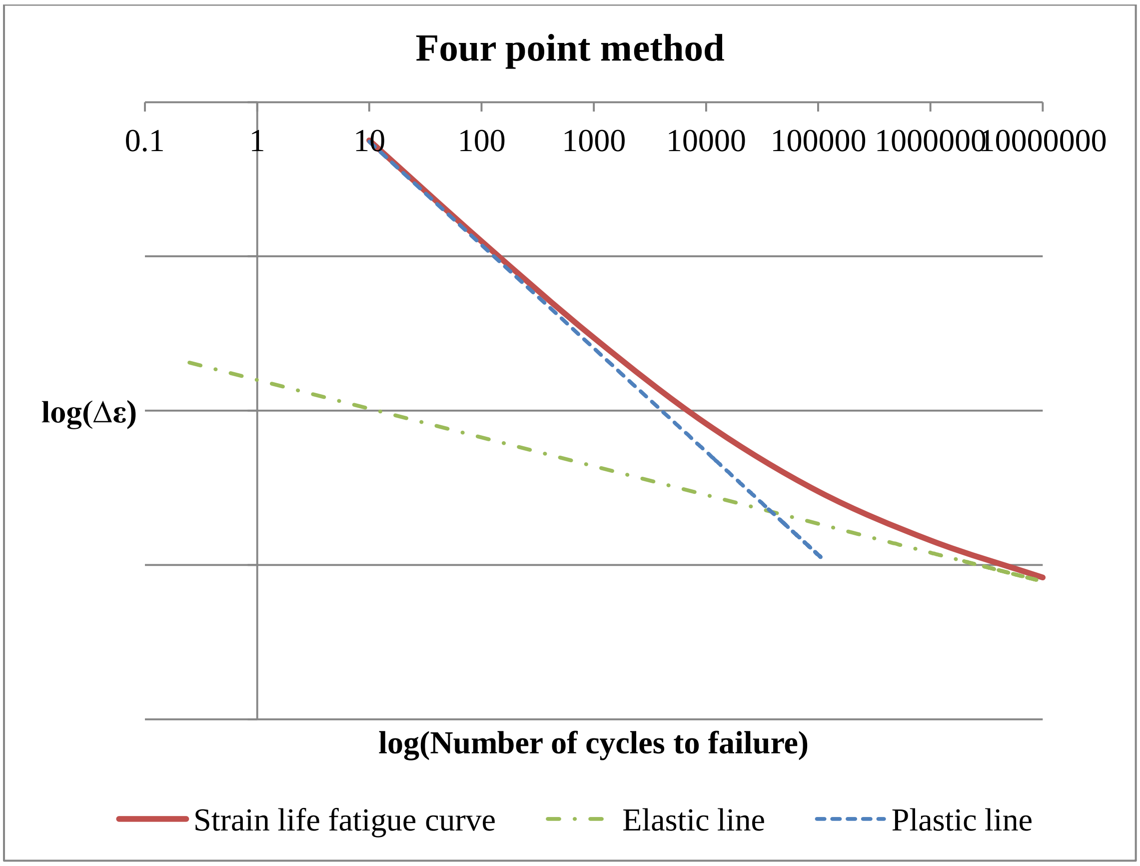

Figure 8; An example of using the four point method to characterise a fatigue curve

4.6 Paris' Law

This method starts with the basis that the component has an initial crack of known length a, and when the crack reaches a critical length, failure occurs. This is described by the Paris-Erdogan equation shown below.

$$\frac{da}{dN} = C(\Delta K)^m \tag{20}$$

[Bishop et al, 2000, P66]

C and m are known as Paris' constants, which are unique to a material, and ΔK is the range of stress intensity at the crack tip, which could be determined from FEA. This method can be used to predict how many more cycles a component will endure by re-arranging the equation to give:

$$dN = \frac{da}{C(\Delta K)^m} \tag{21}$$

4.7 Empirical Methods for Polymer Fatigue

Fatigue analysis for polymers is far from well developed. They are materials which are difficult to model as they exhibit complex stress-strain behaviour. On top of this, polymers are subject to a range of other failure mechanisms (see chapter 13). Research by Opp and associates [1970] suggests that common metal fatigue methods such as the method of universal curves are not suitable for polymers.

There are, however, generally accepted methods that can be used to estimate fatigue life in a polymer component. Popular methods used to characterise polymer fatigue are empirical methods. These are methods based on knowledge and backed up by data to create a general rule for which a range of polymers abide by.

Some of the common empirical polymer fatigue methods are presented in equation 22, 23 and 24 (Maxwell et al, 2005, P46):

$$UTS = \sigma_a N^{-m} \tag{22}$$

This method suggests that at one cycle to failure, the stress amplitude required to induce failure is equal to the UTS of the material. With decreasing σ_a, N increases exponentially thereafter.

$$\sigma_a = UTS - b \log N \tag{23}$$

Similar to equation 22, this method suggests that at one cycle to failure, the stress amplitude required is equal to the UTS of the material. As σ_a reduces, the term blogN increases to compensate meaning that the curve reduces logarithmically.

$$\Delta\sigma = a + \frac{b}{N^x} \tag{24}$$

This method is based on stress range but is again similar to those above with an exponential decaying nature. However, it is not based on easily obtainable material properties and it requires the derivation of constants a, b and x.

Alternatively, the four point method could be reduced to a two point method to characterise the brittle failure region of the curve. Using the UTS as the first point and collected data as the second - this could then be characterised further with more data.

Another useful piece of data that can be used in estimating polymer and metal fatigue is the fatigue endurance limit.

4.8 Fatigue Endurance Limit

Some materials exhibit a fatigue limit. This is a stress value below which fatigue failure does not occur in the material as illustrated in figure 9. This means that if the stress level in the material can be kept below this critical value, the component is safe from failure by fatigue. However, other failure mechanisms could occur, particularly through age, such as degradation and corrosion [Bishop et al, 2000, P25].

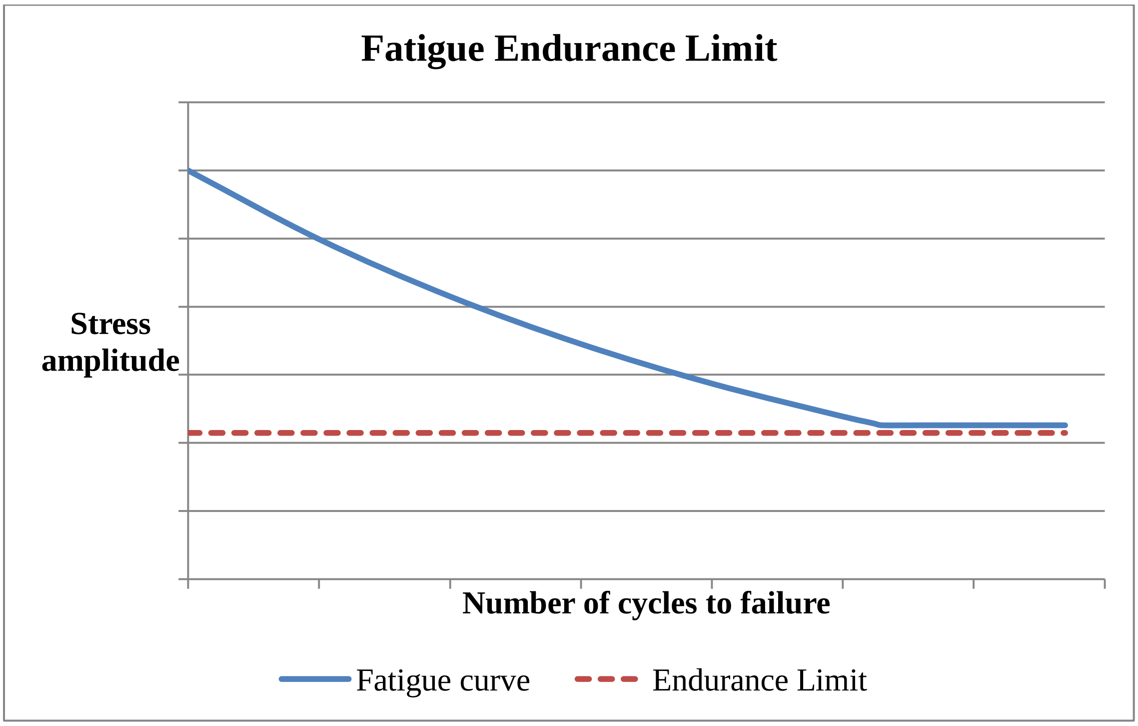

Figure 9; Fatigue endurance limit

4.9 Palmgren-Miner Rule

The Palmgren-Miner rule offers a solution to consider fatigue when a component is subject to a range of different stress/strain states. The equation representing this rule is as follows:

$$\sum_{i=1}^{k} \frac{n_i}{N_i} = 1 \tag{25}$$

[Bishop et al, 2000, P34]

Where n_i refers to the number of cycles the component endures at state i and N_i refers to the total number of cycles to failure for the component at state i. This can also be written:

$$\frac{n_1}{N_1} + \frac{n_2}{N_2} + \frac{n_3}{N_3} + \ldots = 1 \qquad (26)$$

This type of analysis could be used to determine the impact of a varying load profile such as the one in figure 10 and the total life of the component subject to such a complex stress state could be estimated.

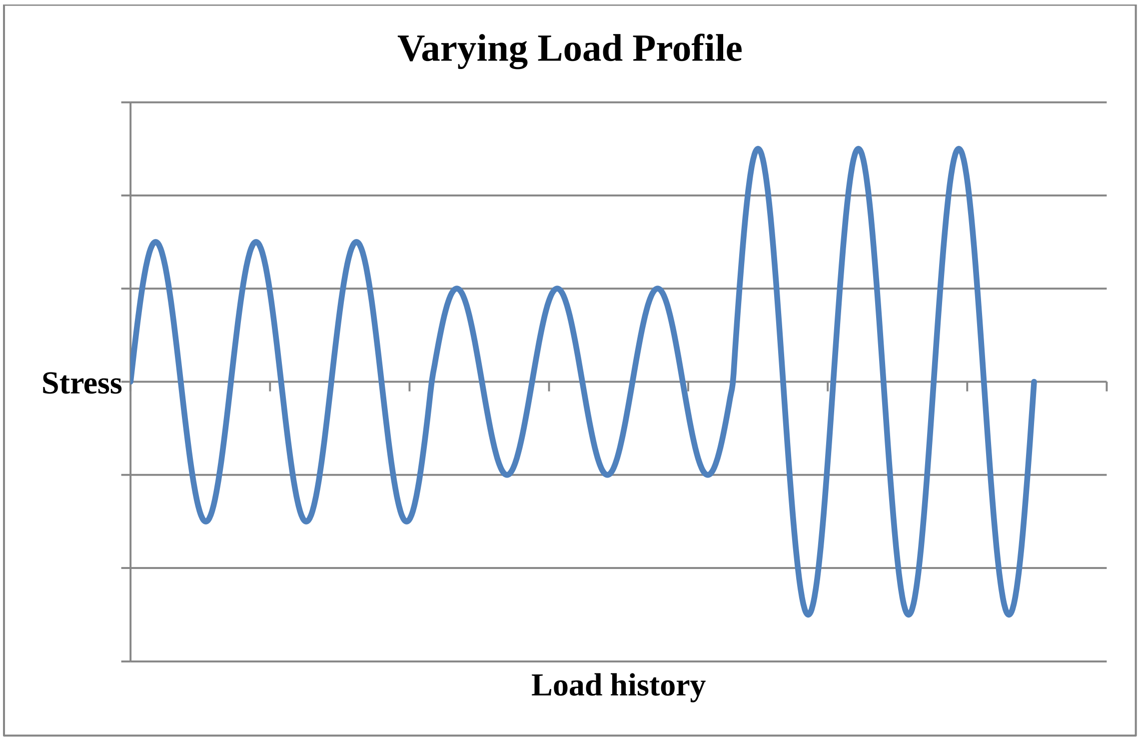

Figure 10; Varying load profile

5.0 Review of Fatigue Test Methods

This Chapter looks at common methods to test a material or components resistance to fatigue and their significance in relation to this project.

5.1 End Loaded Fatigue

End loaded fatigue tests are ones by which a specimen is cyclically loaded at one end and fixed at the other. The tests can be strain controlled or stress controlled. An illustration of this method can be seen in figure 11.

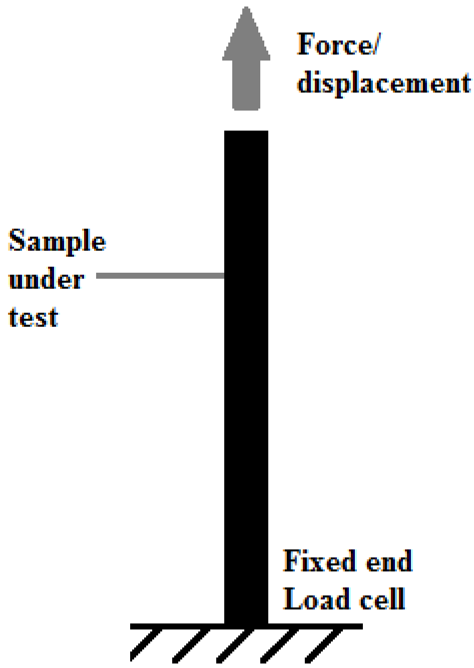

Figure 11; End loaded fatigue illustration

Strain controlled end loaded fatigue tests are when a specimen is fixed at one end and a displacement is applied to the other, putting a strain on the component. This cyclic strain ultimately induces a cyclic stress. Stress controlled end loaded fatigue tests are when a specimen is fixed at one end and a load is applied to the other. This applies a cyclic stress to the specimen. In both scenarios, when failure occurs number of cycles to failure is noted. This type of test can be done on a universal tensile test machine (as pictured in figure 4), when programmed to load cyclically.

A repeated bend flex test is a strain controlled test so the use of the strain controlled end loaded fatigue test could prove useful as the maximum stress induced would effectively be the same, just the method of inducing it would be different.

5.2 Flexural fatigue

There are two main types of flexural fatigue tests. Three point flexural fatigue and cantilevered beam flex.

Three point flexural fatigue test is when the sample is constrained at two points and a load or displacement applied in the middle. Figure 12 is a picture of this method.

Figure 12; Three point flexural fatigue test method [Instron, 2013]

The other type of flexural fatigue test is the cantilevered beam test. This is when the sample is fixed at one end, like a beam, and a transverse load or displacement is applied at the other. Figure 13 is a picture this method.

Figure 13; Cantilevered beam flexural fatigue test [System Integrators, 2011]

5.3 MIT Flex Life Endurance

Initially developed to determine the durability of paper, the MIT flex life test tests the sample to failure by bending a 0.19 mm (typically) thick strip of material through a 0.38 mm bend radius, through an angle of 135 degrees and back on itself (270 degrees in total). Number of cycles to failure is noted. Figure 14 illustrates this method.

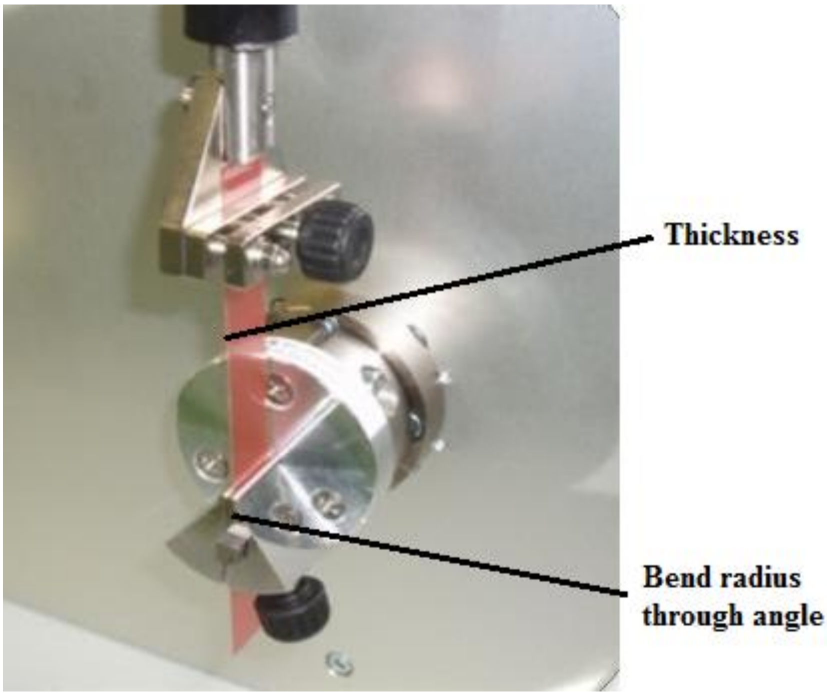

Figure 14; MIT folding endurance test machine (Beijing Shijia Wanlian Scientific Co. LTD)

Polymer flex life data is often presented in this way. However, while it is useful qualitative data, because of the very high frequency rates that the tests are run at, the data may not be representative of a real life application. Also the thickness of the sheet is very small; this can have an effect on the overall mechanical properties of the polymer.

6.0 Review of Cable Flex Test Equipment

A review of cable flex test equipment was carried out at Axon' Cable LTD's parent company in France, where a range of flex tests are employed for various purposes. These flex tests are typical of those available in industry. This chapter looks at the various different methods used and analyses the effectiveness of each.

6.1 Tick-Tock Flex

This method is named tick-tock flex because of its resemblance to a pendulum on a grandfather clock.

Figure 15; Tick-tock flex test

The cable is clamped between the two blocks, the corners of which induce a bend radius to the cable. A tensile load is used to ensure the rest of the cable is kept straight throughout the process. The blocks move from a straight position to 90 degrees either side (through 180 degrees in total).

This method is good as it applies a full reversed bend to the cable, the bend radius can be changed by simply changing the bend radius on the blocks. However the tensile load is not representative of a real application. Also, this tensile load could affect results as it is an additional stress on the cable which could contribute to its failure.

Figure 16 is a variation on the design in figure 15 to allow for multiple samples to be tested simultaneously. It is also a smaller model so it is more suited to testing wires or bare conductor.

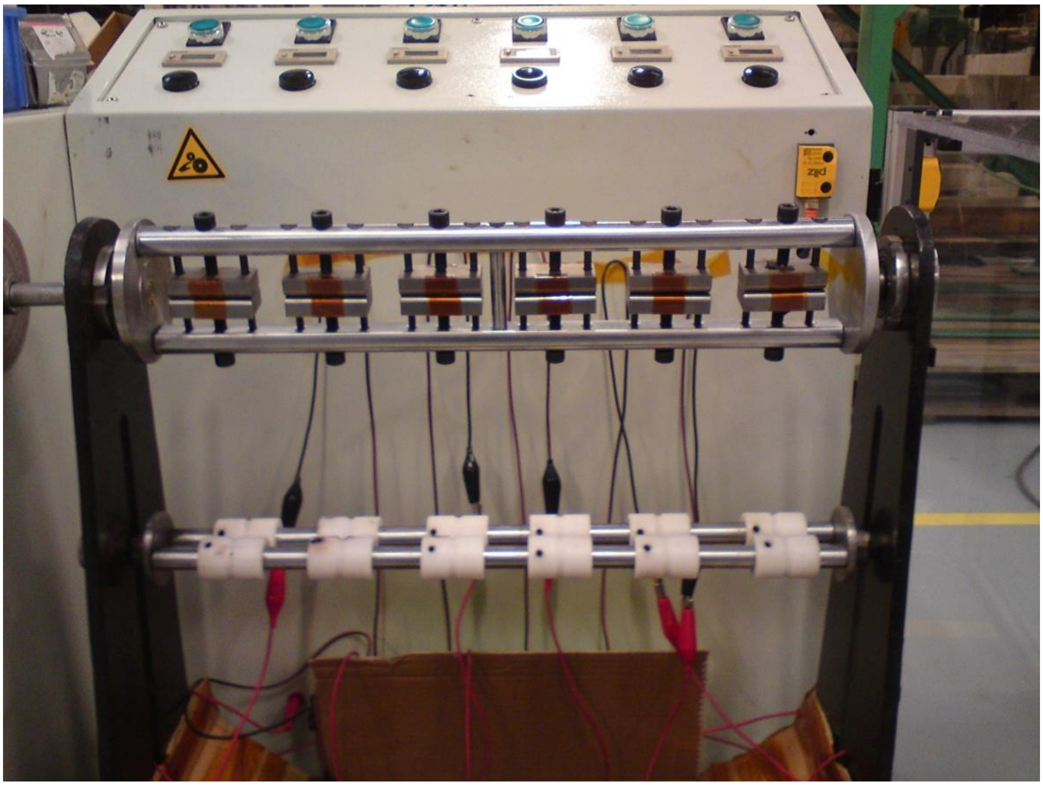

Figure 16; Tick-tock flex test for smaller cables

6.2 Rolling Flex

Figure 17 is a picture of a rolling flex test machine.

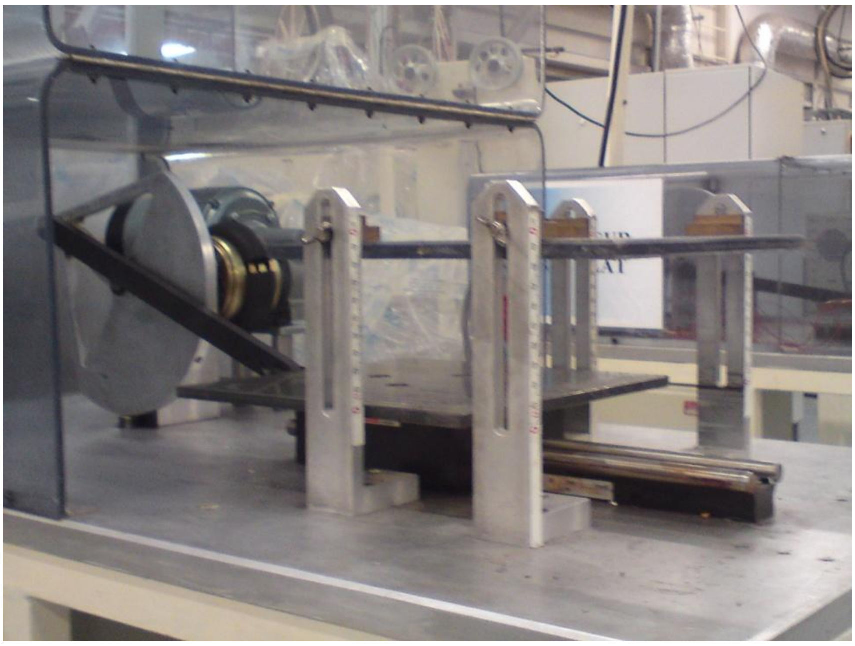

Figure 17; Rolling flex test

The cable sits in between the two plates in the bend position, with the upper plate fixed and the lower plate moving laterally. This rolls the cable along itself. This method is typically used for flat cables or ribbon cables. The bend radius can be changed by changing the plate separation. However, because it is designed for flat cables, it may not necessarily be suitable for round cables or conductors.

This method induces a bend region as the cable is rolled along a portion of its length as opposed to the tick-tock flex test where it is just a single point that is subject to the bend. Since more of the cable is being flexed, this would help to reduce the impact of material inconsistencies in results which is beneficial.

A further illustration of this method is shown in figure 18.

Figure 18; Rolling flex method illustration

6.3 Random Variable Flex

Also known as a manual handling flex test. Figure 19 shows a picture of this flex test setup.

Figure 19; Random variable flex test

The bar at the top of rotates which applies a bend to each cable. Each individual cable is then attached to another fixture which twists to apply torsion to the cable simulating random motion. At the other end, the cables are unconstrained.

This method is suitable for testing umbilical type cables. The cables being tested in figure 19 were being tested for a medical application - the combination of bending and torsion was supposed to mimic the random movement of a surgeon's hand.

Since the movement is designed to be 'random', it would be too problematic for modelling purposes because while the movement is repetitive, it is not reliable.

6.4 Torsion Flex

A torsion flex test machine is pictured in figure 20. The cable is fixed at one end and a twist is applied to the other end, applying a torque along the length of the cable.

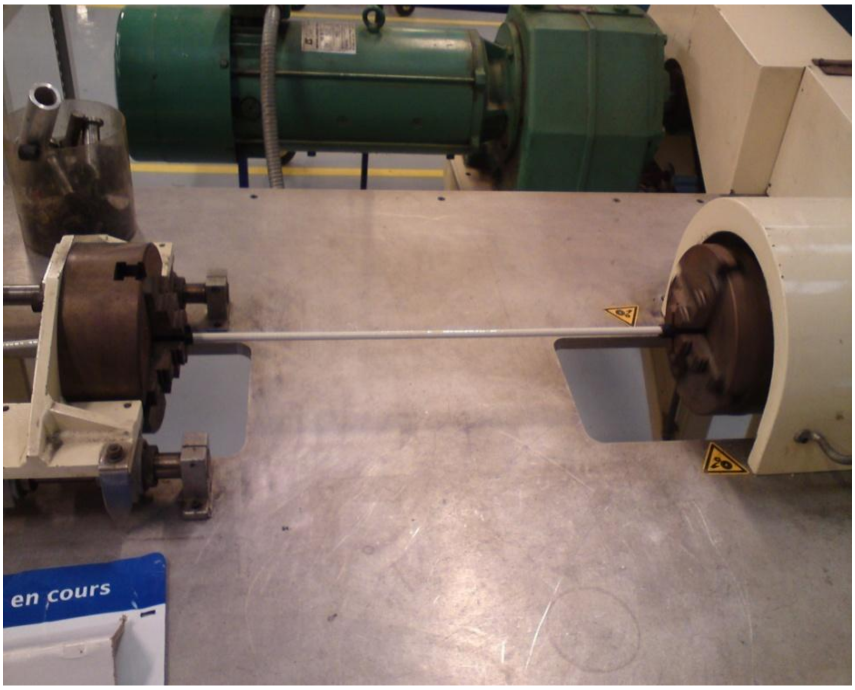

Figure 20; Torsion flex test

This test would be good for testing a direct repeated torsion on the cable, however more dynamic applications are bending rather than torsion. In addition, in most circumstances, design engineers will try to eradicate torsion from the application completely by giving significant consideration to how the cable is routed.

6.5 Pulley Flex

A picture of this test equipment is shown in figure 21. Cables are clamped at either end of the equipment, and fed through the two pulleys to induce a double bend in the cable. The pulleys then move side to side to force this bend through the cable repeatedly.

Figure 21; Pulley flex test

Like the rolling flex test this would induce a bend region which, as discussed previously, would help to improve the quality of test results.

However, due to the design of the pulley test machine in figure 21, different sized pulleys would induce the bend through a different angle. In order to keep testing as consistent as possible, this would need to be eradicated.

7.0 Flex Life Test Regime

As mentioned in chapter 1.0, any flex life models generated must be validated by means of a suitable test regime. This chapter looks at the thought process behind the design of flex test rigs that were used.

At the start of the project, a few options were considered as to how the flex life model would be tested and validated.

- Use of flex test equipment at Axon' LTD's parent company based in France.
- Fatigue test equipment or modifications made to equipment based at Edinburgh Napier University.
- Design and build of new flex test rigs.

It was decided that two flex test rigs would be designed and built in order to test and validate flex life models.

1. A physically small rig that is capable of testing single strand conductor, small multi strand conductor, small wires and insulation filler samples.
2. A larger flex test rig that is capable of testing cable bundles as well as individual cable elements such as multi strand conductor.

Having the rigs designed and built specifically for the project meant that they could be kept on-site and their availability would not be an issue. It also meant that options were not restricted and the rigs could be tailored to their function.

7.1 Flex Test Rig 1

Having carried out a review of cable flex test equipment (chapter 6), it was decided that this flex test rig would be based on the rolling flex method for the following reasons:

- No alternative failure mechanism.
- Appropriate for small scale samples.

Some requirements were put in place before the design of this flex test equipment:

- Based on rolling flex test method.
- Ability to test different size samples.
- Ability to test different bend radii.

The initial concept design was based on two plates, an upper and a lower plate. The upper plate is fixed and the lower plate moves laterally to roll the element along itself when it is constrained in the bend position between the two plates.

Since the rolling flex method is traditionally used on flat cables, the samples needed to be constrained in such a way that would make them behave like flat cables. Grooves were cut in to the top and bottom plates to give the samples a channel to run along. A polyester sheet was used to then constrain the samples to the grooves in the top and bottom plates.

Figure 22 is an annotated CAD model of the concept design with a description of the annotated parts below.

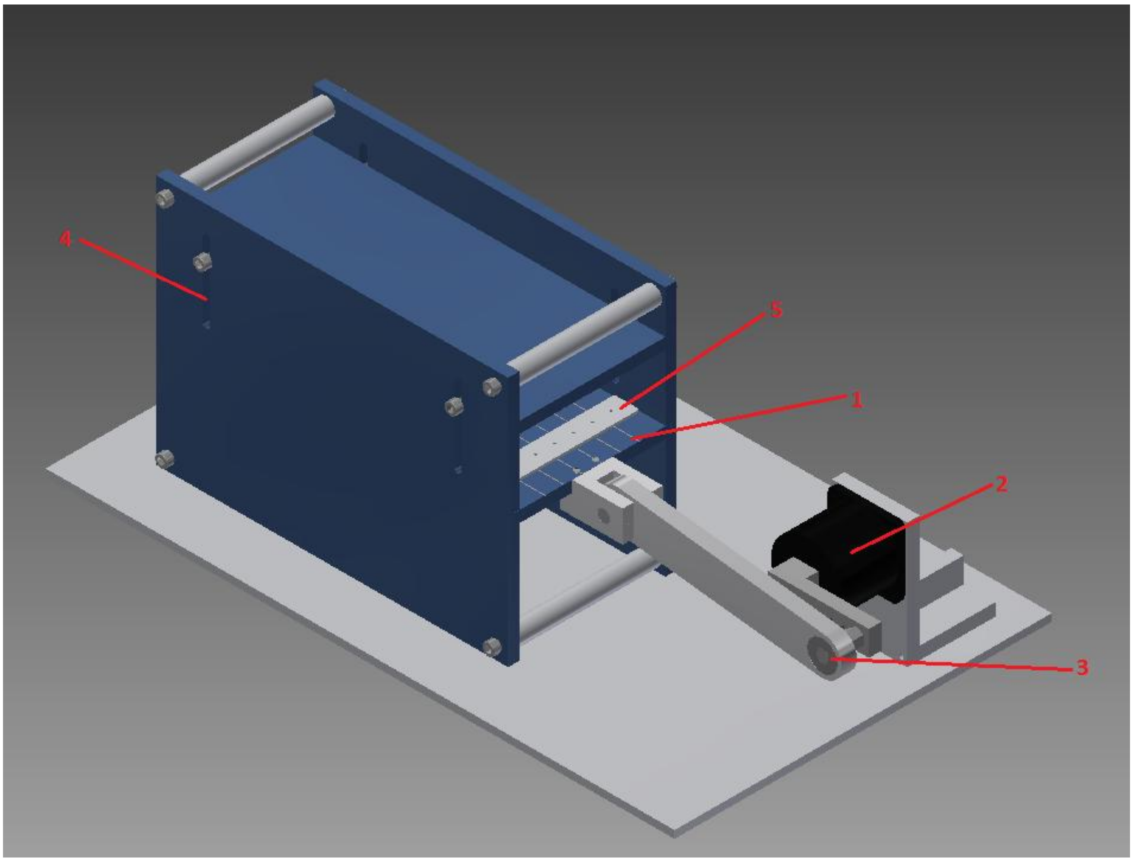

Figure 22; CAD model of rolling flex test rig

Features:

1. Grooves in plates to help constrain the samples.
2. Motor to power lateral movement of lower plate.
3. Bearings to reduce friction and ensure smooth power transmission.
4. Slots in sides to allow for variable plate separation and bend radius.
5. Clamp to constrain samples.

An industrial PVC material is chosen for the upper, lower and side plates. This is because this material cheap and most importantly low friction (typical coefficient of friction = 0.2-0.3, Dotmar) and it can slide along itself with ease. Lubricants can also be used to help with the sliding.

The power transmission system is on a cam so the motor can run in one direction and the lateral movement occurs repeatedly.

A light sensor is used to send pulses to a counter via the conductors. This subsequently counts the number of bends the element is subject to by counting how many times the light is cut off. For a single strand conductor, once the wire breaks, the pulses stop and the counter stops counting. Other elements such as multi strand conductors and insulation fillers require to be monitored more closely.

Figure 23 is a picture of the test rig once built and figure 24 is a picture of the board with the counters.

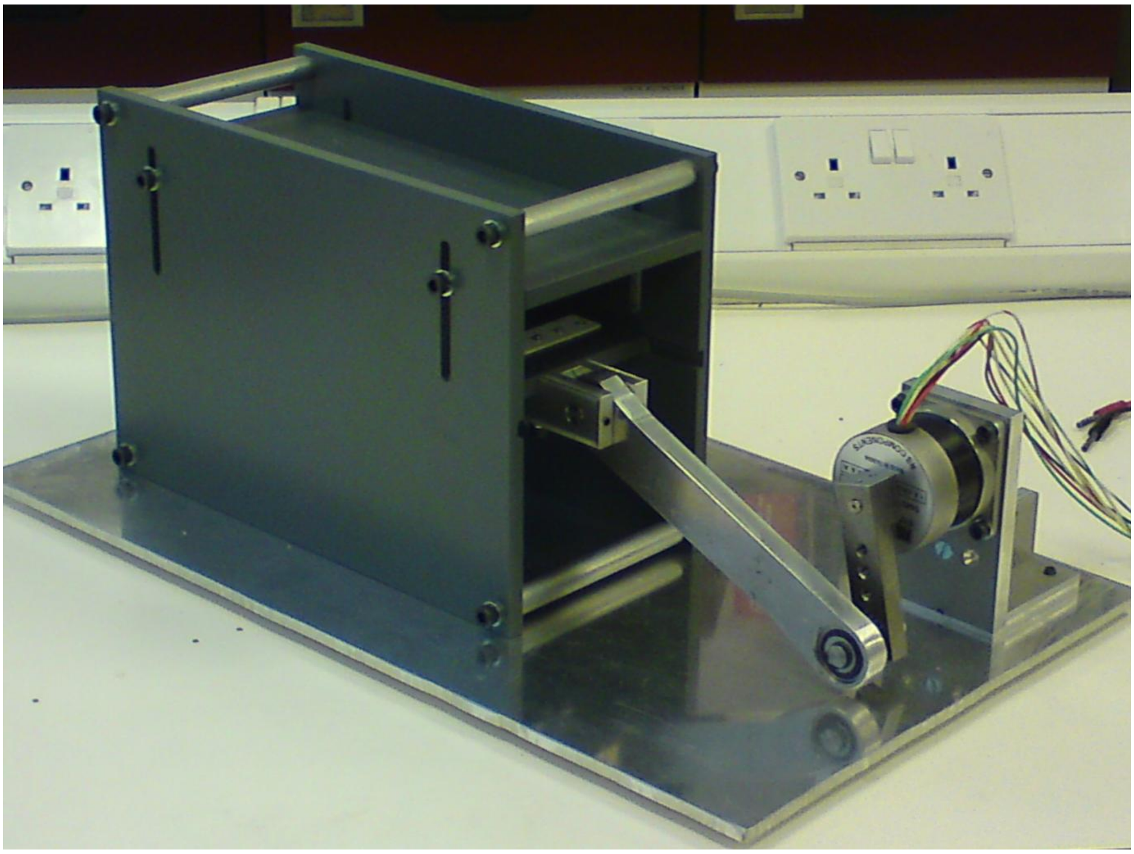

Figure 23; Rolling flex test rig

Figure 24; Counter board

7.2 Flex Test Rig 2

The following specific requirements were put in place before the design of this equipment:

- Reversed bending - to test flex life model under different flex conditions.
- Capable of testing dynamic cables of up to 10 mm diameter.
- Ability to test different bend radii.

A pulley flex method was decided to be the base concept for this equipment. This accommodates the reversed bending requirement and inter-changeable pulleys allow for different bend radii to be tested.

The design was based on two pulleys inducing an S shape bend in a cable. These pulleys then move up and down forcing this S-bend through the pulleys repeatedly. Side to side (instead of up and down) motion was also considered but due to space constraints and the size of the footprint this rig would leave, an up and down motion was more suitable. Various options were explored to achieve this up and down motion:

- Electrically powered linear actuator.

- Hydraulically powered linear actuator.
- A geared cam and motor setup.

It was decided that the pulleys would be encased in a yoke which moves up and down via a linear actuator which is powered by a reversing motor. This was deemed the most reliable option. Figure 25 is an annotated CAD model of this setup. Again the annotations are explained below. The size of the rig is approximately 1250 mm in height, 826 mm width and 425 mm depth.

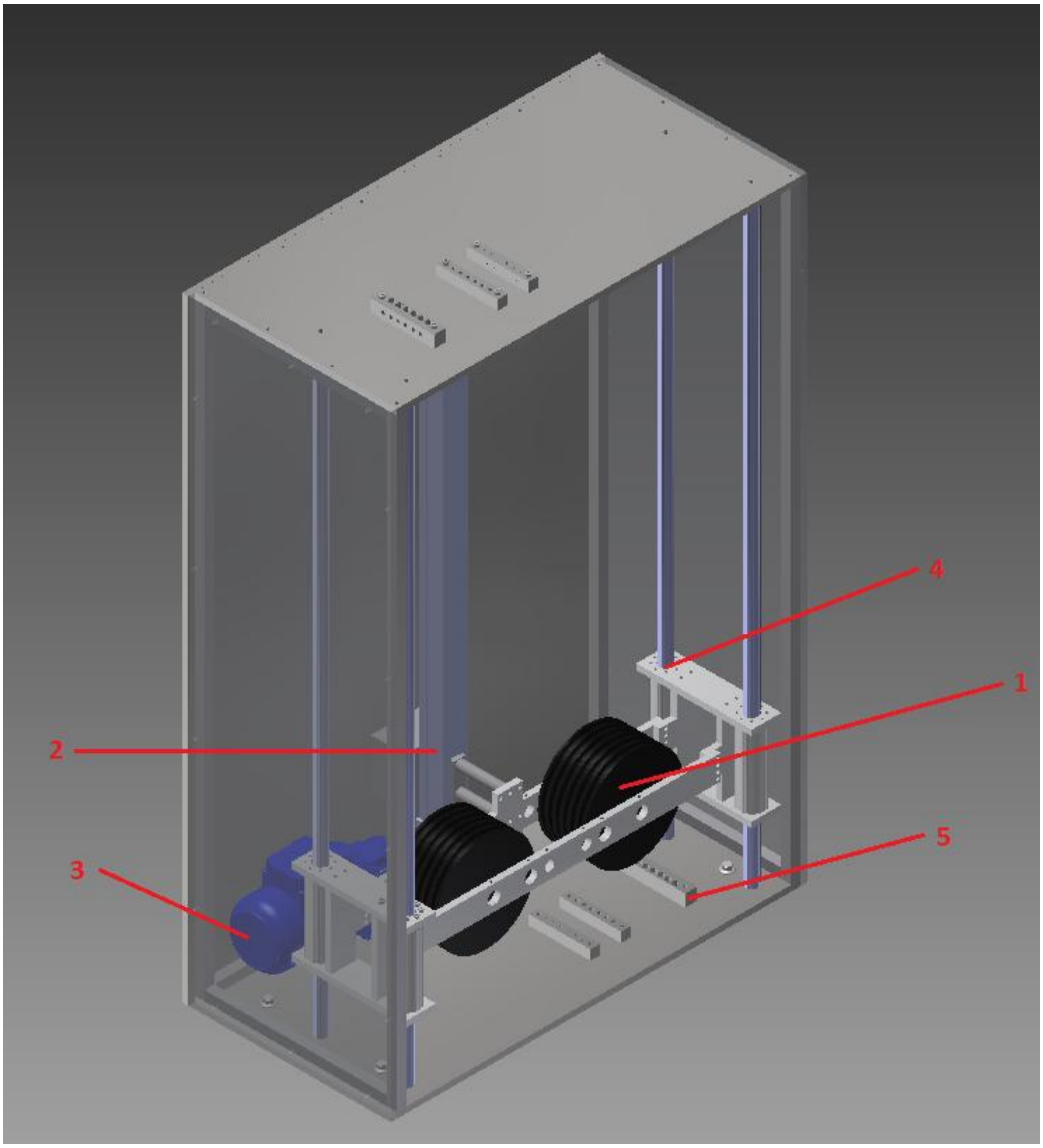

Figure 25; CAD model of pulley flex test rig

Features:

1. Pulleys surrounded by yoke that moves up and down.

2. Linear actuator to achieve up and down motion.
3. Reversing motor to power linear actuator.
4. Poles/ linear bearings to ensure smooth sliding motion.
5. Clamps to constrain samples in place on rigs floor and roof.

To reduce the load on the motor, the design of the pulley and yoke system needed to be lightweight. However, it also needed to be robust in order to withstand repeated loading itself. The material used for the yoke was aluminium due to its low density. The pulleys are made from an industrial PVC material in order to keep them lightweight with low friction so that they are not destructive when coming in to contact with a cable. The poles and pulley axles are made from hardened outer steel to ensure they are resistant to wear.

Magnetic switches are used to trigger the reversal of the motor. These reversals are then counted to record the number of cycles that the cable has endured.

Figure 26 is a picture of the pulley flex test rig once built.

Figure 26; Pulley flex test rig

8.0 Single strand conductor flex life

This stage of the project had two main targets which were to test initial flex life models and to determine the material impact on flex life.

The conductor materials considered at this stage of the project are as follows:

- A1 copper - a low grade of copper regularly used in cable designs.
- C1 copper - another low grade of copper regularly used in cable designs.
- Beryllium copper (CuBe) - a high grade believed to be a top performing product for flex life.
- Silver plated copper alloy (SCA) - a high grade believed to perform well for flex life but not as well as CuBe.

8.1 Strain in Single Strand Conductor

The strain in a single strand conductor, when subjected to a bend, can be calculated using elastic bending theory (equation 3). This theory is then modified to generate an equation more specific to the application.

$$\frac{M}{I} = \frac{E}{R} = \frac{\sigma}{y}$$

$$\frac{E}{R_{bend}} = \frac{\sigma}{R_{strand}}$$

$$\frac{\sigma}{E} = \frac{R_{strand}}{R_{bend}}$$

$$\varepsilon = \frac{R_{strand}}{R_{bend}} \tag{27}$$

It is important to note that the bend radius is taken as the radius through the central axis of the strand. This concept is illustrated by figure 27.

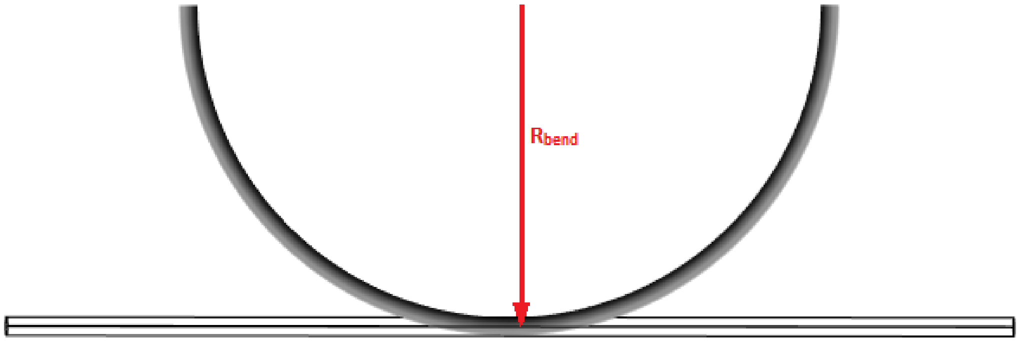

Figure 27; R_{bend} taken from strand central axis

This relationship can also be calculated from basic mathematics: For a strand of length L, when in bend position around a bend radius of R_{bend}, the length of the strand's central axis=L;

$$L = \pi R_{bend} \tag{28}$$

The length of the outer surface of strand can be found by:

$$L_{outer} = \pi(R_{bend} + R_{strand}) \tag{29}$$

The strain induced by the bend can be found using equation 1:

$$\varepsilon = \frac{\Delta L}{L}$$

$$\varepsilon = \frac{L_{outer} - L}{L}$$

$$\varepsilon = \frac{\pi(R_{bend} + R_{strand}) - \pi R_{bend}}{\pi R_{bend}}$$

$$\varepsilon = \frac{R_{bend} + R_{strand} - R_{bend}}{R_{bend}}$$

$$\varepsilon = \frac{R_{strand}}{R_{bend}}$$

8.2 Test procedure

The test machine used for flex life testing single strand conductors was the conductor rolling flex rig (figure 23). Each conductor was connected to a counter and once a wire broke, the counter stopped counting. Figure 28 illustrates this concept. The machine could hold and count up to six wire samples at a time. This allowed a good average to be obtained as well as observing the scatter of results that flex life experiments by this method produce.

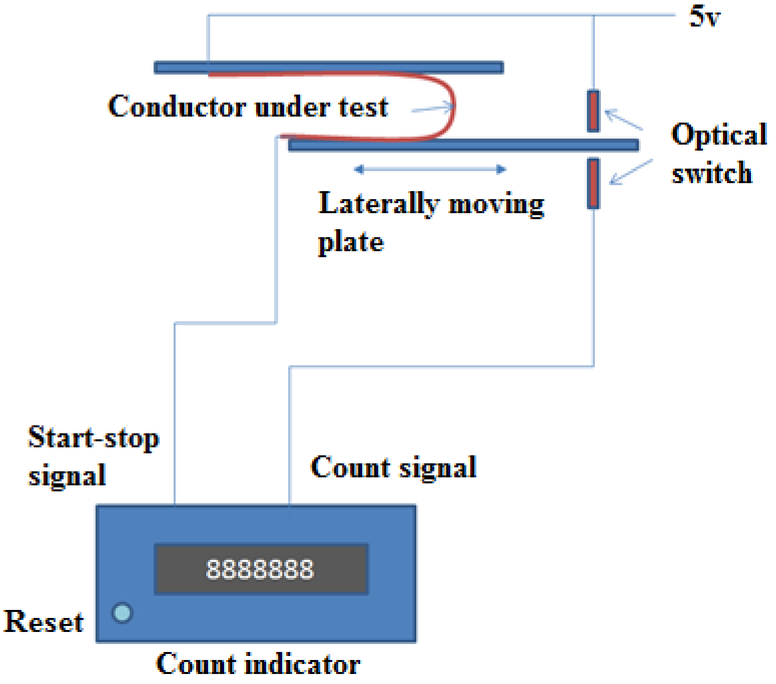

Figure 28; Schematic to illustrate counting mechanism

8.3 Results and discussion

The strain induced from the bend was determined using equation 27 detailed in section 8.1. Once this strain is determined, it is used to make a flex life prediction using one of the fatigue prediction methods detailed in section 4.

The prediction methods investigated for this stage are the method of universal curves and the four point method(s).

Figure 29 shows the results obtained for CuBe compared with the two prediction methods.

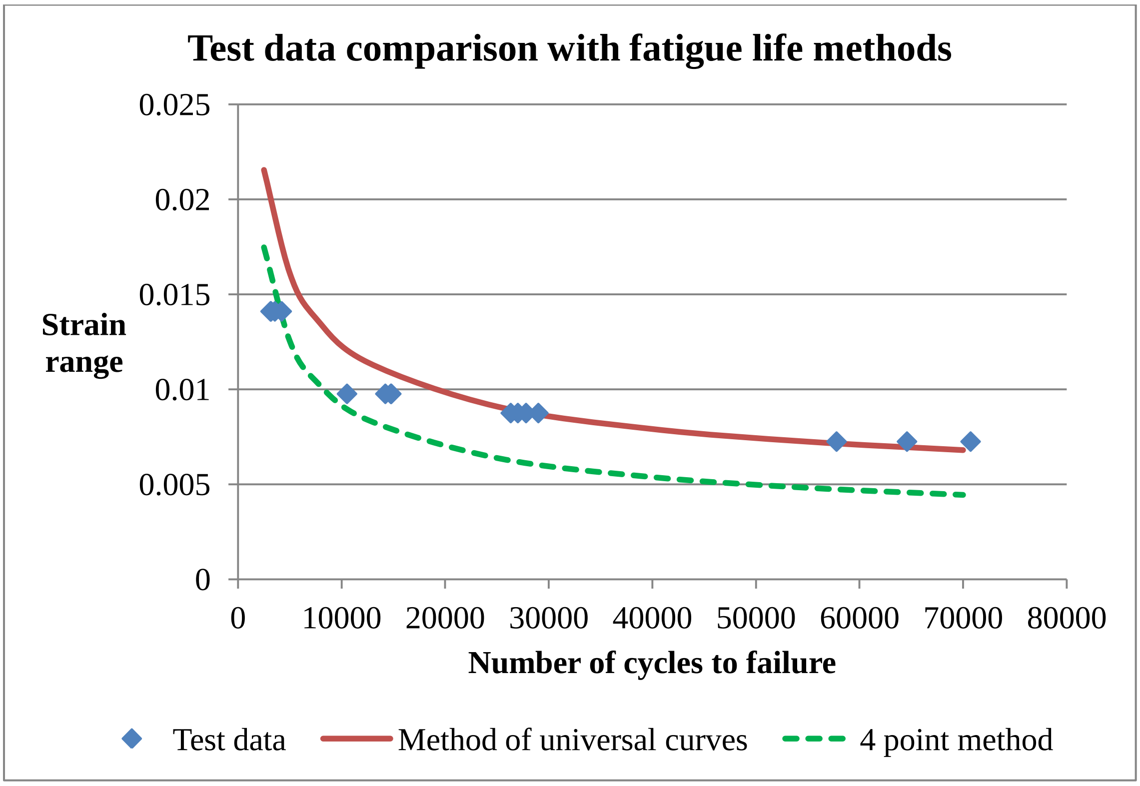

Figure 29; Comparison of universal curves method and 4-point method with test data

It can be concluded from this that the method of universal curves gives a more accurate representation than the four point method, it was therefore decided that the method of universal curves will be the base for any flex life predictions made.

It can be seen, however, that the prediction line deviates from the results in the low cycle region, this is because the two exponents (-0.6 and -0.12) are fixed. When looking at the Coffin-Manson fatigue equation, we can see that these exponents are material specific. Therefore -0.6 and -0.12 may not be suitable for all metals (although a good starting point). It was therefore decided that in order to get a more accurate prediction the exponents could be curve fitted, or derived from the test data. Figure 30 shows this more accurate prediction line which fits most of the points more accurately.

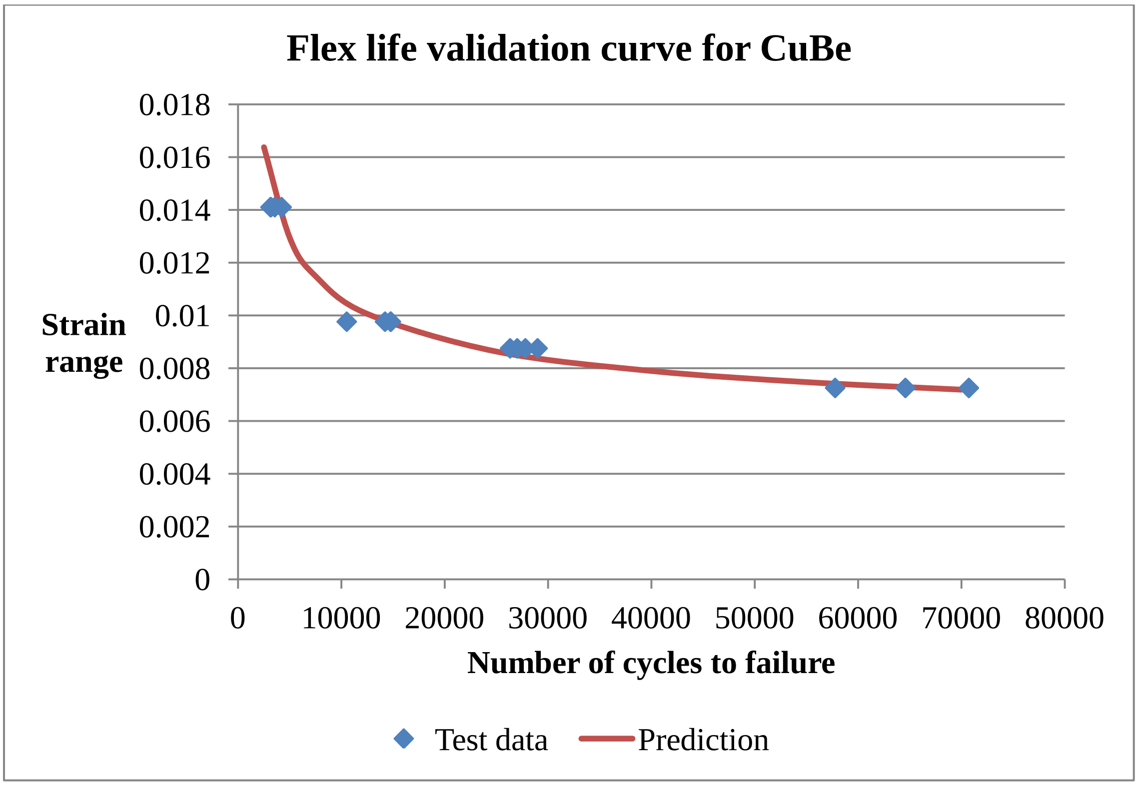

Figure 30; Flex life validation curve for CuBe

The material data used for CuBe is as follows:

E = 127500 MPa [Fisk, 2013]

UTS = 675 MPa

$\varepsilon_f = 2.11$

b = -0.095

c = -0.69

E can be found from data sheets, exponents b and c are curve fitted, UTS and ε_f are characterised from a tensile test. Characterising the material properties UTS and ε_f is discussed in sections 3 and 9.

The flex life model is amended accordingly:

$$\Delta\varepsilon = 3.5\frac{UTS}{E}N_f^{\ b} + \varepsilon_f^{\ -c}N_f^{\ c} \tag{30}$$

Flex life curves and data for other conductor materials can be found in appendix 1.

8.4 Scatter Range

Looking at the data points, it is clear that there is a certain degree of scatter in each test. These inconsistencies could due to various reasons, some of which are explained:

Material deformities and general inconsistencies within a materials structure means there will always be a degree of inconsistency in results. This may vary between different types of materials (e.g. metals and polymers).

The repeatability of the test setup will have an impact on the consistency of results; a small change in bend radius will result in a small change in strain induced which, because of the exponential decaying nature of the fatigue curve, could then result in a significant change in number of cycles to failure.

The errors and tolerances associated with wire drawing could have a similar effect to that above as a larger strain will be induced (for the same bend radius) if the wire tolerance is near its upper limit. Similarly, a smaller strain will be induced (for the same bend radius) if the wire tolerance is near its lower limit. This will have a knock on effect on the number of cycles to failure.

There could be some residual damage done to the sample depending on the handling of the batch that the sample came from. If it has been poorly handled during production or transportation, weak areas could develop which will not be visible or determined by any analysis. This will have a detrimental effect on its mechanical performance.

Finally, errors could also be present from the accuracy of calculations and derivation of material properties. However, these types of error will be more systematic and it would be possible to account for if determined.

In order to quantify this scatter range, we must look at the highest and lowest values of each test. Table 1 presents some randomly selected data that was used to determine this range.

Table 1; Basic scatter range of experimental results

Test sample	Maximum test value	Minimum test value	% Range
1	2,050	1,518	30
2	4,886	3,830	24
3	15,612	21,000	29

The scatter range is fairly consistent throughout at around 28%. This suggests that if predictions can land within this range, they will deviate about ±14% from the mean.

9.0 Multi Strand Conductor Flex Life

This stage of the project also had two main targets. These were to further test flex life model whilst determining the impact of conductor construction on flex life.

In order to consider the construction effect on flex life performance, it is important to note the exact conductor construction and associated geometries. The five main multi strand conductor constructions are as follows:

- True concentric - wires are laid up counter directionally to successive layer with outer layers with a longer lay length. Outer strand lay length is typically 12x overall conductor diameter. This is illustrated in figure 31.

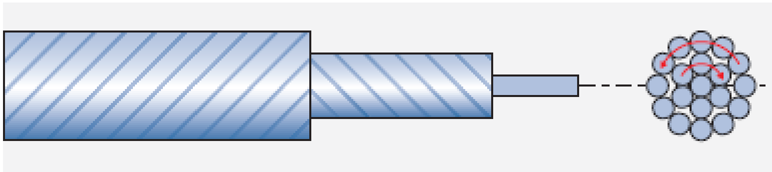

Figure 31; True concentric

- Unidirectional concentric - similar to true concentric, in that outer layer have a longer lay length but direction of lay remains the same for all layers. Outer strand lay length is typically 12x overall conductor diameter. This is illustrated in figure 32.

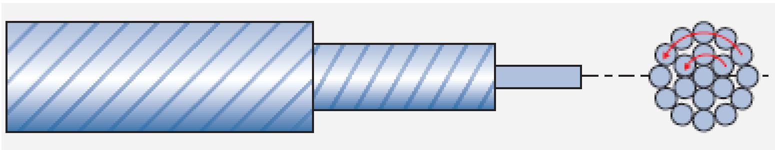

Figure 32; Unidirectional concentric

- Unilay concentric - direction of lay is the same for all layers as is lay length. Lay length is typically 10x overall conductor diameter. This is illustrated in figure 33.

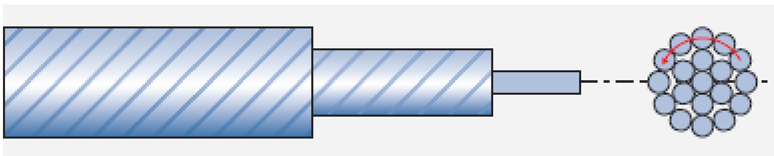

Figure 33; Unilay concentric

- Ropelay - composed of groups of the above conductor construction making up a 'rope'. Outer group lay length is typically 12x overall conductor diameter. This is illustrated in figure 34.

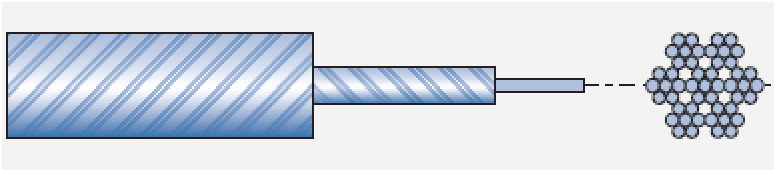

Figure 34; Ropelay

- Bunch - unidirectional configuration with random positioning of strands and random lay length. With this being the case, it is unlikely that a bunch construction would be used in designs for a high flex application. However if it was then the worst case scenario would have to be modelled.

9.1 Strain in Multi Strand Conductor

Research paper Bending of Helically Twisted Cables by Papailiou (1995), suggests the strain induced by bending in a multi stand cable is dependent on the outer dimensions of the element, however, initial flex life tests quickly show that this does not appear to be the case. Equation 31 summarises this approach.

$$\sigma = E\frac{1}{R_{bend}}\frac{d_L}{2}\sin\varphi\cos^2\beta \qquad (31)$$

In equation 31, $d_L/2$ is the distance from the centre to outer strand. However, actual flex life results for multi stranded conductors are not far off what the individual single strand flex life results would produce and this equation would yield significant differences in strain and therefore flex life. Therefore the basis of the strain calculation will be based on individual strand size. However, the strain induced is still a function of lay angle (dictated by lay length) and distance from the conductor and cable central axis. This is because the individual strands central axis is offset from the conductor central axis. Also, since the position angle ϕ would be 90 (outer strand), the term sin ϕ can be simplified to 1. The following equation is proposed:

$$\varepsilon = \frac{R_{strand}}{R_{bend} - d}\cos^2\beta_1 \qquad (32)$$

Where d represents the distance from the conductor central axis and β represents the resulting lay angle.

When considering this construction in a cable bundle or for a ropelay construction there will be a second angle of lay on the element. Further parameters are introduced to include this:

$$\varepsilon = \frac{R_{strand}}{R_{bend} - (d_1 + d_2)} \cos^2 \beta_1 \cos^2 \beta_2 \tag{33}$$

These further parameters can be introduced every time there is an additional lay and distance on the element (e.g. in the case of a twisted pair). Within a bundle, an individual conductor strand (within a cable) could have up to 4 angles of lay and distances. This would generate the equation:

$$\varepsilon = \frac{R_{strand}}{R_{bend} - (d_1 + d_2 + d_3 + d_4)} \cos^2 \beta_1 \cos^2 \beta_2 \cos^2 \beta_3 \cos^2 \beta_4 \tag{34}$$

Where subscripts denote the following:

1. Primary - required in all multi stranded conductors.
2. Secondary - only required for ropelay construction.
3. Twisted bundle - only required if conductor makes up part of a twisted pair or bundle.
4. Element - defining element position within cable.

9.2 Test Procedure

Both the rolling flex life test rig and the pulley flex test rig were used for testing in this stage of the project. For bare conductor samples, failure is taken to be when it is visible that strands are broken. At this stage of failure, a DC resistance increase would not be detected so it is a relatively early point of failure.

True concentric, unilay concentric and ropelay constructions of A1 and C1 copper were tested.

9.3 Results and Discussion

The strain induced from the bend was determined using equation 28 detailed in section 8.1.

Figure 35 shows the graph of strain range against number of cycles to failure for multi stranded constructions of A1 copper.

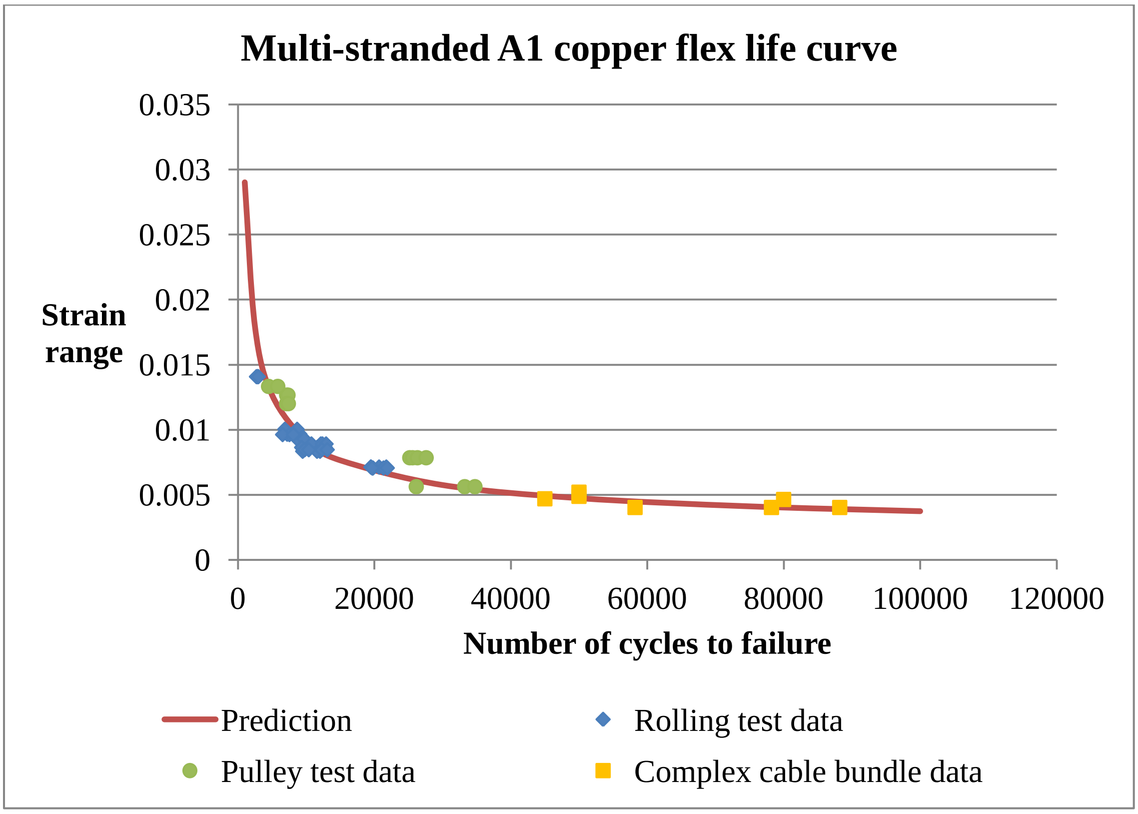

Figure 35; Multi strand validation curve for A1 copper

The diamond shaped markers represent data obtained from the rolling flex test, the circular markers represent data from the pulley flex test and the square markers represent data which is also obtained from the pulley flex test, however the sample was in the form of a cable bundle (discussed in more detail in chapter 15).

The data points fit the flex life curve well so we can be confident that the construction effect of the conductor is captured well by the strain calculation. Since the strain range is plotted and a good comparison is observed, it is apparent that mean stress/strain effects do not need to be considered as part of the strain calculation for these metals. The strain range is a sufficient estimator of flex life for both single (R=0) and reversed bending (R=-1).

Notably, cable bundle data fits the flex life curve as well as bare conductor data. This is the ultimate aim of the tool - to model elements within a cable.

Again, there is scatter on the data points, of similar magnitude to that discussed in the single strand section.

A point of note that was observed while using the pulley flex test method is that in some instances there was some torsion on the sample. This could be for a few reasons; the sample could have been clamped with a slight twist along its length which would cause this torsion. Also, the sample had been previously wound round a reel, and its natural shape is slightly curved meaning that when ‘relaxed’ the sample will try to assume this position and therefore twist.

It was therefore important to observe if and when this was apparent as it would have an impact on results. The method used to do this was to simply mark a point on the sample that was exerted to the full double bend. It was then possible to see if the sample twisted judging by the position of this mark.

The graph for C1 copper can be found in appendix 1.

10.0 Temperature regime

The flex life model in place considers material properties and stress-strain curves. The idea behind this stage of the project is to characterise these properties and curves at different temperatures, allowing temperature dependencies to be introduced in to calculations.

This is done by tensile testing to characterise the material when the sample is enclosed in a temperature chamber. The equipment pictured in figure 36 was used to do this.

Figure 36; Tensile machine and temperature chamber used to characterise materials

Carrying out these tests at a range of temperatures allows temperature dependant material parameters to be generated. Using these temperature dependant material parameters or curves in calculations and models means that flex life predictions at different temperatures can be made.

10.1 Metal properties at temperature

In order to perform a fatigue prediction calculation for metals, we need to know certain material properties. Therefore in order to make this fatigue life prediction at temperature, a temperature corrected material property must be used. For metals, considering the flex life model used and validated in section 8.3, the following properties are required:

- Young's Modulus
- UTS
- Ductility coefficient

10.2 Young's Modulus at temperature

The graph in figure 37 below shows how the Young's modulus of a metal changes with temperature. Accurately determining Young's modulus by tensile testing wires can be difficult so supplier data or data from research needs to be used in this instance.

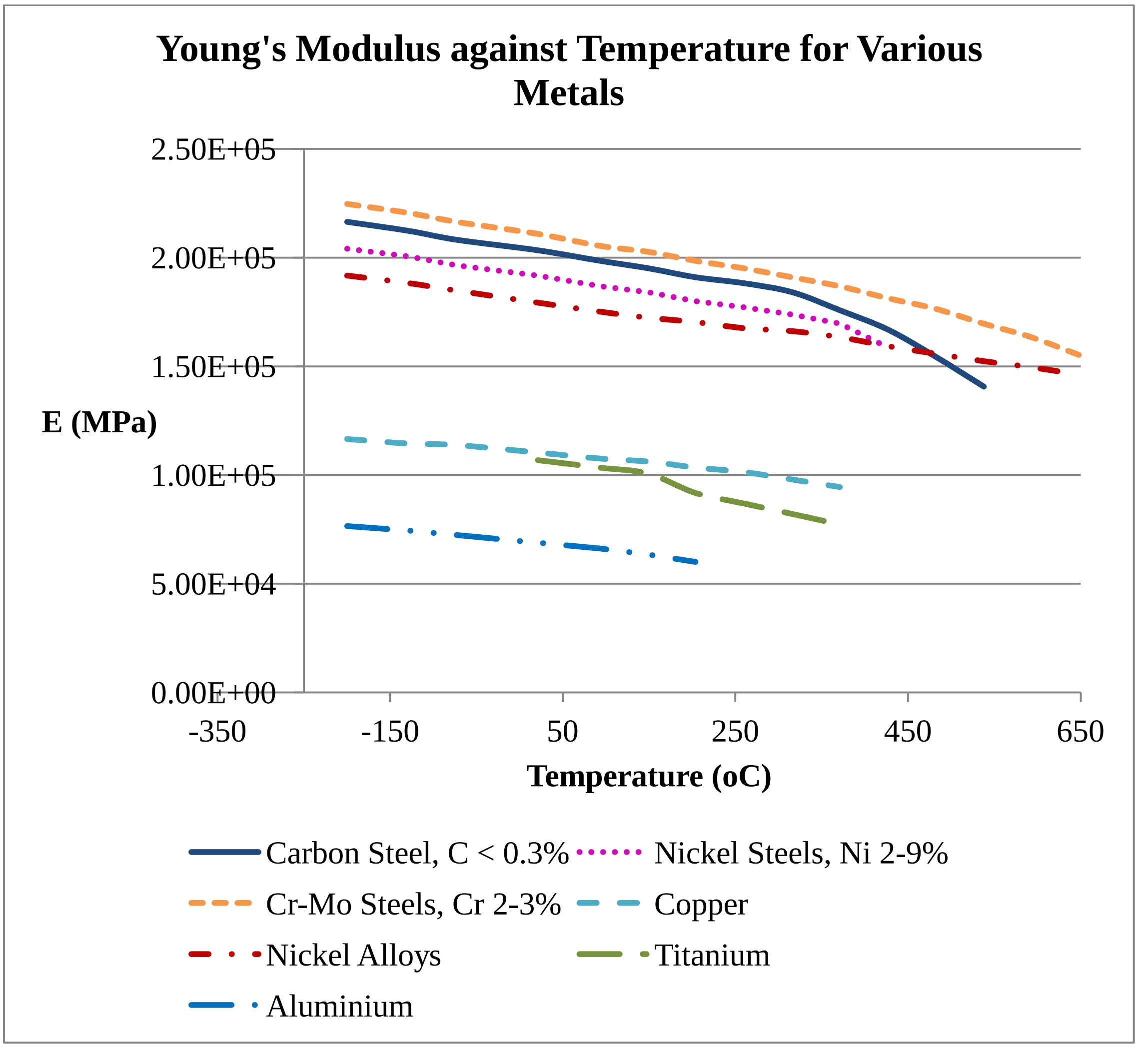

Figure 37; Change in Young's modulus with temperature

The data used to compile the graph in figure 37 is taken from an online source referenced to ASME, 1995. It can be seen that this change can be approximated linearly over a relatively small temperature range, up to a certain value.

In this project, the main metal families of interest are steel, copper and aluminium as these are the more common cable conductor materials. Taking data from the graph and plotting in excel to get a correlation of this property with temperature gives the graph shown in figure. Since the temperature range chosen to do this over is much smaller than that in figure 37, it is safe to assume a linear relationship.

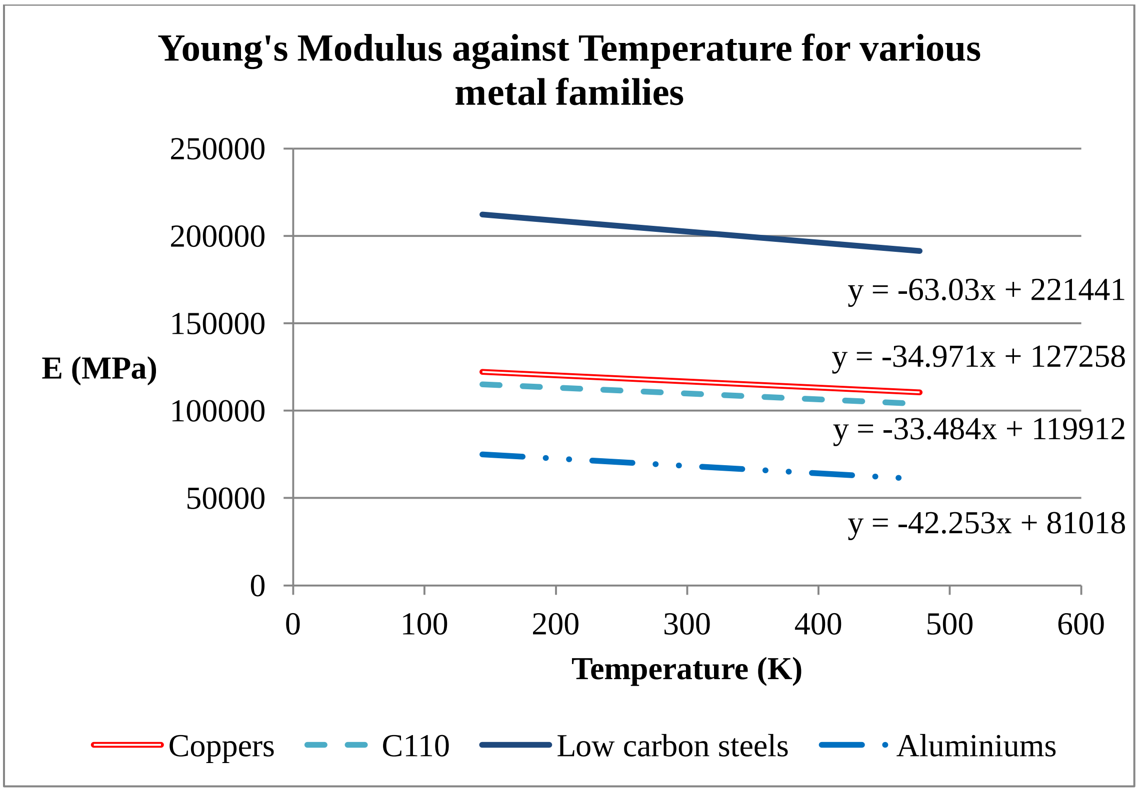

Figure 38; Young's modulus against temperature linear approximations for low carbon steels, coppers and aluminiums

The equations are displayed on the graph against their respective curves. We can see from the equations the change in E with each degree. This is summarised in the table below:

Table 2; Summary of change in E at temperature

Metal Family	Change in E (MPa/ ^{o}C)
Low carbon steels	-63
Coppers	-35
Aluminiums	-42

It is important to compare and calibrate these values to supplier datasheet values for the specific the conductor metal (at room temperature). Calibrating to supplier values is acceptable here because looking at the graphs, the linear approximations are all quite similar (i.e. their general behaviour is the same, but with different initial values) and the specific grade of metal within the metal family will be even more so.

10.3 UTS at Temperature

In order to obtain temperature dependant UTS values, tensile tests were carried out at different temperatures and changes noted. These tests were conducted on the Lloyd tensile machine with temperature chamber that is pictured in figure 36. The UTS of a metal can be found using equation 11 (from chapter 3):

$$UTS = \frac{F_{\max}}{A_{initial}} \tag{11}$$

The graph of UTS against temperature for CuBe is shown below in figure 39.

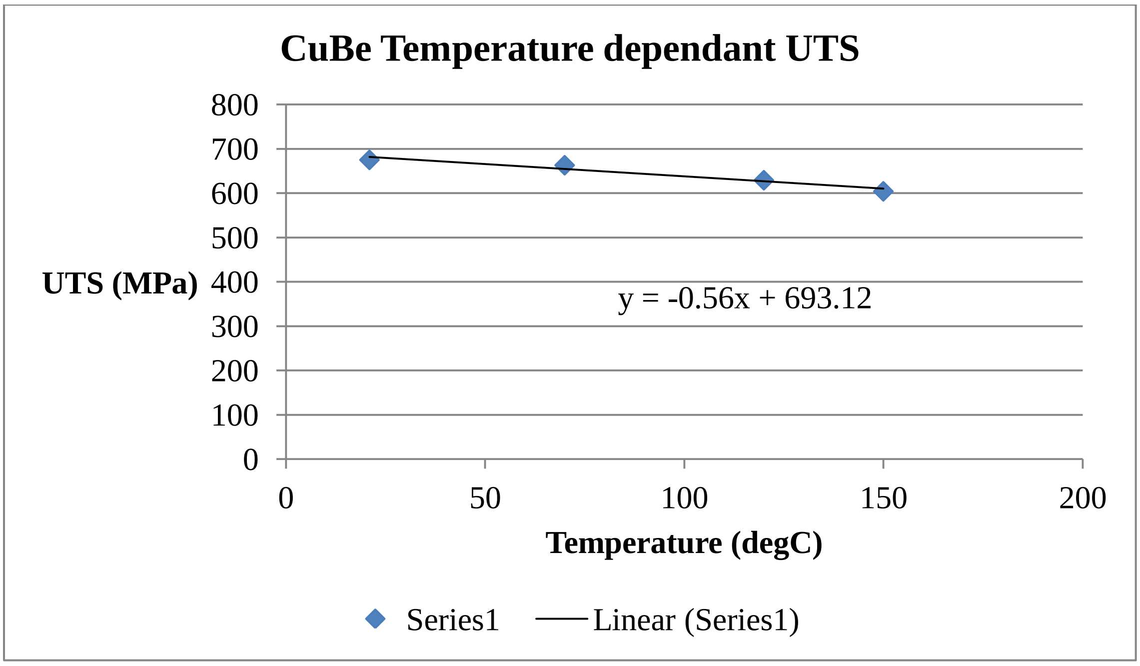

Figure 39; UTS against temperature for CuBe

It can be seen that this property changes by -0.56 MPa per degree Celsius.

10.4 Ductility at Temperature

The samples from the set of tensile tests conducted were kept and used to determine the metals ductility change with temperature. Ductility is calculated in the following manner:

$$\varepsilon_f = \frac{1}{1-RA} \tag{35}$$

Using an optical measuring microscope, RA measurements were taken on the samples and the corresponding ε_f values calculated. Graphs of ε_f against temperature were then plotted to characterise the change as shown in figure 40.

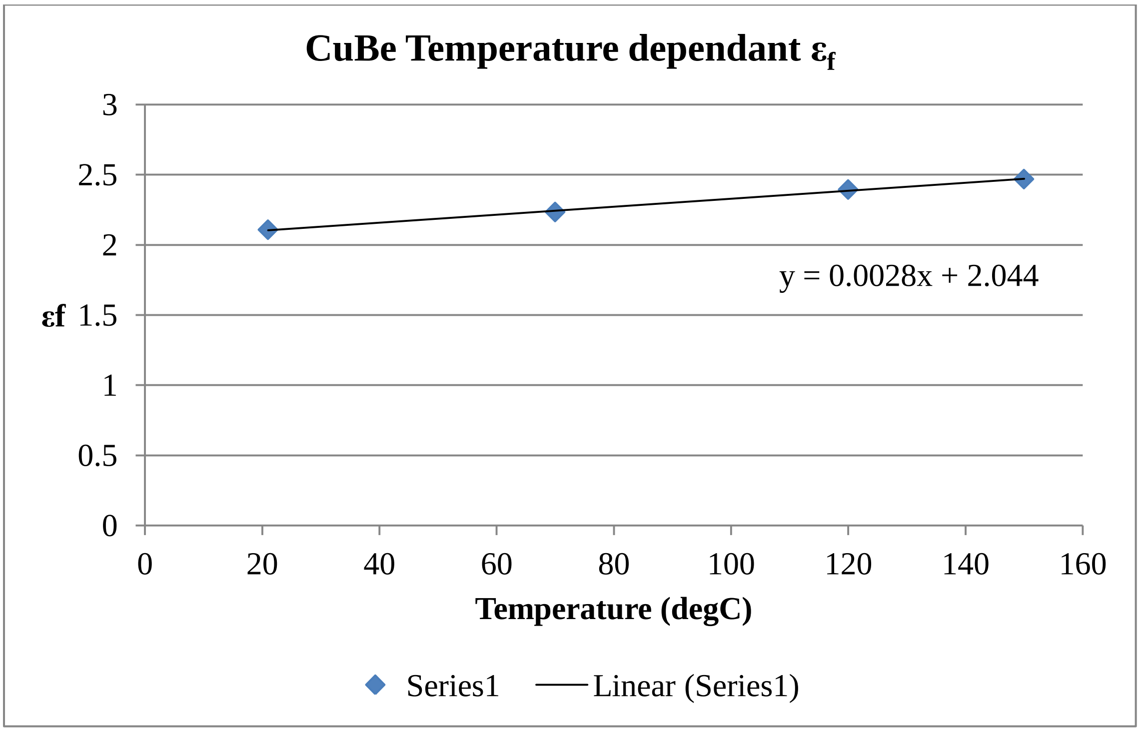

Figure 40; Ductility against temperature for CuBe

From this graph, it can be seen that the change in ductility for CuBe is about 0.0028 per degree Celsius.

These temperature dependant material properties were then used to generate and flex life tests for CuBe were carried out at -20°C. The flex life curve was then plotted and compared with data as shown in figure 41.

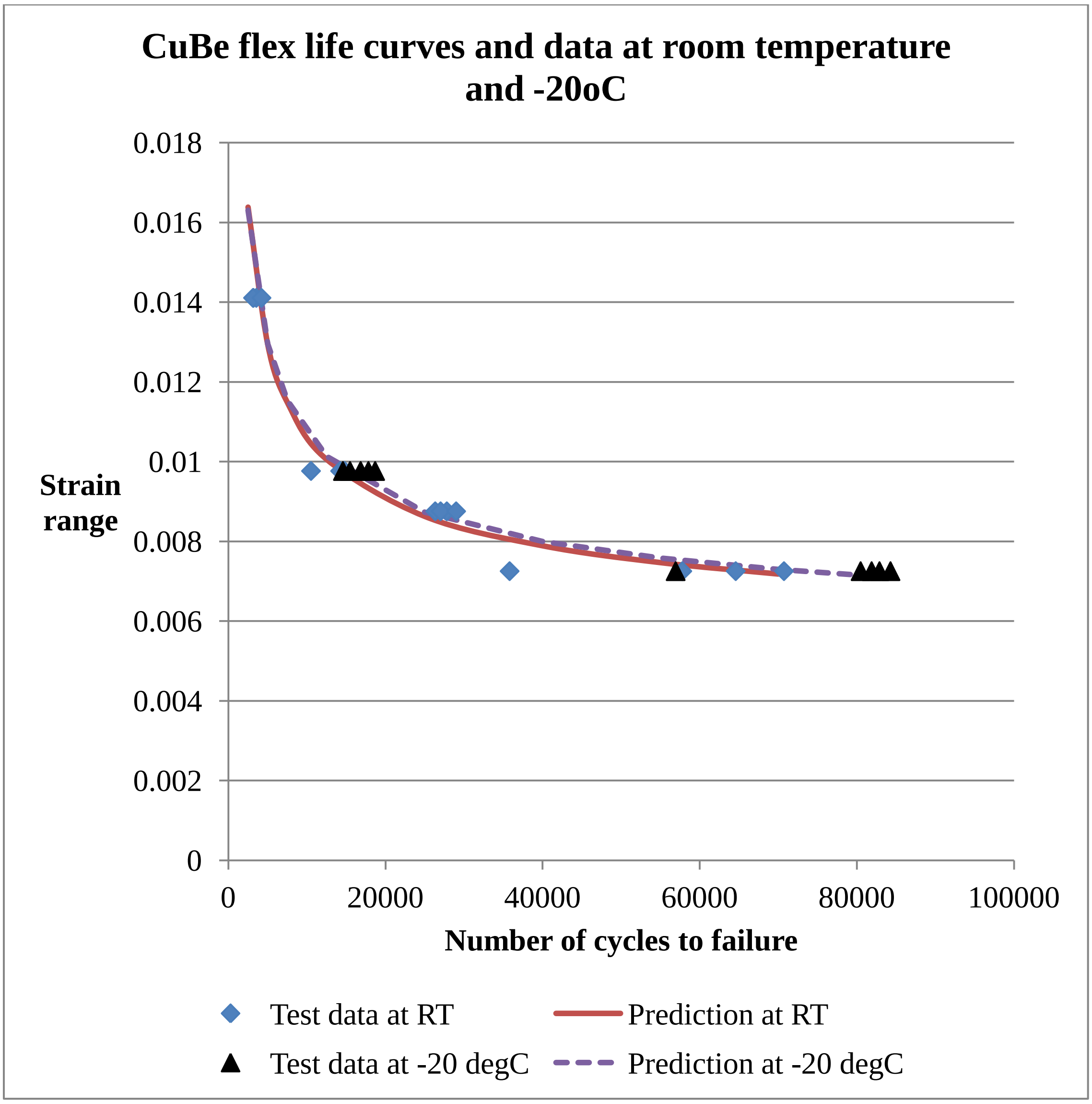

Figure 41; Flex life curves and data at -20°C for CuBe

As can be seen the curves and data are very close together so it could be hard to differentiate between them and the effect of temperature may be offset by other errors. However there is a correlation and this capability can be introduced to predictions.

Generating temperature dependant flex life predictions in this manner does mean that an assumption is being made that the fatigue exponents are independent of temperature. This assumption is backed up by research from Kohout who states that the slope of the fatigue curve at different temperatures is approximately constant on a log-log graph.

11.0 Insulation flex life

This stage of the project was carried out to determine how insulation materials perform under repeated bending. In general, polymer plastics are more resistant to fatigue failure than metals. However, there are some factors that could have a significant influence on the overall flex life of the component.

- The point of highest strain in a cable is likely to be in the insulation, as this is often the furthest away point from the cable's central axis.
- The cable's metal part is made up of smaller individual strands with a relatively small diameter, which reduces the strain in the metals.
- Polymer behaviour is dependent on temperature.
- Polymer behaviour is dependent on time.

Some cable applications can be over a range of temperatures and thermal cycling can also take place. Therefore it is of high importance to have a temperature model for insulations.

Plastics have a time dependency to their behaviour, however customers to the cable industry cannot always define times, rates and frequencies so any work done in this area would be good to know but not necessarily useful in terms of a final product. In addition, research from DuPont (2000, P22) suggests that in polymer fatigue, frequency of loading below 1800 cpm does not have an explicit effect on number of cycles to failure. It was therefore decided not to consider the polymer materials time dependence. In order to keep results and measurements consistent, tensile testing is carried out in line with DEF STAN 61-12 part 31. Specifically, a gauge length of 20 mm and an elongation rate of 50 mm/minute will be used. This standard is generally used when characterising cable sheath materials [Ministry of Defence, 2006].

11.1 Strain in Insulation

Since the insulation in a cable is effectively a jacket around a conductor or series of conductors making up a central core, the calculation to determine the maximum strain in the outer insulation is the same as that for a single strand conductor. This is because an assumption is applied; that the central core is solid and the insulation jacket surrounding it will act as an addition to this. Therefore, when calculating the strain in the outer insulation, the element can be considered as one piece. Equation 27 is modified to determine the maximum strain in the insulation in an insulated wire or cable.

$$\varepsilon = \frac{R_{insulation}}{R_{bend}} \tag{36}$$

If it is desired to calculate the strain in the insulation of a coiled wire, the same techniques to calculate strain in multi stranded conductors can be implemented. As the insulation can only have 2 angles of lay and distances from central axis, only subscripts 3 and 4 apply (twisted bundle and element position respectively - these values will be the same as for the conductor it surrounds).

$$\varepsilon = \frac{R_{insulation}}{R_{bend} - (d_3 + d_4)} \cos^2 \beta_3 \cos^2 \beta_4 \tag{37}$$

11.1 Polymer Material Models

It is understood that polymers have much more complex stress-strain behaviour than metals.

In order to generate realistic stress strain curves for insulation polymer materials, extruded filler samples of insulation materials were taken and tensile tested in a Lloyd tensile machine. Stress-strain curves, in the form of high order polynomials, were then fitted to the raw tensile data to create a stress-strain model.

This is done and presented in figure 42 for a grade of FEP.

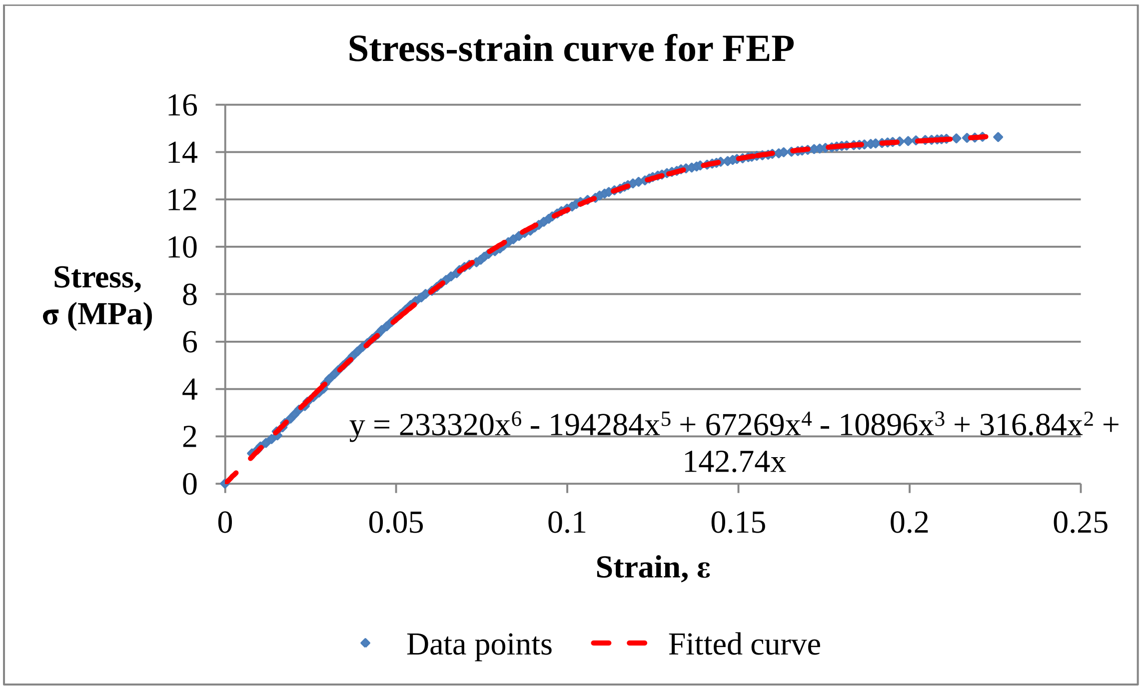

Figure 42; Stress-strain curve and model for FEP at room temperature

It can be seen from the graph that the stress induced by the strain for this grade of FEP at room temperature can be given by the following relationship:

$$\sigma = 233320\varepsilon^6 - 194284\varepsilon^5 + 67269\varepsilon^4 - 1089\varepsilon^3 + 316.84\varepsilon^2 + 142.74\varepsilon$$

11.2 Polymer Fatigue Curve

In general, polymer fatigue curves are more complex than that of a metal fatigue curve. While they both exhibit ductile and brittle failure regions, the transition between them in metals is usually a lot smoother and often less of an issue. Figure 43 is a representation of the type of curve a complex polymer could exhibit. It has been annotated to highlight its key features.

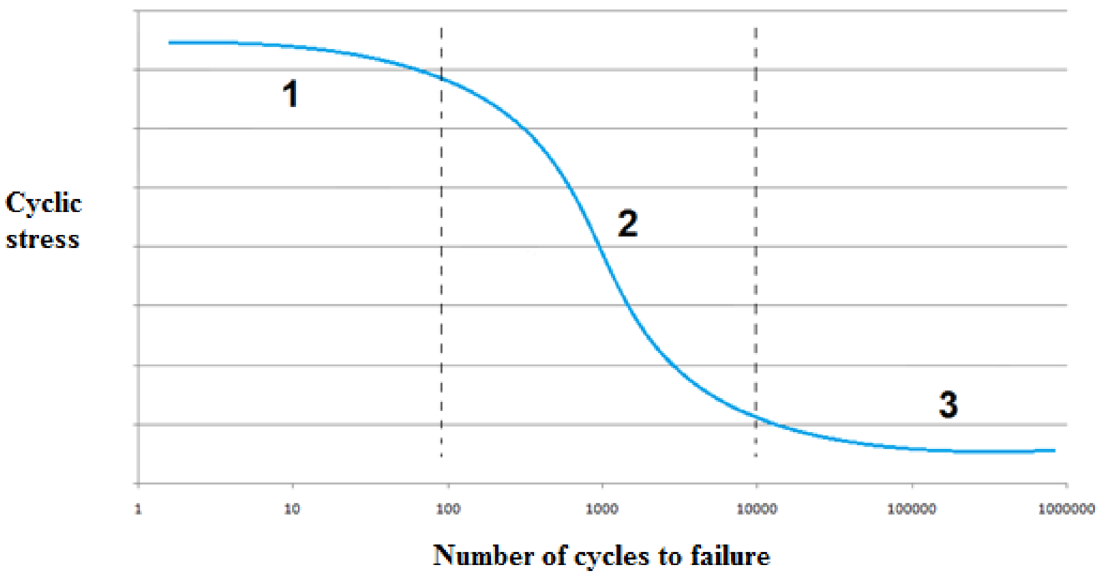

Figure 43; Polymer fatigue curve and regions

The key features to this curve are listed:

1. Ductile failure region - the region where the material is taken beyond yield and the polymer is susceptible to ductile fatigue.
2. Ductile-brittle transition region - the steep slope where the polymer undergoes a transition from ductile to brittle working.
3. Brittle failure region - when the polymer is flexing in its elastic region and failure will be brittle failure.

[Smithers Rapra, 2012a]

Unlike for metals, there are not any well developed models or templates that can be used to characterise polymer fatigue curves. The only genuine way is to collect enough data points to do so. This would be extremely time consuming and inappropriate for a short term project.

In most dynamic cable applications, if the insulation was to fail in the ductile or ductile-brittle region, it would be considered either poor material selection or poor customer specifications. Therefore, it was decided that this project will only consider the brittle failure region. This will allow for some known material parameters to be used in addition to data points to help characterise the brittle failure region of the fatigue curve.

Since only the brittle failure region is being considered, it is important to highlight that the prediction method would not be appropriate for anything other than brittle fatigue failure, i.e. for stresses below yield.

11.3 Test Procedure

Both the rolling flex test rig and, where possible, the pulley flex test rig were used to carry out flex life tests for insulations. In some cases, however, the pulley flex test could not be used due to the torsional aspect that was occasionally apparent when testing bare conductor. These polymer materials seemed to be much more sensitive to this effect. This produced too many invalid results, wasting material and time.

The sample forms that were used for flex testing were:

- Extruded filler samples.
- Extruded filler over Kevlar.

Materials for testing are as follows:

- FEP grade 1
- FEP grade 2
- ETFE
- PTFE

It was deemed important to test extruded samples because for the materials chosen, this is the process used to create a jacket or to insulate a wire.

11.4 Results and Discussion

Flex tests were carried out on the grade of FEP on both the rolling flex rig and the pulley flex rig. The maximum stress induced by the repeated bend was calculated by the polymer material model for FEP as detailed in section 11.1. The flex life results obtained were plotted and are displayed in figure 44.

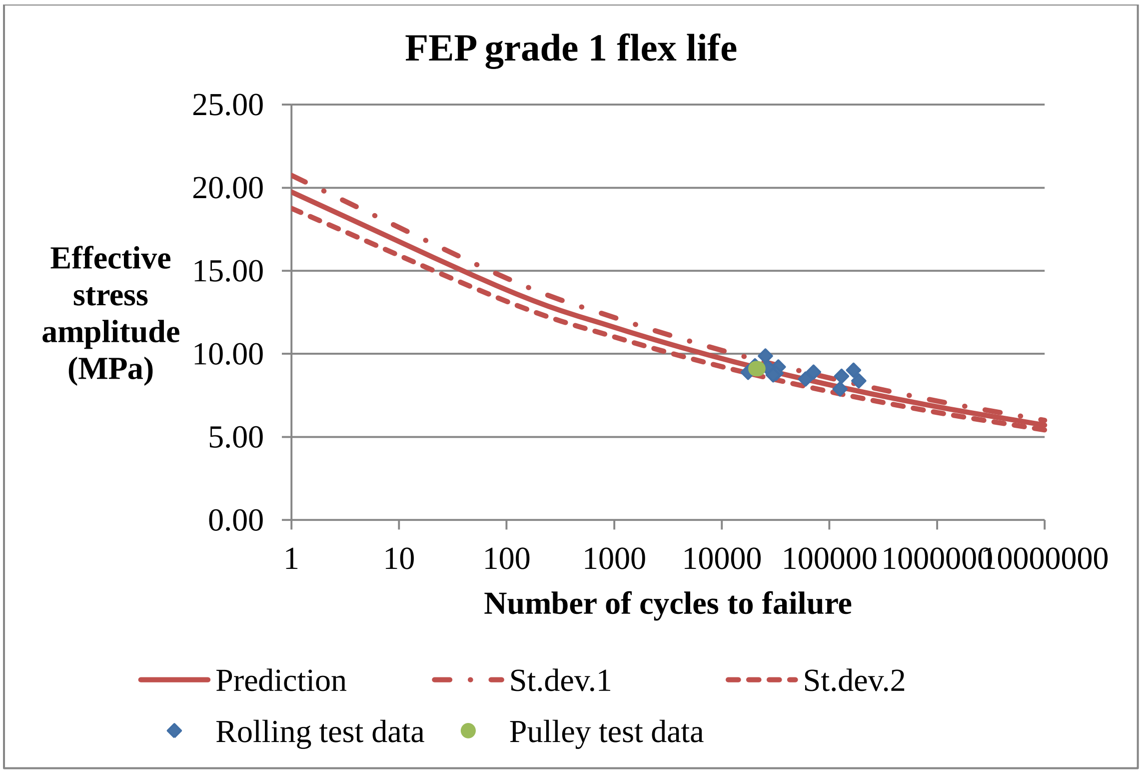

Figure 44; FEP grade 1 flex life curve and validation

Using equation 22 (from section 4.7), with a value of -0.077 for the fatigue exponent, the data fits the line well. The different shaped points in the graph denote different test methods. The diamond shaped points are data collected from the rolling flex test (R=0), and the circular points are data collected from the pulley flex test (R=-1).

From this data and graph, it is apparent that mean stress effects (as plotted) need to be accounted for and this effective stress is determined by use of the SWT mean stress model as discussed in section 2.3.

As can be seen there is significant scatter on the data points. Upper and lower prediction lines based on deviations in UTS have been introduced in order to justify this scatter. If working to a worst case scenario, the lower prediction line should be used.

There are a number of reasons for this scatter. One explanation is that because of the polymers fibrous nature, deformities causing initial cracks are irregular. Therefore the stress that induces the crack may not always be the true maximum stress on the outer surface of the material. However, this phenomenon cannot be accounted for so just has to be worked around.

The heating of the motor powering the equipment could affect consistency of results as the temperature of the air surrounding the sample may not be constant. In particular, polymers are a lot more sensitive to such temperature changes than metals.

In addition, other factors such as material inconsistencies, batch handling, test setup and sample production tolerances will also have an impact on reliability of results as discussed in section 8.4.

Results and prediction plots for the other materials specified can be found in the appendix 2.

11.5 PTFE

The PTFE filler of diameter 1.55 mm was flex tested around an extremely tight bend radius of 5.225 mm (6 mm plate separation, much tighter bend than a wire is likely to see in service). This induced a cyclic strain of 0.1483, a maximum stress of 13.34 MPa and an effective stress of 9.44 MPa.

All samples tested lasted over 810,000 cycles at which point testing was stopped in order to free up the test machine. An endurance limit was assumed at this effective stress (9.44 MPa). The UTS of the PTFE is 29.7 MPa at room temperature. This would mean an endurance ratio (σ_{ar}/UTS) of 0.32.

12.0 Polymers at Temperature

As can be determined from the model being used (equation 22), it is the ratio of stress to UTS that determines the flex life performance of the material.

Tensile stress-strain data was collected and material models were generated for the insulation samples. Stress strain graphs at different temperatures for FEP grade 2 can be seen in figure 45.

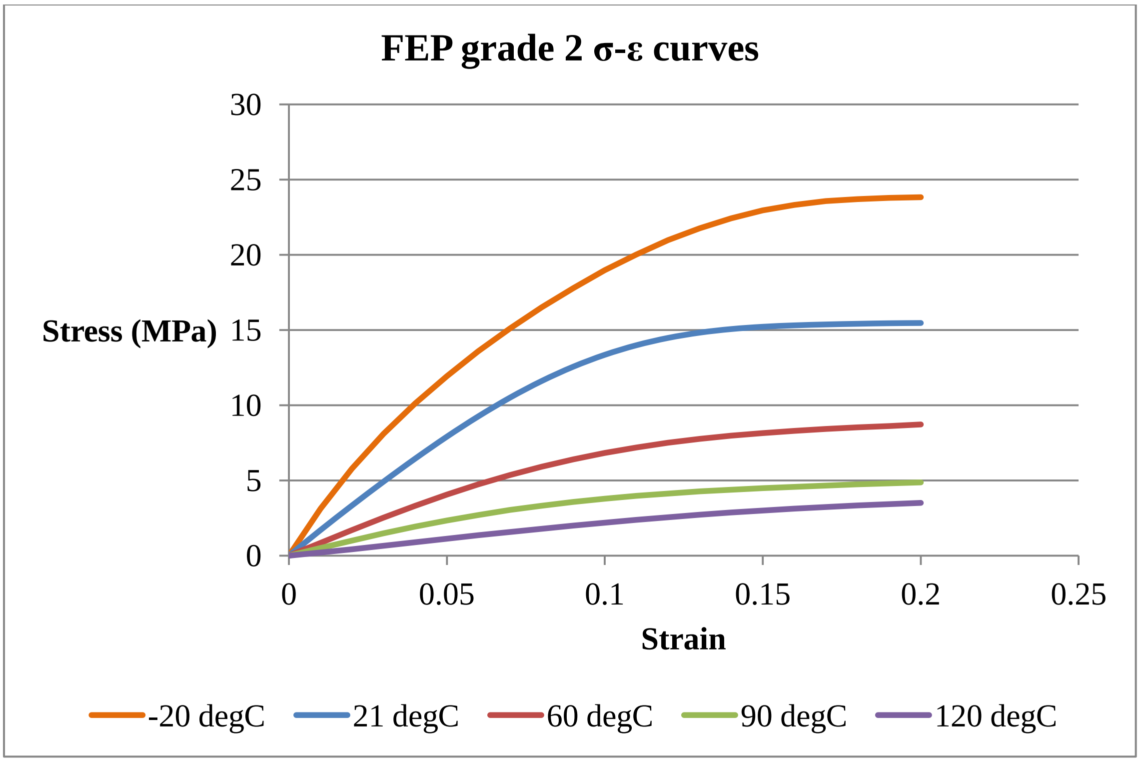

Figure 45; FEP grade 2 stress-strain curves

Flex life tests were then carried out on appropriate samples of FEP in a freezer at -20^{o}C. In order to then validate the model at -20^{o}C, the results needed to be compared with the materials stress-strain curve at -20^{o}C.

12.1 Results and Discussion

A problem when conducting low temperature tensile tests was that significant slip occurred. This could be to do with the low temperature affecting clamp performance or the increased stiffness of the material, making the sample more prone to slip.

Typical low temperature stress-strain results for FEP grade 2 at -20^{o}C are displayed in figure 46.

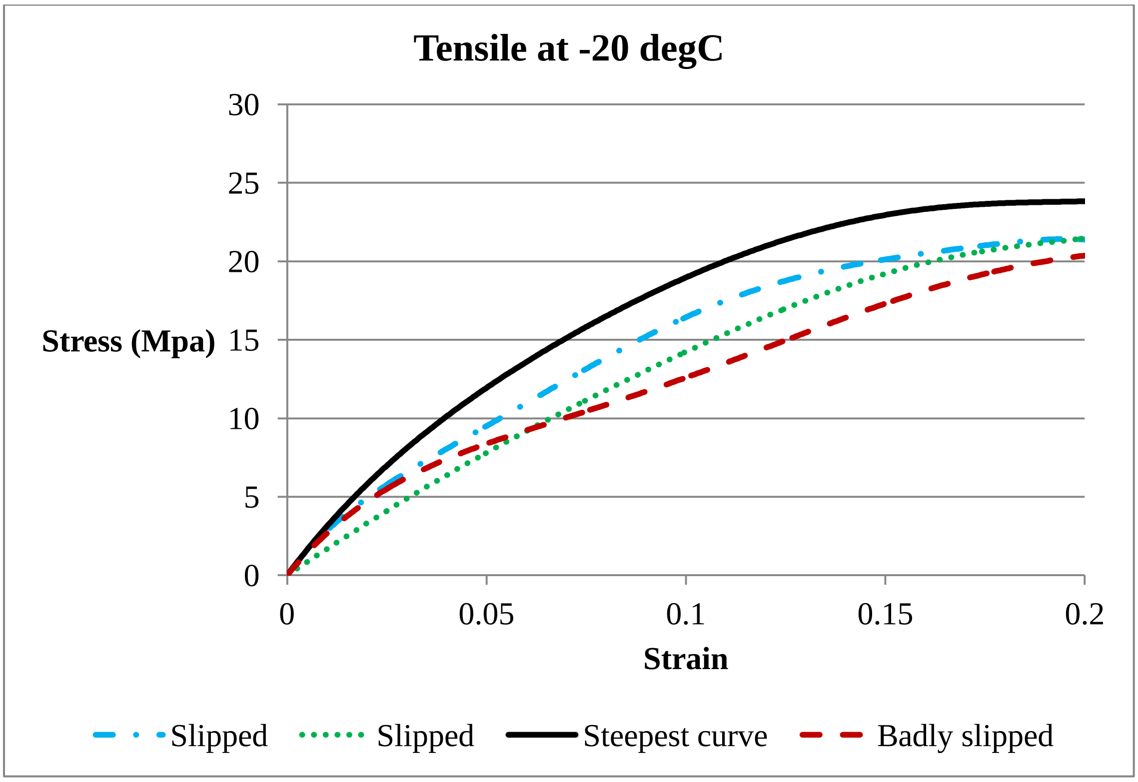

Figure 46; Tensile results at -20°C for FEP grade 2

As can be seen from the graph, there is significant slippage in some of the curves and this would significantly affect calculations of stress induced and therefore invalidate flex life predictions.

In order to overcome this, the steepest curve was used. This is because with the steepest curve, it is likely that the sample was less affected by slip and is more representative of the materials stress-strain behaviour at low temperature.

This issue could potentially be further remedied by using dumbbell polymer samples. These sample types allow the clamps to grip the sample more effectively and therefore slip less likely to occur. However, using dumbbell samples would also mean an extra cost and also the polymer processing method would be different and therefore may affect the properties in a different way.

This stress-strain model, correlated with flex life data produces the validation curve in figure 47 for FEP grade 2.

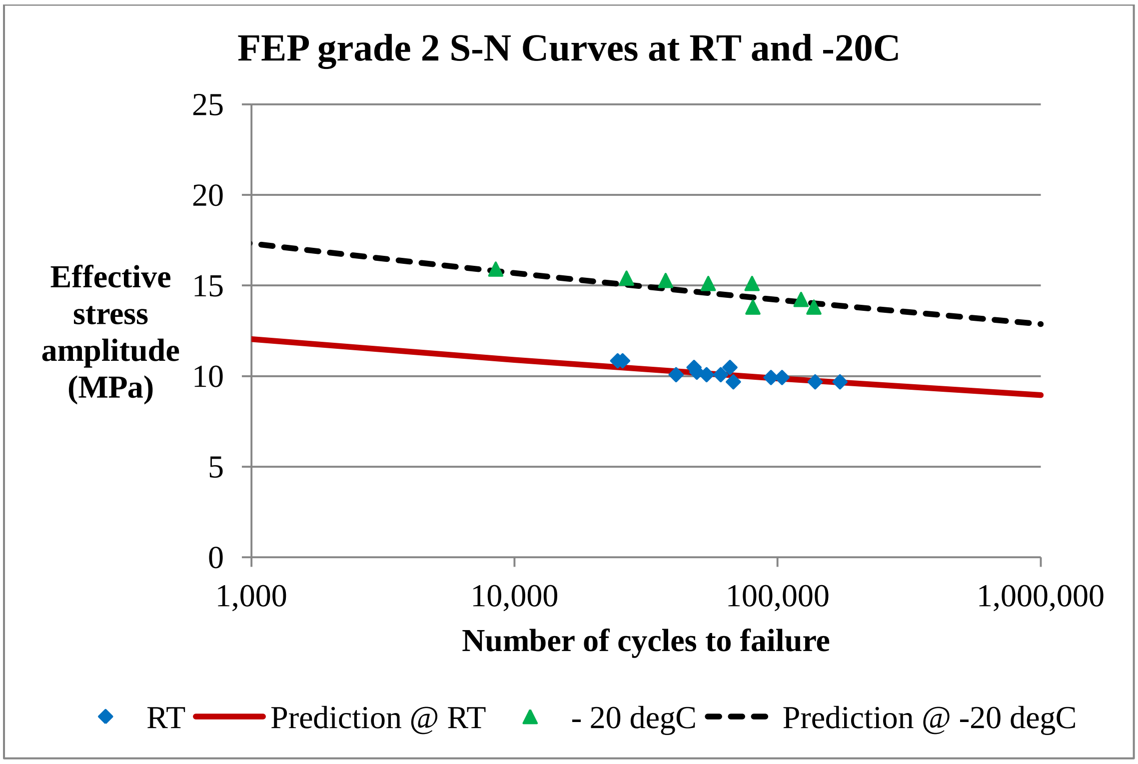

Figure 47; FEP flex life at room temperature and -20°C

As can be seen, there is a good correlation between predicted flex life behaviour and actual flex life results at both -20°C and room temperature (21°C). Low temperature flex life and stress strain analyses were also carried out on FEP grade 1 and a good correlation was also found. Results for this, along with temperature dependant data for other polymer samples can be found in appendix 2.

13.0 Alternative Failures in Polymers

Fatigue is just one of many possible failure mechanisms for polymers. In fact, as the pie chart in figure 48 below suggests, only 15% of plastic failures are due to fatigue. The pie chart is generated from research done by a leading polymer consultancy company, Smithers Rapra (2012b).

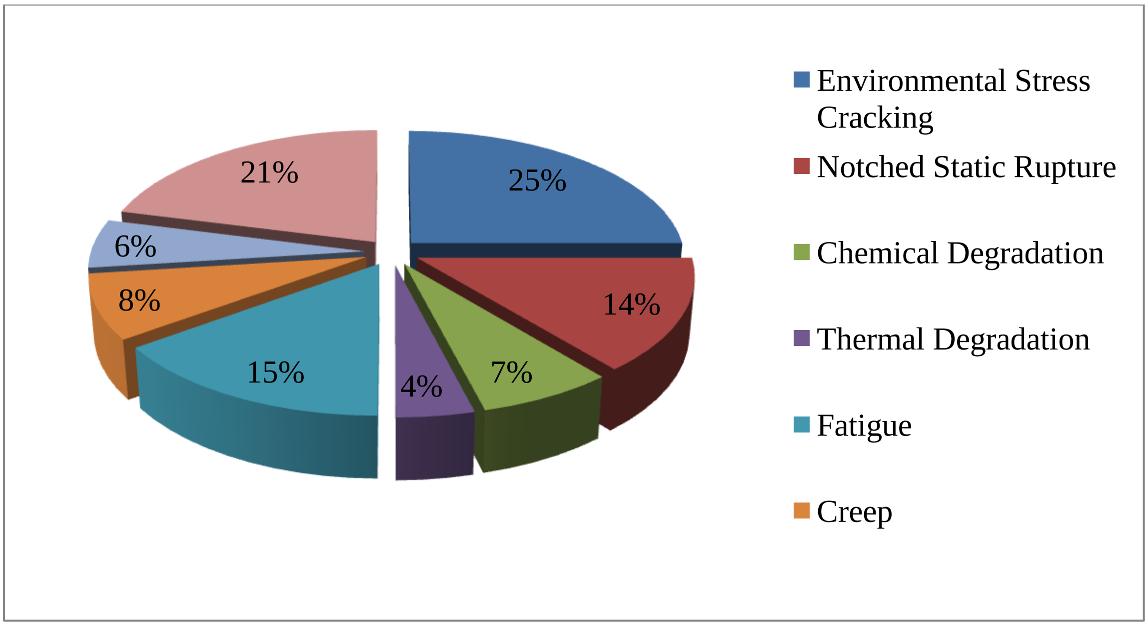

Figure 48; Plastic failure mechanisms [Smithers Rapra, 2012b]

The process of dynamic fatigue has been covered in this paper, below summarises the other potential failure mechanisms that are represented in the above chart.

13.1 Environmental Stress Cracking

Environmental stress cracking (ESC) is the premature cracking of a plastic as a direct result of the combination of stress and chemical presence, where neither the stress or substance present would have a significant effect individually and therefore the failure is unexpected [Jansen, 2004].

This can be a significant killer of plastics. It is not always picked up immediately as the exposure to the ESC agent can simply accelerate a long term stress failure mode, such as fatigue or creep.

13.2 Thermal Degradation

It is understood that the mechanical properties of polymers vary significantly with temperature. However, these changes are only in the short term. If a polymer material is exposed to increased temperature for a prolonged period of time, then chemicals that contribute to the structure of the polymer can escape due to the energy gained from the heating. This, over time changes the properties of the material and unlike any short term changes resulting from temperature, this process cannot be reversed [Zeus, 2005a].

13.3 UV Degradation

Photo-induced degradation, also known as photolysis, can happen when the material is exposed to waves from the electromagnetic spectrum for prolonged periods. A very common method of this is UV degradation. As with thermal degradation, chemicals within the polymer can get excited, escape and change the structure of the polymer [Zeus, 2005b].

A good example of this is a plastic garden chair left outside. After a number of years, the colour of the chair will have faded, as well as the chair losing strength. This is due to the lengthy exposure to the light and UV rays from the sun.

13.4 Chemical Degradation

Chemical degradation can occur in a polymer when in the presence of a chemical, similar to UV/ thermal degradation, a reaction takes place which alters the materials properties. There are many different kinds of chemicals that can induce degradation, one of the most common being oxygen.

13.5 Creep

Creep is a time dependant phenomenon which can induce failure in a material under constant deformation or load. Since polymers exhibit both elastic and viscous behaviour, they are more prone to creep than linear elastic materials because of their viscous characteristics. The effects of creep can be heightened by increased temperature [French, 1991].

13.6 Notched Static Rupture

Notched static rupture, or stress rupture is a form of creep [Nondestructive Testing]. It occurs under static loading when there is a 'stress raiser' present in the material and this stress raiser accelerates the creep process. This is usually in the form of a notch in the material that could have been induced from mishandling or processing.

13.7 Impact on Cable Materials

The graph in figure 48 represents a generalisation of engineering plastics. Cable materials may not be subject to all of these failure mechanisms, or the proportions of failure may not fully represent that of cable materials.

The probability of some of these failure mechanisms happening can be significantly reduced by careful planning and design. The following points summarises ways in which this can help prevent these failure mechanisms: The risk of creep or fatigue can be by good cable management. Cable routing methods can be used to maximise the radius of any bend the cable is subject to, reducing the stresses within. Notched static rupture could be prevented by taking care when handling and ensuring high quality extrusions and production methods. ESC/ chemical degradation could be prevented ensuring any chemicals or products used in production and in service are not harmful to the polymer. It is therefore important to know of any chemicals that are harmful to the materials used. UV/ light/ thermal degradation could be prevented by ensuring use in an environment where it will be protected or if this is not feasible, the impact of these factors could be reduced by ensuring proper material selection.

In any process that irreversibly degrades polymer properties, such as thermal degradation, this effect combined with another, such as dynamic fatigue, will reduce the overall life of the material further. For example, a cable jacket subject to 1,000,000 bends per year may last for 10 years in bending and 10 years in a heated environment. However, combine the two and thermal degradation will degrade it's insulation's properties. As a result, it may not fulfil its required 10 years in bending.

14.0 Screen Flex Life

The screen on a cable is usually a layer of material which has two main protective purposes:

1. To protect the inner elements and signals against electromagnetic interference (EMI).
2. To help prevent electromagnetic signals escaping and interfering with other signals.

There are two main types of screen that Axon' uses in its products; helical screens and braids. Figure 49 is a picture of a helical screen.

Figure 49; Helical screen

A helical screen is basically a helix of wires surrounding an element that it is protecting from EMI. Often double helical screens are used to improve the EMI performance of the screen. A double helical screen is a helical screen with a second helix of wires on top of it. With a double helical screen, the direction of lay of the two layers will be opposite.

Figure 50 is a picture of a braid.

Figure 50; Braided screen

A braid differs from a helical screen by its construction, the two layers on a braid are weaved together to form one layer. In general, it is believed that braided screens provide better EMI protection than helical screens. Helical screens, however, are believed to offer better flex life performance and in a dynamic application it is often important to consider both.

14.1 Strain in Screen

Because of its construction, the maximum strain in a helical screen when it is subjected to a bend is effectively the same as the maximum strain in the outer strands of a multi stranded conductor. However to keep things clear, subscript SC will be used (instead of 1). Therefore the following equation is used in this instance.

$$\varepsilon = \frac{R_{strand}}{R_{bend} - d_{SC}} \cos^2 \beta_{SC} \tag{38}$$

A braid has an additional effect of the 'weave'. What this weave effect does is induce a higher strain than would be calculated using equation 39, this is known as a stress or strain raiser. This strain raiser can be accounted for by introducing a strain concentration factor (SCF) into equation.

$$\varepsilon = SCF\left[\frac{R_{strand}}{R_{bend} - d_{SC}} \cos^2 \beta_{SC}\right] \tag{39}$$

14.2 Test Procedure

Flex life tests were carried out on both the rolling flex test rig and the pulley flex test rig. When testing bare screen elements, failure was considered to be when strands had visibly broken.

It was decided that the best way to determine the braid SCF was from test results. Test results were to be gathered and then an SCF assigned to the braid by calibrating it to a flex life model for a known material. Trends were then observed and plotted to determine whether or not the SCF for the braid is predictable or not. The following characteristics of braids could have an impact on the SCF.

- Strand diameter.
- Braid angle.
- Outer diameter.
- Bend radius.

While some of these aspects are considered in the initial strain calculation, they could also have an impact on the braids SCF.

Any helical screen testing took place only as part of a cable bundle and results can be seen in chapter 15.

14.3 Results and Discussion

Raw flex life data for various braid constructions was collected. These raw data results were then assigned an SCF to calibrate the data points to the materials flex life curve as shown in figure 51.

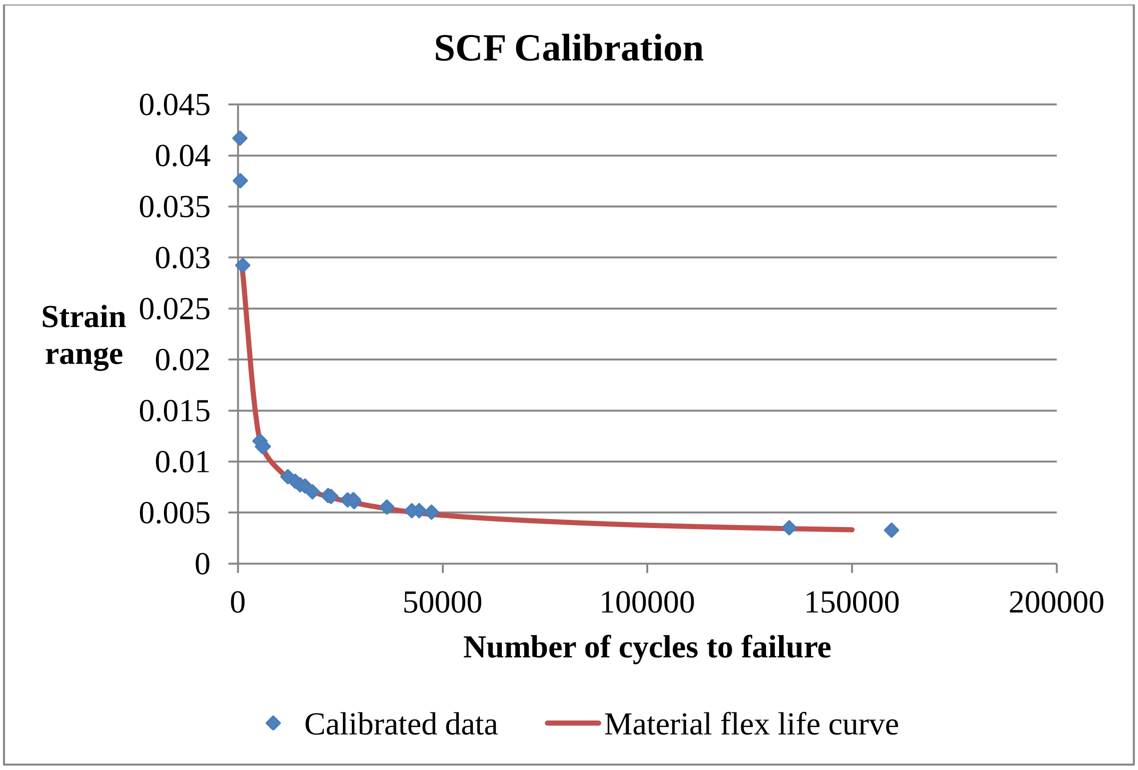

Figure 51; Graph calibrating braid flex life data

Each individual SCF was then plotted against factors that could affect the braids SCF (mentioned in the previous section 14.2). Trends were acknowledged and the graph with the best trend is used as the basis for calculating the SCF.

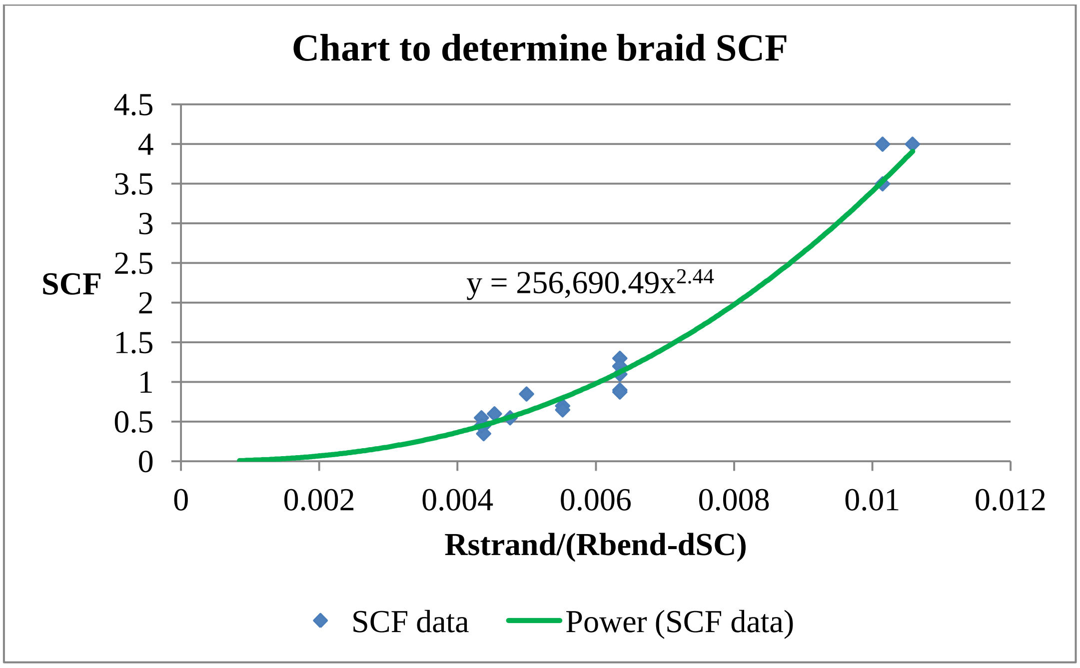

Figure 52; Graph to estimate braid SCF

As can be seen from figure 52, the equation used to estimate the braids SCF is:

$$SCF = 1 + 256690.49\left(\frac{R_{strand}}{R_{bend} - d_{SC}}\right)^{2.44} \qquad (40)$$

Using this SCF in strain calculations and plotting results, the validation in figure 53 is achieved.

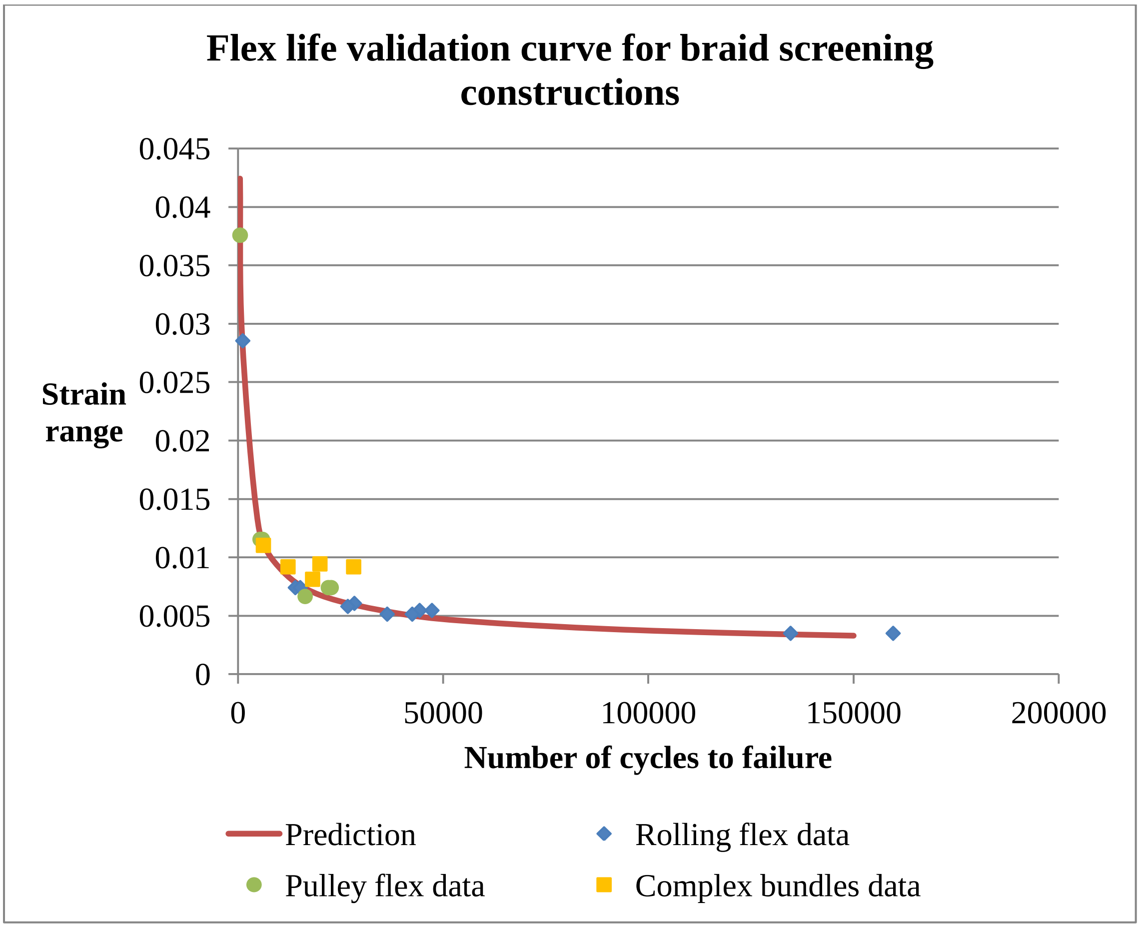

Figure 53; Braid validation curve

Since failure was taken to be when strands started to visibly break, this model determines the number of cycles to initial strand failure. However, an observation made is that different braid materials behave differently after initial strand failure. Low grade coppers, such as A1 copper, generally embrittle very soon once strands start to break. This results in the braid falling apart quite easily and therefore the braids EMI performance deteriorating rapidly. High grade alloys, such as SCA, do not embrittle soon after. So even though there is strand breakage, the braid is still intact and providing a good degree of EMI protection and although a mechanical failure, the product is still fulfilling its purpose.

However, if a broken strand was to escape from the cable by threading through its outer covering (often dynamic cables have a fabric outer nomex instead of a jacket), this could be potentially dangerous depending on the application. So it is important to acknowledge when this initial strand failure is likely to occur. In terms of defining a failure point, there is some leeway here and when the screen is actually considered failed after initial strand failure is down to some of the following points:

The application or environment that the cable is operating in; if a loose strand was to escape from the cable it could interfere with other components around it. For example, it could cause jamming in mechanical equipment or a short circuit if there is electrical circuitry present.

As discussed, the material used would appear to have an impact on the performance of the screen. A high grade material will stay intact for longer than a low grade material which will become brittle and fall apart quickly.

A significant degree of engineering discretion would need to be used here with particular thought given to the cable’s environment, the importance of the EMI performance of the screen and how the screen material will behave after it has begun to fatigue.

15.0 Cable bundle flex life testing

Using the pulley flex test method, cable bundles were tested around an inner bend radius of 20 mm (true bend radius = 20 mm + ½ cable diameter). Individual elements within the cable were monitored to determine their condition.

Three measurement techniques were used to do this:

- DCR measurements to determine the conductive state of metallic components. Failure determined by either an increase of >5% DCR or intermittent readings.
- High voltage isolation checks to ensure isolation between metallic components. Failure determined by a DCR reading on meter.
- Visual inspection. Failure determined when visible damage on component.

A 5% increase in resistance or a broken strand on a braid does not necessarily mean a catastrophic electrical or screen failure, however, it does indicate the state of the component is deteriorating and is an early indication of mechanical failure. Therefore from this point, while there would still be more time before catastrophic failure, it would a good stage to replace the cable.

The typical test set up for these cable bundle tests is shown in figure 54.

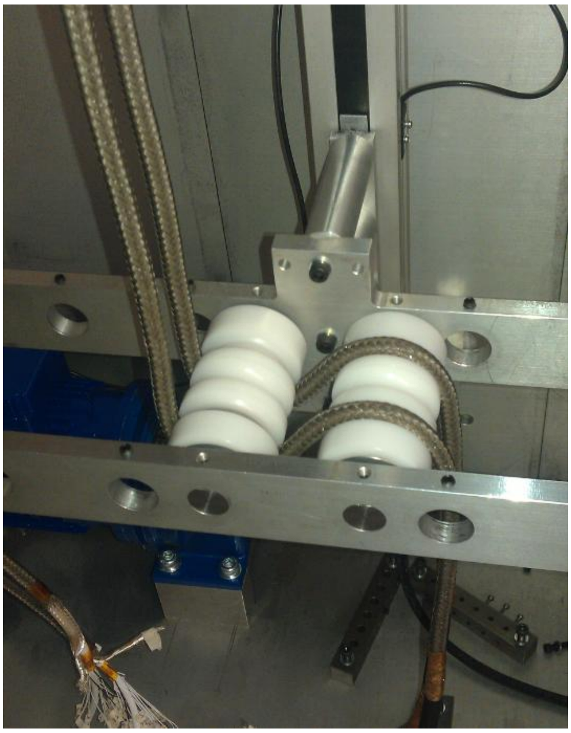

Figure 54; Test setup for cable pulley flex test

15.1 Cable 1 Flex Test

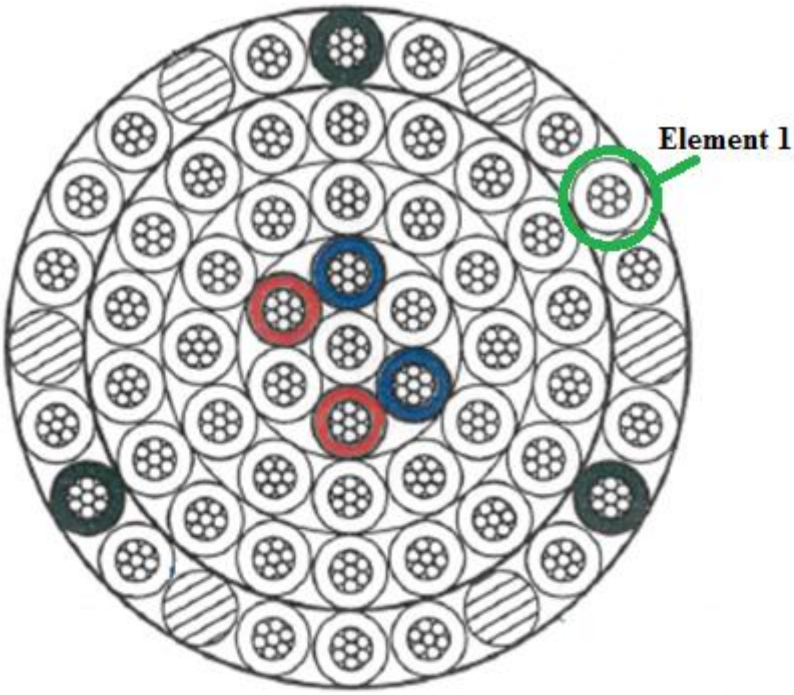

Figure 55; Cable 1 cross section

The cable shown in figure 55 is made up of 56 of the same element and some fillers to ensure the cable is balanced and structurally sound. This one element (element 1.1) is in 5 different positions (different pitch circle diameters) within the bundle. On top of this bundle there is a soft, protective tubing over which there is a SCA braid and a nomex, which is a protective fabric covering for the cable. All the input data is displayed in table 3.

Table 3; Geometry of cable 1 for flex test

<table>
<tr><th colspan="5">Element 1.1</th></tr>
<tr><td colspan="5">Conductor
• D_{strand} = 0.127 mm
• Distance 1 = 0.127 mm
• Lay length 1 = 4.572 mm
• Distance 2 = N/A
• Lay length 2 = N/A
• Material: A1 copper</td></tr>
<tr><td colspan="5">Wire insulation
• OD = 0.7 mm
• Material: ETFE</td></tr>
<tr><td colspan="5">Element position</td></tr>
<tr><td>1
• Distance from centre = 0 mm
• Lay length = N/A</td><td>2
• Distance from centre = 0.7 mm
• Lay length = 16.32 mm</td><td>3
• Distance from centre = 1.4 mm
• Lay length = 32.64 mm</td><td>4
• Distance from centre = 2.1 mm
• Lay length = 48.96 mm</td><td>5
• Distance from centre = 2.8 mm
• Lay length = 65.76 mm</td></tr>
<tr><td colspan="5">Outer screen over bundle
• D_{strand} = 0.127 mm
• OD = 8.8 mm
• Lay angle = 24 degrees
• Material: SCA</td></tr>
</table>

15.2 Cable 2 Flex Test

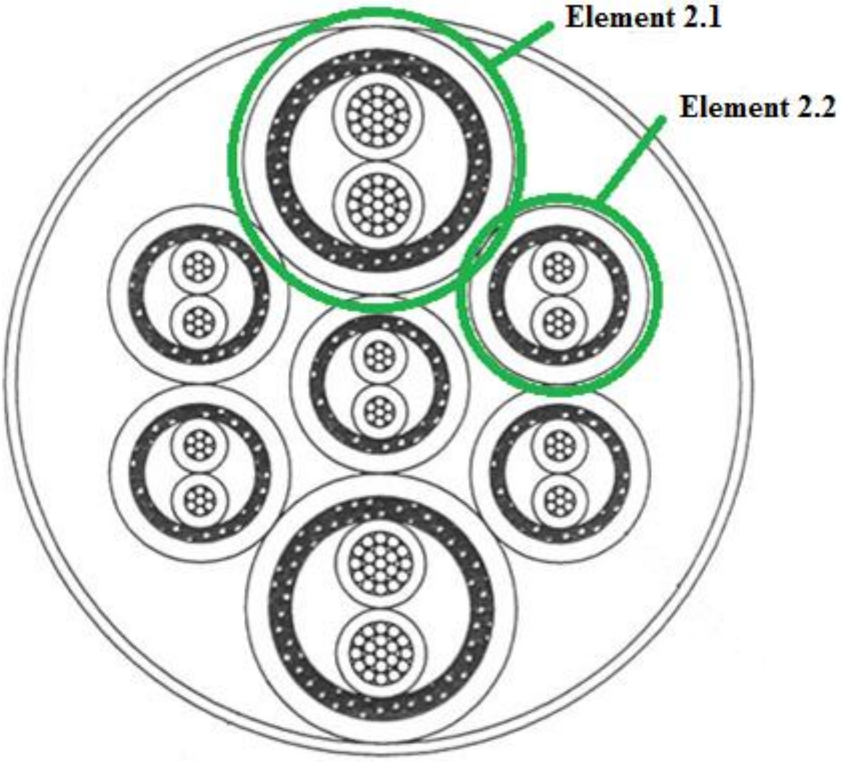

Figure 56; Cable 2 cross section

The cable shown in figure 56 has 2 different elements in three different positions within the bundle. There is a nomex covering this bundle. The input data is displayed in table 4 below.

Element 2.1 is the larger of the two twisted pair elements.

Element 2.2 is the smaller of the two twisted pair elements.

Table 4; Geometry of cable 2 for flex test

<table>
<tr><th>Element 2.1</th><th colspan="2">Element 2.2</th></tr>
<tr><td>Conductor
• D_{strand} = 0.16 mm
• Distance 1 = 0.32 mm
• Lay length 1 = 9.6 mm
• Distance 2 = N/A
• Lay length 2 = N/A
• Material: A1 copper</td><td colspan="2">Conductor
• D_{strand} = 0.127 mm
• Distance 1 = 0.127 mm
• Lay length 1 = 4.572mm
• Distance 2 = N/A
• Lay length 2 = N/A
• Material: A1 copper</td></tr>
<tr><td>Wire insulation
• OD = 1.13 mm
• Material: PTFE</td><td colspan="2">Wire insulation
• OD = 0.7 mm
• Material: PTFE</td></tr>
<tr><td>Twisted pair
• Distance 3 = 0.565 mm
• Lay length 3 = 13.36 mm</td><td colspan="2">Twisted pair
• Distance 3 = 0.7 mm
• Lay length 3 = 8.4 mm</td></tr>
<tr><td>Screen
• D_{strand} = 0.127 mm
• OD = 2.8 mm
• Lay angle = 25 degrees
• Material: A1 copper</td><td colspan="2">Screen
• D_{strand} = 0.079 mm
• OD = 1.75 mm
• Lay angle = 25 degrees
• Material: A1 copper</td></tr>
<tr><td>Element jacket
• OD = 3.35 mm
• Material FEP</td><td colspan="2">Element jacket
• OD = 2.2 mm
• Material: FEP</td></tr>
<tr><td>Element position
• Distance from centre = 2.775 mm
• Lay length = 67.8 mm</td><td>Element position 1
• Distance from centre = 0 mm
• Lay length = N/A</td><td>Element position 2
• Distance from centre = 2.2 mm
• Lay length = 67.8 mm</td></tr>
</table>

15.3 Cable 3 Flex Test

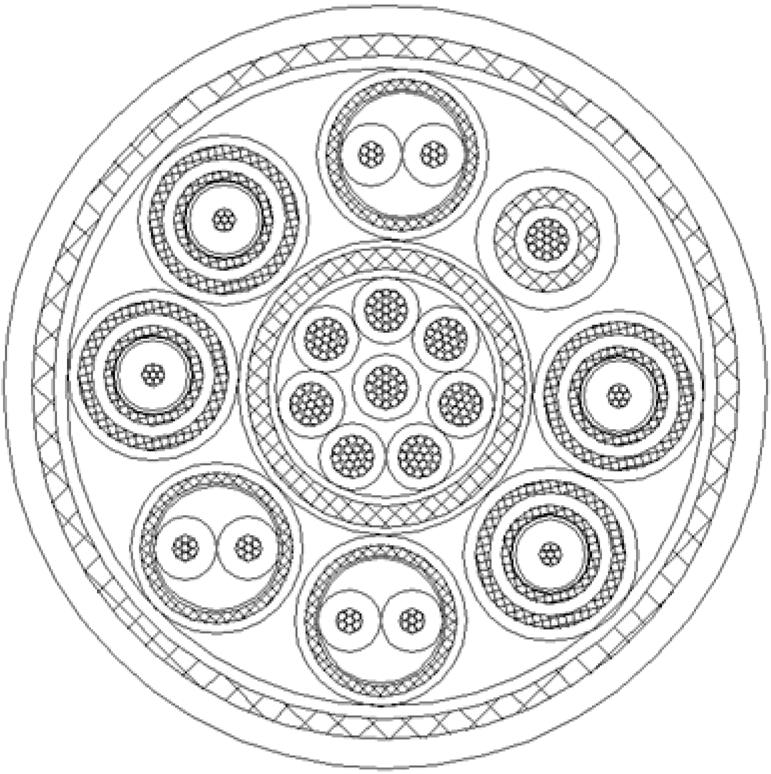

Figure 57; Cable 3 cross section

Figure 57 shows a cable which is a lot more complex, with four different elements and two separate individual screens. Tables 5 –7 summarise the inputs for the elements.

Element 3.1 is the conductor element making up the in the central bundle. See figure 58.

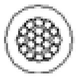

Figure 58; Element 3.1

Element 3.2 is the single coaxial element in the outer layer. See figure 59.

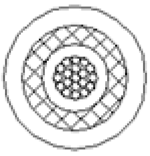

Figure 59; Element 3.2

Table 5; Geometry of elements 3.1 and 3.2

<table>
<tr><th colspan="2">Element 3.1</th><th>Element 3.2</th></tr>
<tr><td colspan="2">Conductor
• D_{strand} = 0.102 mm
• Distance 1 = 0.204 mm
• Lay length 1 = 6.12 mm
• Distance 2 = N/A
• Lay length 2 = N/A
• Material: A1 copper</td><td>Conductor
• D_{strand} = 0.102 mm
• Distance 1 = 0.204 mm
• Lay length 1 = 6.12 mm
• Distance 2 = N/A
• Lay length 2 = N/A
• Material: A1 copper</td></tr>
<tr><td colspan="2">Wire insulation
• OD = 0.8 mm
• Material: ETFE</td><td>Wire insulation
• OD = 0.8 mm
• Material: ETFE</td></tr>
<tr><td colspan="2">Screen
N/A</td><td>Screen
• D_{strand} = 0.102 mm
• OD = 1.25 mm
• Lay angle = 65 degrees (Lay angle = 25)
• Material: A1 copper</td></tr>
<tr><td colspan="2">Element jacket
N/A</td><td>Element jacket
• OD = 1.7 mm
• Material: FEP</td></tr>
<tr><td>Element position 1
• Distance from centre = 0
• Lay length = N/A</td><td>Element position 2
• Distance from centre = 0.8 mm
• Lay length = 31.8mm</td><td>Element position
• Distance from centre = 2.62 mm
• Lay length = 82.8 mm</td></tr>
</table>

Element 3.3 is the (double) screened coaxial element in the outer layer. See figure 60.

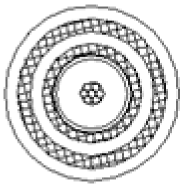

Figure 60; Element 3.3

Element 3.4 is the screened twisted pair element in the outer layer. See figure 61.

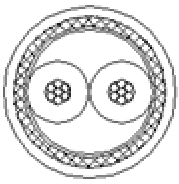

Figure 61; Element 3.4

Table 6; Geometry of elements 3.3 and 3.4

Element 3.3	Element 3.4
Conductor • D_{strand} = 0.091 mm • Distance 1 = 0.204 mm • Lay length 1 = 6.12 mm • Distance 2 = N/A • Lay length 2 = N/A • Material: SCA	**Conductor** • D_{strand} = 0.127 mm • Distance 1 = 0.254 mm • Lay length 1 = 4.572 mm • Distance 2 = N/A • Lay length 2 = N/A • Material: SCA
Wire insulation • OD = 0.84 mm • Material: PTFE	**Wire insulation** • OD = 0.8 mm • Material: Celloflon/PFA
Screen 1 • D_{strand} = 0.051 mm • OD = 1.1 mm • Devis angle = 65 degrees (Lay angle = 25) • Material: A1 copper	**Screen** • D_{strand} = 0.079 mm • OD = 2 mm • Lay angle = 65 degrees (Lay angle = 25) • Material: A1 copper
Twisted pair N/A	**Twisted pair** • Distance 3 = 0.8 mm • Lay length 3 = 19.2 mm
Element jacket • OD = 1.48 • Material: FEP	**Element jacket** • OD = 2.42 mm • Material: FEP
Screen 2 • D_{strand} = 0.1 mm • OD = 2 mm • Devis angle = 63 degrees (Lay angle = 27) • Material: A1 copper	**Screen 2** N/A
Element position • Distance from centre = 2.8 mm • Lay length = 82.8 mm	**Element position** • Distance from centre = 2.8 mm • Lay length = 82.8 mm

Central bundle braid is the braid surrounding the central bundle made up of 7 x element 1.1.

Outer braid is the braid surrounding the cable.

Table 7; Geometry of braids on cable 3

Central bundle braid	Outer braid
Screen • D_{strand} = 0.13 mm • OD = 4 mm • Devis angle = 63 degrees (Lay angle = 27) • Material: A1 copper	**Screen** • D_{strand} = 0.13 mm • OD = 10 mm • Devis angle = 63 degrees (Lay angle = 27) • Material: A1 copper

15.4 Results and Discussion

Flex life predictions for the three cables were compiled and are presented in tables 8-10 below. The flex life prediction column indicates the number of cycles to failure for that element, considering its different positions where appropriate. The number of cycles to failure column indicates the earliest detected number of cycles to failure for that element.

Table 8; Cable 1 predictions and results

Cable 1	Position	Flex life prediction (number of cycles)	Number of cycles to failure	Notes
Element 1.1 conductor	All 5 layers	36,288 – 46,209	50,000	
Element 1.1 insulation	All 5 layers	No failure in time frame	No failure	
SCA screen	Outer	16,635	60,000 17,000	Separate braid test conducted showed good correlation for **strand failure** only.

As can be seen from these results there is a good correlation between results and predictions for the conductor and insulation, however the SCA braid on the cable appeared to last a lot longer. A separate braid test was carried out under the same conditions. This showed a good correlation with predictions; however this was for stand failure which could be detected a lot earlier as there was no nomex hiding the damage. While there were broken strands on the braid, it remained intact quite well. This is believed to be to do with the SCA material not embrittling as quickly as a lower grade of copper.

Table 9; Cable 2 predictions and results

Cable 2	Position	Flex life prediction (number of cycles)	Number of cycles to failure	Notes
Element 2.1 conductor	1 layer	22,561	20,000	
Element 2.1 insulation	1 layer	No failure in time frame	No failure	
Element 2.1 screen	1 layer	12,148	40,000	
Element 2.1 jacket	1 layer	20,379	Failure observed at end of test	Model for different grade of FEP
Element 2.2 conductor	All 2 layers	39,397 - 43,266	45,000	
Element 2.2 insulation	All 2 layers	No failure in time frame	No failure	
Element 2.2 screen	All 2 layers	157,560 – 176,814 (No failure in time frame)	No failure	
Element 2.2 jacket	All 2 layers	No failure in time frame	No failure	Model for different grade of FEP

There is a good correlation with the conductors, however the braid (on element 2.1) is again predicted below its actual result. This is again believed to be to do with the measurement method. Since there was no visual inspection possible, the only way to determine braid failure was by DCR measurement, this takes much longer to show in a braid compared to a conductor.

The jacket on element 2.1 was a grade of FEP which was uncharacterised. Having modelled it with FEP grade 1, it was expected to fail around 20,000 cycles. However, this failure could not be detected until after the cable was dissected.

The exact point of failure however is unknown as this failure was not picked up electrically. It was found after the test when dissecting the cable. Figure 62 shows the element jacket cracked in a number of places.

Figure 62; Cracked jacket on element

The predictions and results for the test conducted on cable 3 are presented in table 10.

Table 10; Cable 3 predictions and results

Cable 3	Position	Flex life prediction (number of cycles)	Number of cycles to failure	Notes
Element 3.1 conductor	All 2 layers	76,270 – 78,101	60,000	
Element 3.1 insulation	All 2 layers	No failure in time frame	No failure	
Element 3.2 conductor	1 layer	63,330	No failure	
Element 3.2 insulation	1 layer	No failure in time frame	No failure	
Element 3.2 screen	1 layer	40,164	80,000	

Element 3.2 jacket	1 layer	No failure in time frame	No failure	
Element 3.3 conductor	1 layer	No failure in time frame	No failure	
Element 3.3 insulation	1 layer	No failure in time frame	No failure	
Element 3.3 screen 1	1 layer	No failure in time frame	No failure	
Element 3.3 screen 2	1 layer	37,047	12,000* 40,000	
Element 3.4 conductor	1 layer	No failure in time frame	No failure	
Element 3.4 insulation	1 layer	No failure in time frame	No failure	
Element 3.4 screen	1 layer	104,402	No failure	
Element 3.4 jacket	1 layer	No failure in time frame	No failure	
Central bundle braid	1 position	11,338	18,000	
Outer braid	1 position	5,863	6,000	

As the results show, there is a respectable comparison. The second screen on element 3.3 has a questionable result (marked with an asterisk), believed to be a flawed reading during the test. The next corresponding screen to go was at the predicted time.

One other reason to explain general discrepancies between results and predictions could be to do with the position of the element in the bend region. Depending on the cables orientation, the element modelled may not have been in the extreme position in the bend region and it will be subject to lower strain than calculated. However, for modelling purposes the element must be modelled in the extreme position in order to work to a worst case scenario.

16.0 User Interface

The user interface is a key part to the project as it is essential that flex life analyses are automated so that it does not take up too much additional time of engineers. The interface is designed, programmed and run in MATLAB.

The user interface requires the following inputs from the engineer, all of which should be specified on a cable drawing or by the customer.

Conductor

- Strand diameter
- Distance 1
- Lay length 1
- Distance 2 (if applicable)
- Lay length 2 (if applicable)
- Distance 3 (if applicable)
- Lay length 3 (if applicable)
- Material

Insulation

- Outer diameter
- Material

Screen

- Individual strand diameter
- Outer diameter
- Devis angle (lay angle subsequently calculated)
- Material

Jacket

- Outer diameter
- Material

Element position within bundle

- Element distance from central axis
- Lay length on element

Application

- Temperature
- Bend radius

The program then takes these inputs and puts them into a process-able form so that calculations can be done and flex life predictions can be made. A picture of the final user interface can be seen in figure 63.

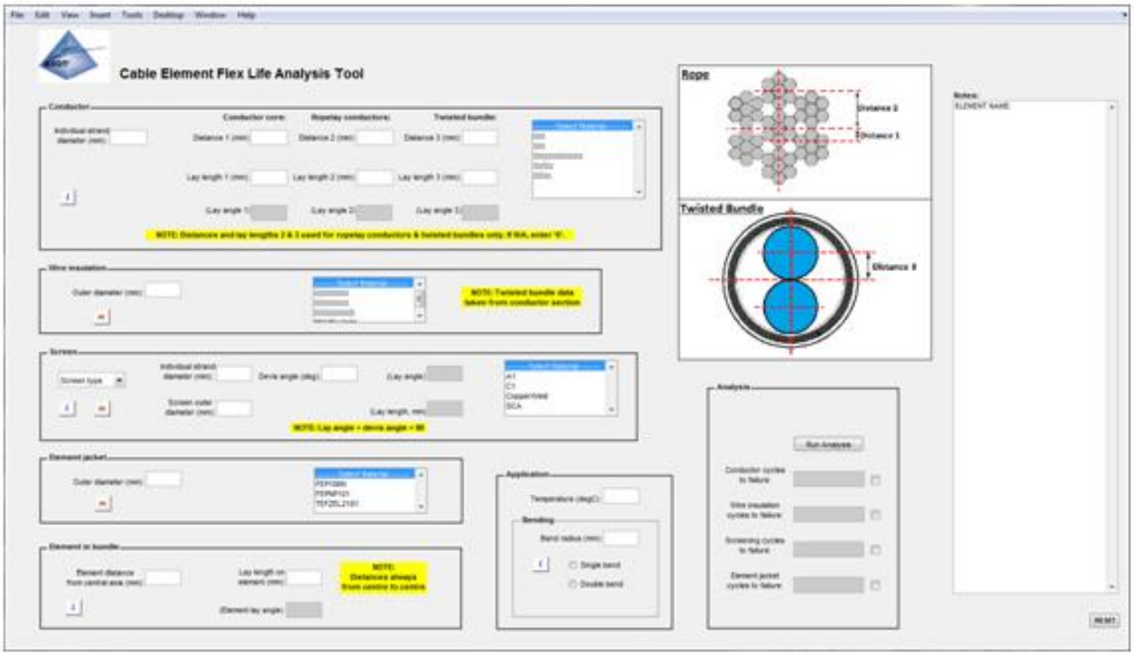

Figure 63; Screenshot of user interface

Having selected a material, the material script is then called up at the appropriate place in the flex life analysis script, at which point the program logs the materials properties and uses them where appropriate.

Two additional 'manual' GUI's were developed, one for insulations/ jackets and one for screens. These are to be used when an element needs to be analysed alone (i.e. without the conductor). The conductor can be analysed alone in the main GUI.

There are also 'information' buttons that can be used to call up schematics which clarify what certain required inputs mean if the user is unsure.

Pictures of these additional GUI's and the code that was developed to create the GUI's can be found in appendix 3.

17.0 Conclusion and Project Review

To conclude; the project meets the primary objectives set out at the beginning. Over the course of the project, the company has increased its knowledge of fatigue in materials and its application in cable flex life through training and presentations made during the course of the project.

Axon' Cable now has a cable flex life analysis tool which can be used to predict cable flex life based on materials, flex conditions, cable construction and temperature. With the correct approach, flex life predictions for composite cables can be compiled and used in the design process, providing Axon' and their customers with a capability that reduces the need for costly and time consuming cable flex life testing.

Axon' engineers can easily implement these flex life calculation methods by means of a user friendly interface to quickly and easily conduct analyses.

Overall, the tool gives Axon' a competitive edge over competitors who do not possess the same knowledge. It gives the customer peace of mind that the product is suitable for the application. It will result in more effective design reviews by allowing engineers to identify and reinforce weak areas of the cable or re-design over engineered areas of the cable resulting in potential cost savings.

As a piece of research, the project has demonstrated that there is a degree of predictability in a failure mode that is often perceived as a substantial uncertainty. The content of the project is transferrable to other applications that involve fatigue failure mechanisms such as tugboat hawsers that bend around a large spindle, although there is of course an additional tension here. It has also looked at the predictability and repeatability of polymer mechanical behaviour, another area often considered taboo. This is an area that would be interesting and beneficial to many industries to further investigate as polymers are a desirable material, because of their lightweight and aesthetic properties, but are often dismissed due to their reliability.

There are limits to the tool, however and these need to be considered when compiling predictions. The tool should not be used 'blindly'.

Alternative polymer failure mechanisms mean that predictions may be made invalid due to a wide range of other failure mechanisms that may induce failure before flex fatigue. The fact that a small change in bend radius can have a significant impact on flex life means that some predictions may not necessarily be accurate to the application depending on how the bend radius is induced or specified. There have also been some assumptions applied to theories such as the extrapolation of data which should be kept in mind by engineers. Finally, errors and accumulation of tolerances will always affect calculations and therefore predictions.

There are some areas where the project could have been improved. Some of these are highlighted and explained below:

There is a lack of raw flex life data in the insulation section. This is because of the time consuming nature of the flex testing process for polymers. An additional flex test rig would have been valuable here as more data could have been collected and perhaps more materials could have been covered. A reversed bending rig custom designed for flex testing insulation fillers would be most beneficial as it would give more reversed bending results, when only few could be obtained on the pulley flex test rig. Also, because of the greater stress range the sample would be subject to, the testing process would take less time.

In most cases, it would be expected for metal part of the cable to fail by fatigue before a plastic part. Therefore, in future it would perhaps be beneficial to focus the tool on metals and low grade plastics only. A few reasons for this are that high grade polymers are generally considered good in high flex applications – focussing on lower grade polymers will give more confidence that they can also withstand repeated flexing. Also, high grade polymers are more time consuming to test to failure and more time would need to be allocated to each of the testing processes.

It was of importance that the project demonstrated correlation between predictions and cable bundle flex test results because this achieved the ultimate aim of the project; to develop a fatigue analysis tool to predict cable flex life.

As mentioned, more data, materials and perhaps capabilities from the tool are desired so in that sense, the final tool is not complete. However it does provide foundations for Axon’ Cable to build on.

18.0 References

ASM (1996). ASM Handbook volume 19; Fatigue and Fracture. ASM International.

ASME (1995). ASME B31.1-1995 Edition: Power Piping. American Society of Mechanical Engineering. http://www.engineeringtoolbox.com/young-modulus-d_773.html <accessed 15/02/13>

Beijing Shijia Wanlian Scientific Co. LTD (N.D). The application of Yasuda MIT type folding endurance tester in DuPont. http://en.shijiawanlian.com/_d275447566.htm <accessed 11/04/13>

Bishop. N. W. M, Sherratt. F. (2000). Finite Element Based Fatigue Calculations. NAFEMS.

Dotmar (N.D.) Plastic properties tables; Co-efficient of friction of plastics. http://www.dotmar.com.au/co-efficient-of-friction.html <accessed 29/07/13>

Dowling. N. E. (2004). Mean Stress Effects in Stress-Life and Strain-Life Fatigue. Society of Automotive Engineers, Inc. Virginia, USA.

DuPont (2000). General Design Principles for DuPont Engineering Polymers. DuPont Engineering Polymers. http://plastics.dupont.com/plastics/pdflit/americas/general/H76838.pdf <accessed 15/02/13>

Fisk (2013). C172 Beryllium Copper Alloy Wire. http://www.fiskalloy.com/product/c172/ <accessed 10/04/13>

French. D. N. (1991). Creep and creep failures. http://www.nationalboard.org/Index.aspx?pageID=181 < accessed 15/02/13>

Instron (2013). 3 and 4 point flexure fixtures. http://www.instron.us/wa/acc_catalog/prod_list.aspx?cid=833&cname=3%20and%204%20Point%20Flexure%20Fixtures <accessed 10/04/13>

Jansen. J. A. (2004). Environmental Stress Cracking – The Plastic Killer. Advanced Materials and Proceses. http://www.madisongroup.com/publications/Janse_ASM_ESC_TMG2011.pdf <accessed 15/02/13>

Kohout. J. (N.D.). Anomalies in Temperature Shift of S-N Curves. University of Defence. Czech Republic. http://portal.zmne.hu/download/bjkmk/bsz/bszemle2006/4/Kohout.pdf <accessed 19/02/13>

Maxwell. A. S, Broughton W. R, Dean. G, Sims. G. D. (2005). Review of accelerated ageing methods and lifetime prediction techniques for polymeric materials. National Physical Laboratory Report. www.npl.co.uk/upload/pdf/depc_mpr_016.pdf <accessed 10/02/13>

Ministry of Defence (2006). Wires, Cords and Cables; Electrical – Metric Units; Part 31: Sheath – Limited Fire Hazard. Defence Standard 61-12 (Part 31), Issue 2.

Nondestructive testing (N.D). Creep and stress rupture. http://www.ndt-ed.org/EducationResources/CommunityCollege/Materials/Mechanical/Creep.htm <accessed 11/04/13>

Opp. D. A, Skinner. D. W, Wiktorek. R. J. (1970). Polym. Eng. Sci. 9(2), 121.

Papailiou. K. O. (1995). Bending of helically twisted cables under variable bending stiffness due to internal friction, tensile force and cable curvature. http://www.pfisterer.com/download_download_us/d_11085.pdf <accessed 05/04/13>

RoyMech (N.D). Elastic bending theory. http://www.roymech.co.uk/Useful_Tables/Beams/Beam_theory.html <accessed 05/04/13>]

Smithers Rapra (2012a). Plastic Design and Material Selection. http://www.rapra.net/consultancy/product-design-and-manufacture-plastic-design-and-material-selection.asp <accessed 15/02/13>

Smithers Rapra. (2012b). Why Plastic Products Fail. http://www.rapra.net/consultancy/failure-analysis-trouble-shooting-why-plastic-products-fail.asp < accessed 15/02/13>

System Integrators L. L. C. Fatigue testing, sheet and plate bending. http://syintegrators.com/fatigue_testing_sheet_plate_bending.shtml <accessed 10/04/13>

Zeus Industrial Products, Inc. (2005a). Thermal Degradation of Plastics. Zeus Technical Whitepaper.
http://www.zeusinc.com/UserFiles/zeusinc/Documents/Zeus_Thermal_Degradation.pdf <accessed 15/02/13>

Zeus Industrial Products, Inc. (2005b). UV Properties of Plastics: Transmission & Resistance. Zeus Technical Whitepaper.
http://www.zeusinc.com/UserFiles/zeusinc/Documents/Zeus_UV_Properties.pdf <accessed 15/02/13>

19.0 Appendices

19.1 Appendix 1

Flex life curve and data for conductor materials:

Table 11; Conductor material data

Material	E (MPa)	UTS (MPa)	εf	Change in E/°C	Change in UTS/°C	Change in εf /°C	b	c
A1	117000	260	2.2	-35	-0.39	0.0173	-0.112	-0.6
C1	115000	256	2.9	-35	-0.39	0.0173	-0.112	-0.595
CuBe	127500	675	2.11	-35	-0.56	0.0028	-0.095	-0.69
SCA	117000	437	2.35	-35	-0.55	0.0075	-0.091	-0.62

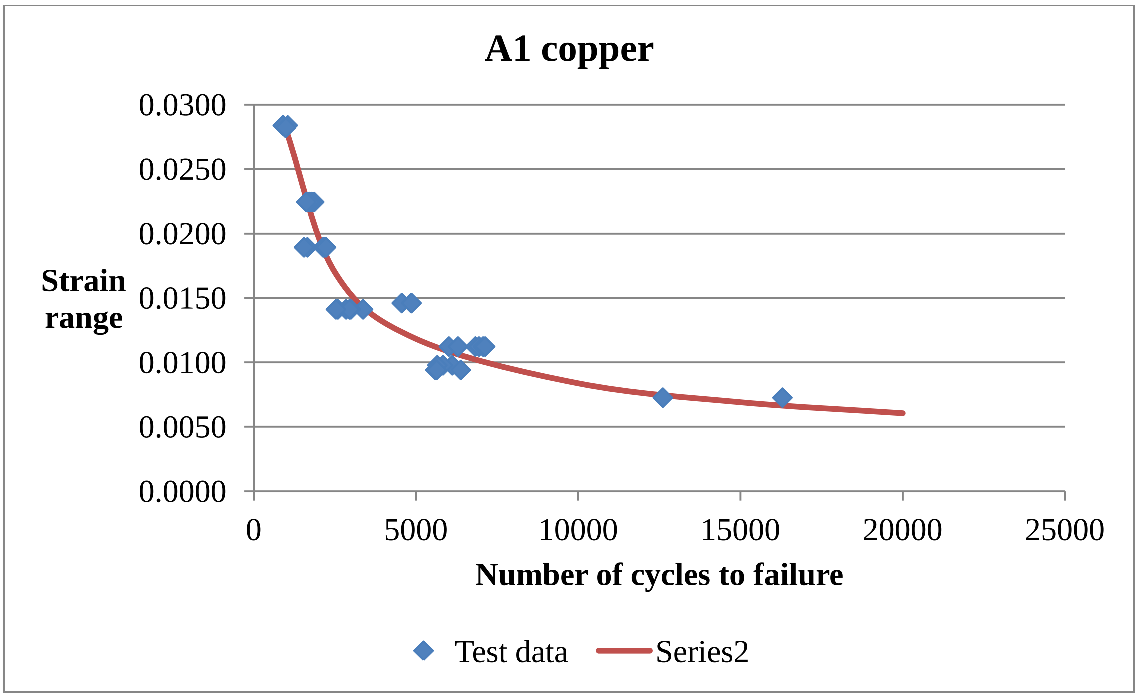

Figure 64; A1 copper flex life curve

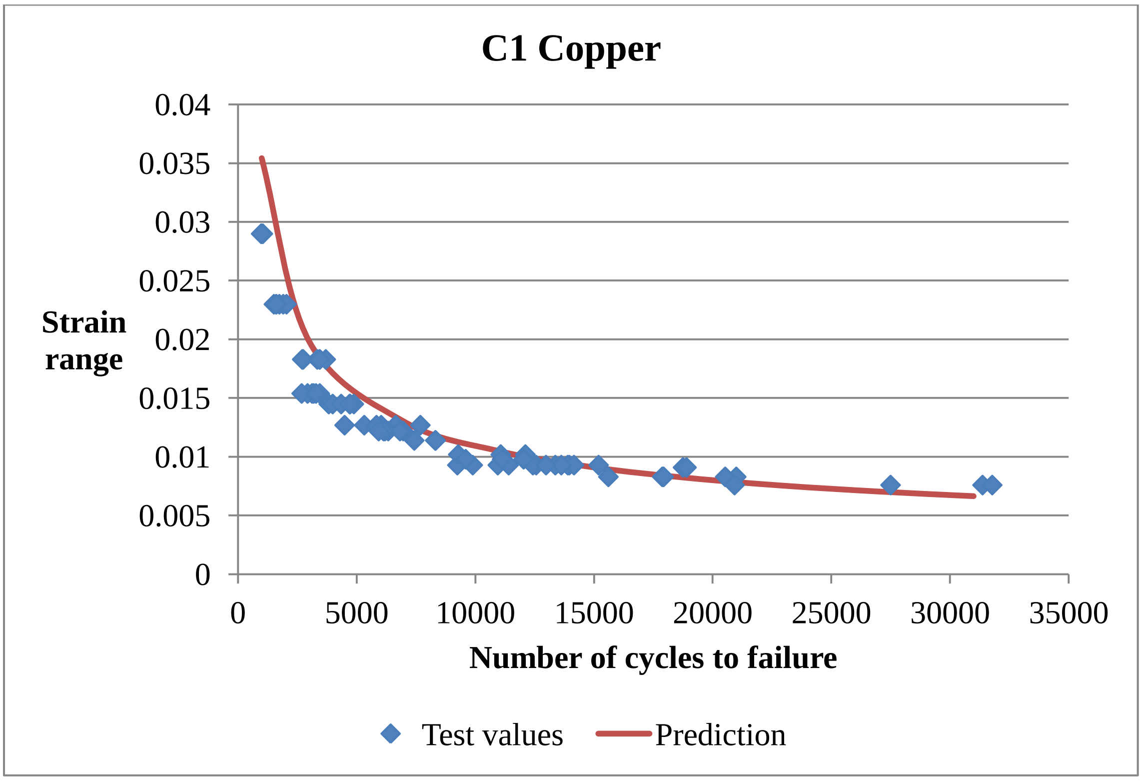

Figure 65; C1 copper flex life curve

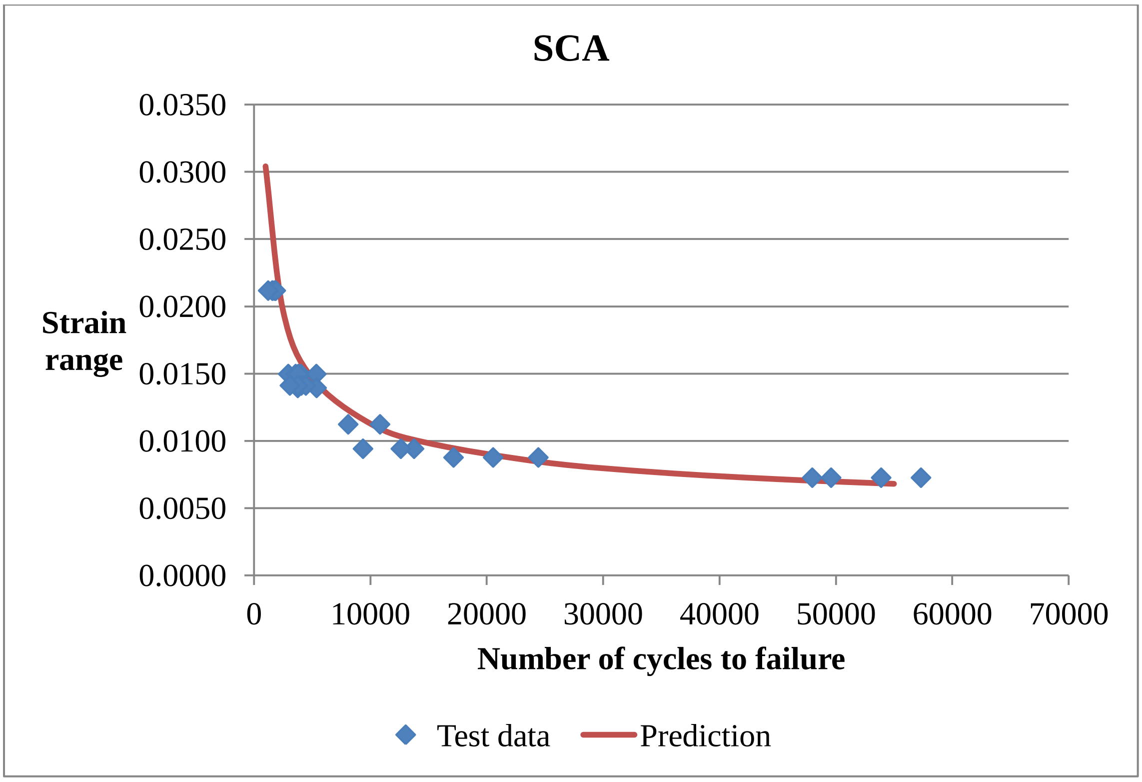

Figure 66; SCA flex life curve

19.2 Appendix 2

ETFE flex life curve, temperature model and data:

Table 12; ETFE data

Temperature (^oC)	UTS (MPa)	σ-ε curve
21	31.5	$\sigma = 53608\varepsilon^6 - 75146\varepsilon^5 + 38347\varepsilon^4 - 8019.1\varepsilon^3 + 269.37\varepsilon^2 + 149.15\varepsilon$
60	27.1	$\sigma = 2647.9\varepsilon^6 + 171.99\varepsilon^5 - 3517.4\varepsilon^4 + 2585.3\varepsilon^3 - 834.74\varepsilon^2 + 148.62\varepsilon$
90	22.37	$\sigma = -1412.5\varepsilon^6 + 3638\varepsilon^5 - 3774.3\varepsilon^4 + 2043.8\varepsilon^3 - 631.26\varepsilon^2 + 115.58\varepsilon$
120	13.57	$\sigma = 30370\varepsilon^6 - 34360\varepsilon^5 + 14421\varepsilon^4 - 2579.5\varepsilon^3 + 81.851\varepsilon^2 + 42.137\varepsilon$

m = -0.078

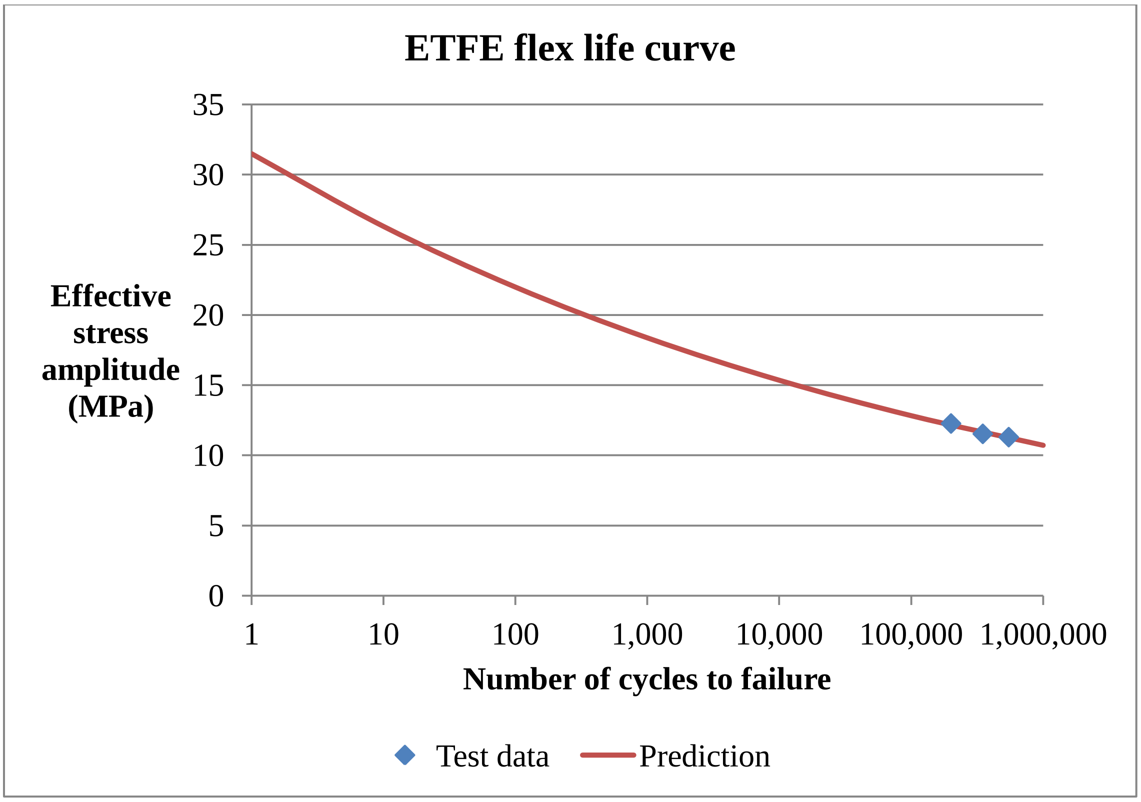

Figure 67; ETFE flex life curve

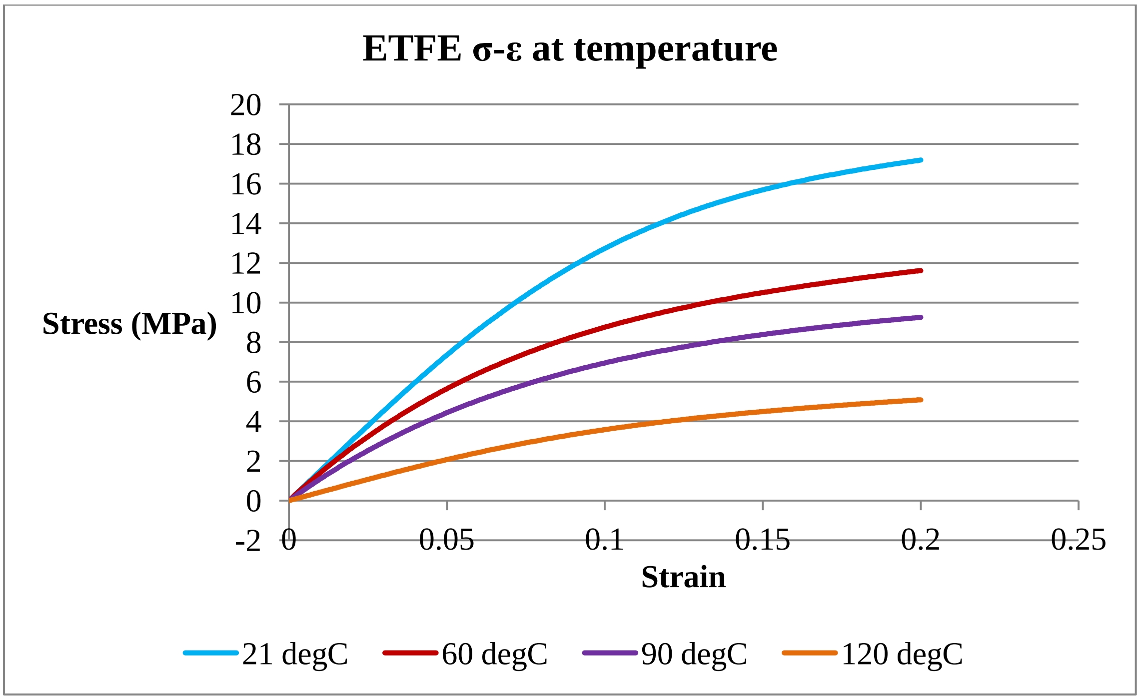

Figure 68; ETFE stress-strain at temperature

FEP grade 1 data and flex life curve at -20^{o}C:

Table 13; FEP grade 1 data

Temperature (^{o}C)	UTS (MPa)	σ-ε curve
-20	23.54	$\sigma = -306476.3\varepsilon^6 + 305635.02\varepsilon^5 - 117509.31\varepsilon^4 + 21901.32\varepsilon^3 - 2301.6\varepsilon^2 + 235.6\varepsilon$
21	19.75	$\sigma = 233320\varepsilon^6 - 194284\varepsilon^5 + 67269\varepsilon^4 - 10896\varepsilon^3 + 316.86\varepsilon^2 + 142.74\varepsilon$
60	13	$\sigma = 1779578\varepsilon^6 - 1356629\varepsilon^5 + 392380\varepsilon^4 - 51362\varepsilon^3 + 2396.3\varepsilon^2 + 86.772\varepsilon$
90	11	$\sigma = 88901\varepsilon^6 - 91627\varepsilon^5 + 34841\varepsilon^4 - 5534.3\varepsilon^3 + 148.95\varepsilon^2 + 59.288\varepsilon$
120	9.43	$\sigma = 157.72\varepsilon^4 - 57.769\varepsilon^3 - 42.513\varepsilon^2 + 27.685\varepsilon$

m = -0.077

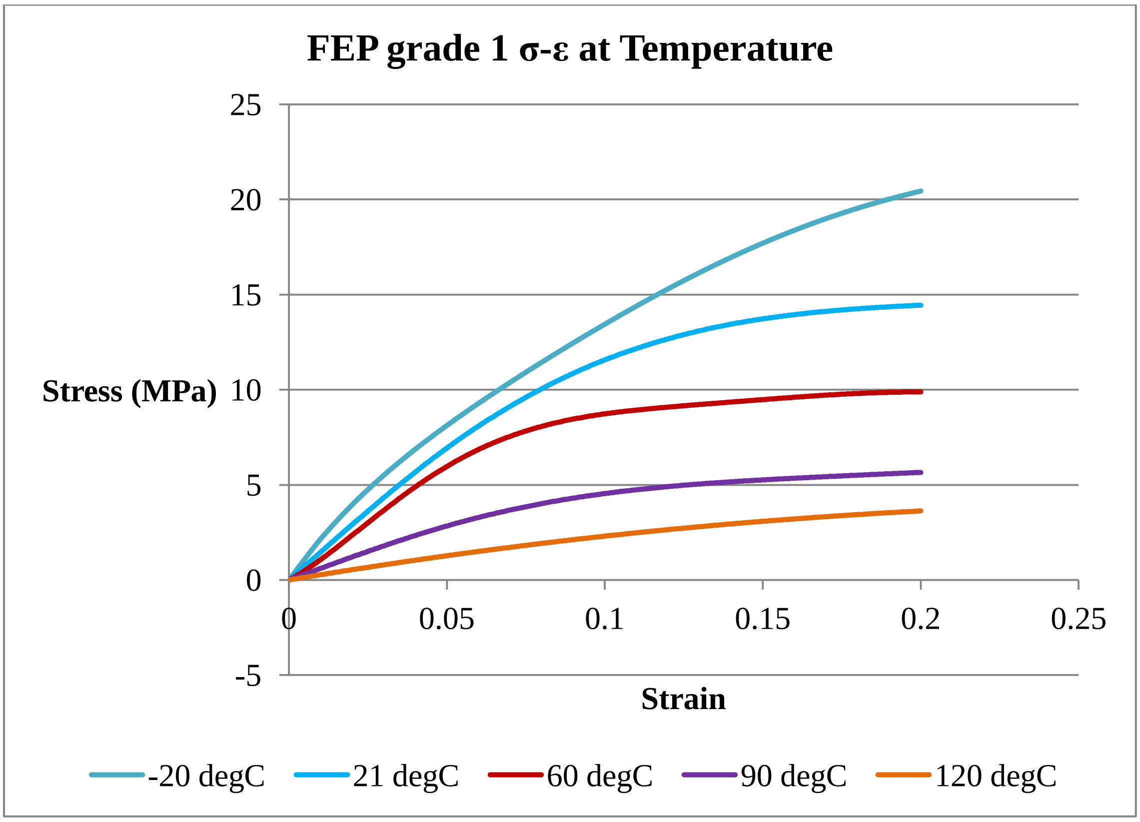

Figure 69; FEP grade 1 stress-strain at temperature

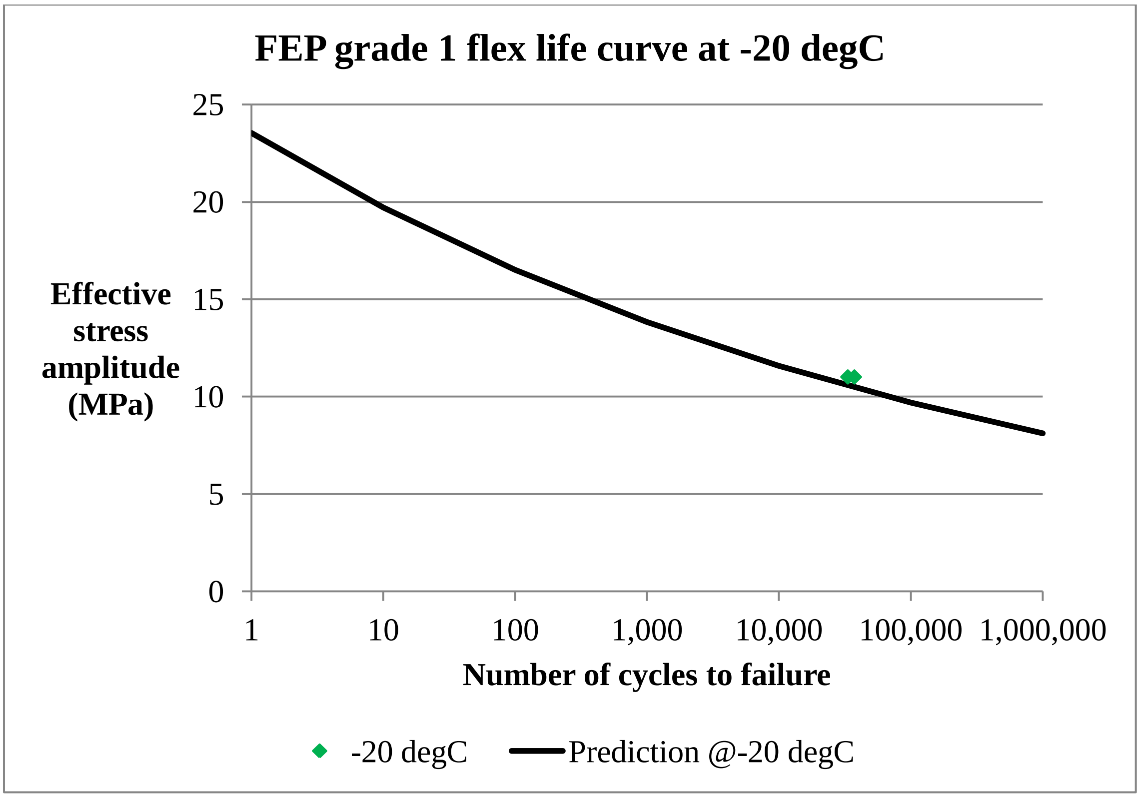

Figure 70; FEP grade 1 flex life at -20^{o}C

FEP grade 2 data:

Table 14; FEP grade 2 data

Temperature (^oC)	UTS (MPa)	σ-ε curve
-20	23.2	$\sigma = 198950.02\varepsilon^5 - 112418.42\varepsilon^4 + 23789.97\varepsilon^3 - 2957.62\varepsilon^2 + 340.09\varepsilon$
21	16.2	$\sigma = -1065632.06\varepsilon^6 + 627040.49\varepsilon^5 - 119764.36\varepsilon^4 + 7236.4\varepsilon^3 - 451.59\varepsilon^2 + 174.02\varepsilon$
60	12.32	$\sigma = -5036.4\varepsilon^6 - 21283\varepsilon^5 + 17221\varepsilon^4 - 4001.2\varepsilon^3 + 82.359\varepsilon^2 + 85.028\varepsilon$
90	9.15	$\sigma = 38963\varepsilon^6 - 44741\varepsilon^5 + 18234\varepsilon^4 - 2954.6\varepsilon^3 + 25.189\varepsilon^2 + 50.744\varepsilon$
120	6.76	$\sigma = 2307.9\varepsilon^6 - 4235.6\varepsilon^5 + 2974.6\varepsilon^4 - 931.1\varepsilon^3 + 84.173\varepsilon^2 + 20.22\varepsilon$

m = -0.043

PTFE data and stress-strain curves:

Table 15; PTFE data

Temperature (^oC)	UTS (MPa)	σ-ε curve
21	29.7	$\sigma = 58787\varepsilon^6 - 73901\varepsilon^5 + 32554\varepsilon^4 - 5015\varepsilon^3 - 303.41\varepsilon^2 + 170.62\varepsilon$
60	24.2	$\sigma = 41058\varepsilon^6 - 51175\varepsilon^5 + 23108\varepsilon^4 - 4112.2\varepsilon^3 + 19.758\varepsilon^2 + 84.41\varepsilon$
90	21.9	$\sigma = 34205\varepsilon^6 - 39689\varepsilon^5 + 17098\varepsilon^4 - 3098.3\varepsilon^3 + 83.518\varepsilon^2 + 54.303\varepsilon$
120	13.34	$\sigma = 172.18\varepsilon^3 - 137.94\varepsilon^2 + 45.01\varepsilon$

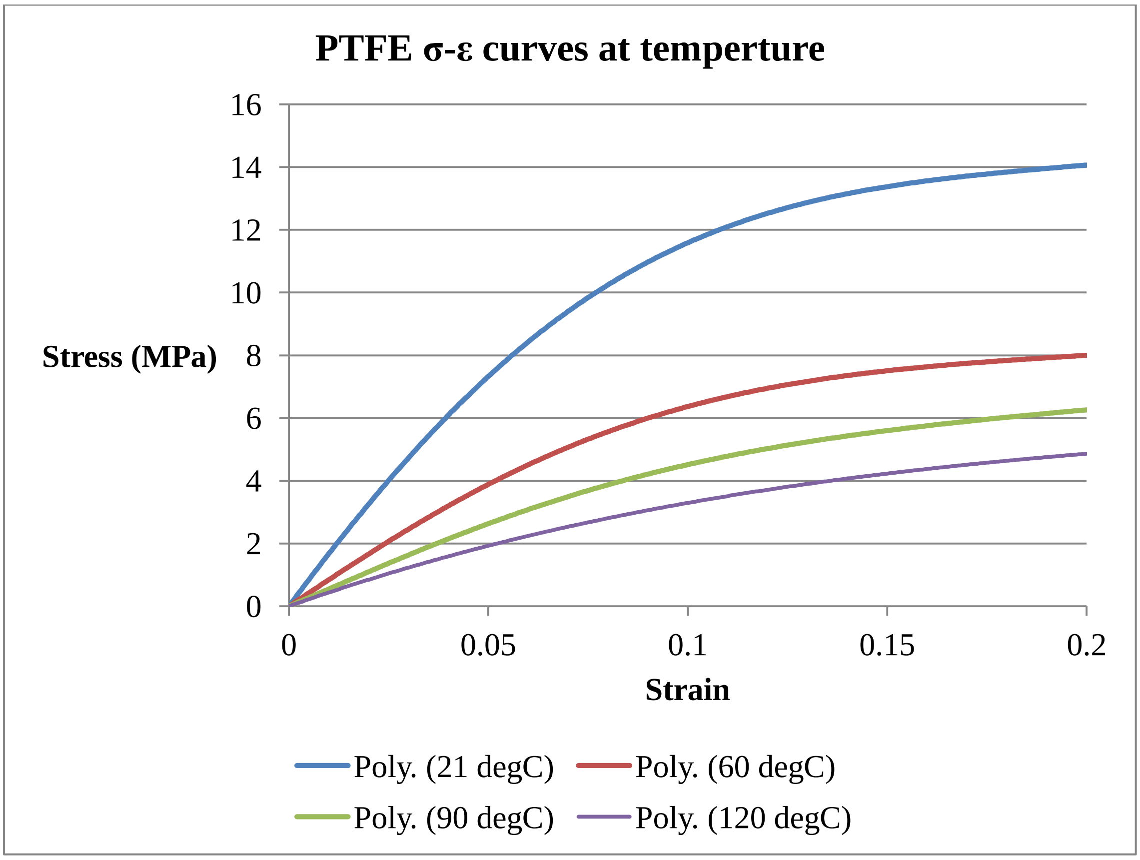

Figure 71; PTFE stress strain at temperature

19.3 Appendix 3

See attached CD for files with MATLAB code.

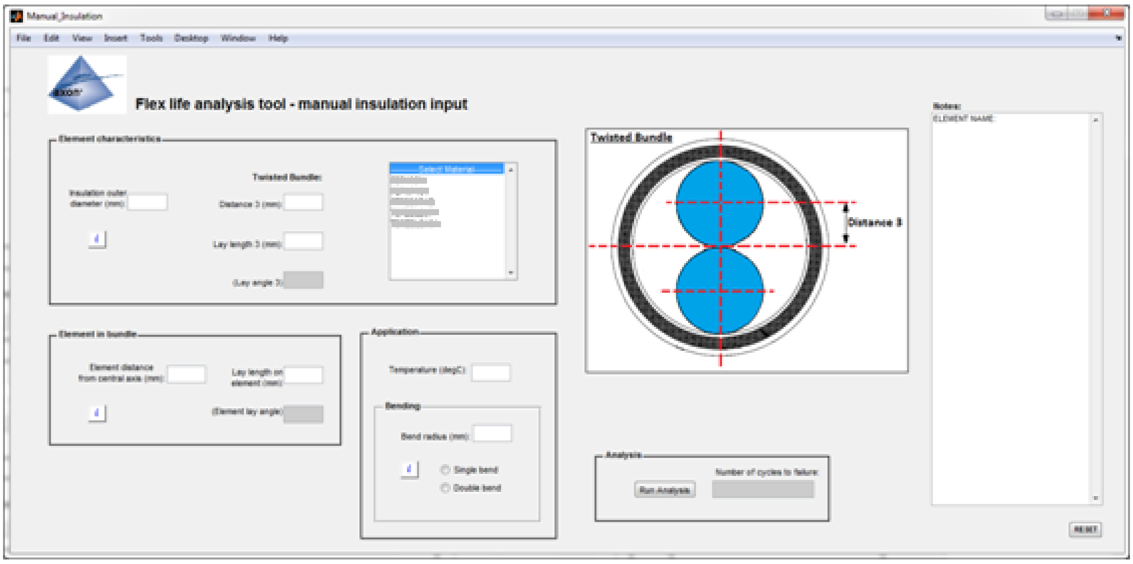

Figure 72; Manual insulation input GUI

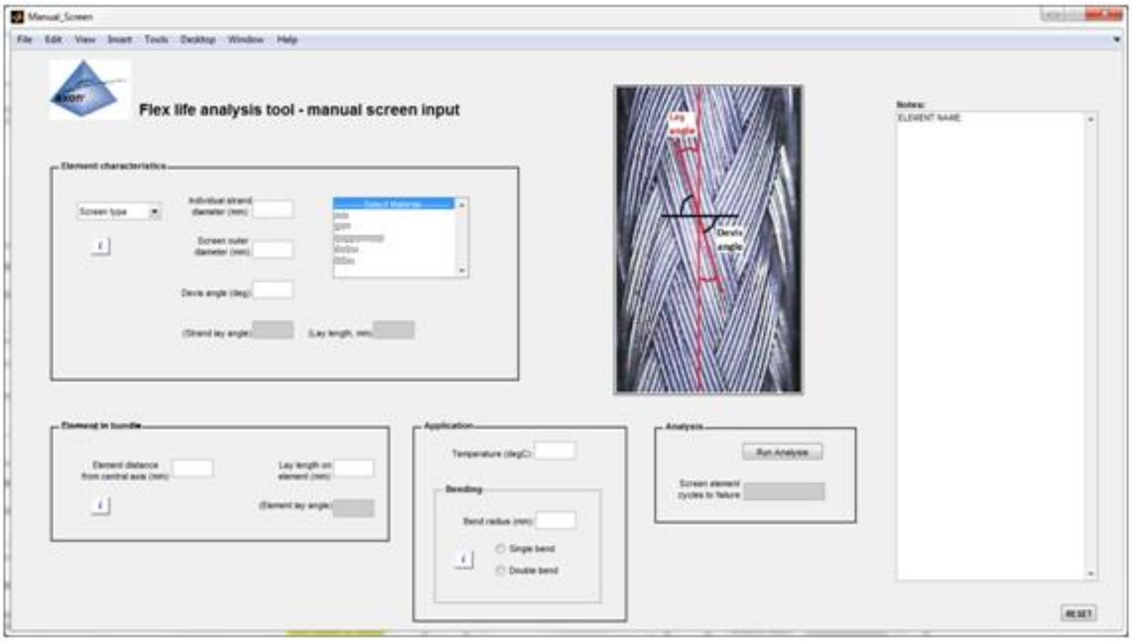

Figure 73; Manual screen input GUI